Mendel University in Brno
Faculty of Forestry and Wood Technology
Department of Wood Science

Heat transfer in wood and wood-based materials

Doctoral Thesis

Author: Ing. Eva Troppová
Supervisor: Ing. Jan Tippner, Ph.D.

2015

Declaration

I declare I have written the presented dissertation titled “Heat transfer in wood and wood-based materials” independently and that I have listed all references. I agree that my dissertation is published in compliance with § 47b of Act no. 111/1998 Coll., on universities, stored in the library of the Mendel University in Brno and available for study purposes in compliance with the MENDELU Rector’s Decree on archiving the electronic form of final studies.

Prohlášení

Prohlašuji, že jsem předloženou disertační práci na téma “Heat transfer in wood and wood-based materials ” zpracovala samostatně a uvedla jsem všechny použité prameny. Souhlasím, aby moje disertační práce byla zveřejněna v souladu s § 47b Zákona č. 111/1998 Sb., o vysokých školách a uložena v knihovně Mendelovy univerzity v Brně, zpřístupněna ke studijním účelům ve shodě s Vyhláškou rektora MENDELU o archivaci elektronické podoby závěrečných prací.

Brno, 15.10.2015 Eva Troppová

Preface

The presented work has been made possible by financial support from the European Social Fund and the state budget of the Czech Republic (project no. CZ.1.07/2.3.00/20.0269– InWood, “The Establishment of an International Research Team for the Development of New Wood-Based Materials”) as well as the Internal Grant Agency (IGA) of the Faculty of Forestry and Wood Technology, Mendel University in Brno – project 8/2011 (Shape and topology optimization of structural parts in wood based buildings), project 25/2013 (Variety of factors influencing the thermal conductivity of insulation wood-based fibreboards) and project 19/2014 (Heat transfer in wooden construction including an air cavity).

The work has been carried out as a Ph.D. thesis at the Department of Wood Science, the Mendel University in Brno. First of all, I would like to thank Doctor Jan Tippner for being my supervisor, for his support and encouragement. My gratitude also belongs to Associate Professor Petr Koňas, who showed me the potentials of a research work. I also want to thank my colleagues and friends from the Department of Wood Science for discussions and good company throughout the years.

Finally, not least, thanks to my parents, my family and close friends for moral support, Elenka for being my pleasure of life.

Brno, October 2015

Eva Troppová

Abstract

Troppová E. (2015) „*Heat transfer in wood and wood-based materials*“, Dissertation thesis, Mendel University in Brno.

The main goals of the dissertation thesis were to investigate thermal properties of wood and wood-based materials using different measurement methods and to study the influence of specific parameters on the measuring processes and, furthermore, on the thermophysical parameters in particular cases. This thesis deals with the description of all heat transfer modes occurring in wooden constructions, as well as with laboratory measurements, theoretical analyses and analysis of the possibilities of in-situ measurement of thermal behavior of wooden structures. The work is structured into three themes: a) on the thermal measurement methods including assessment of their limitations; b) on investigation of influence of materials´ parameters on their thermal properties and c) on contribution of all three heat transfer modes - conduction, convection and radiation, in studied phenomena.

The experimental part of this study consists of evaluation of thermophysical parameters of materials based on three different methods: the heat-flow meter method, the pulse-transient method and the quasi-stationary method. Within the work the medium density fiberboards, Lignamon (ammonia-treated compressed beech wood) and insulation wood-based fiberboards have been studied. For these materials, thermal conductivity, thermal diffusivity and specific heat were evaluated depending on density, moisture content and temperature.

Furthermore, parametric numerical models were employed to study the impact and limitations of chosen measurement methods on the thermal response of each material. Numerical modeling carried out in computing environment ANSYS enabled sensitivity studies of influence of selected parameters on the thermal response of materials. Probabilistic numerical analyses served for both a verification of the experiments and assessment of parameters´ impact on results. Coupled thermal-fluid analysis was solved in ANSYS Flotran software. The contribution of radiation heat transfer on the final heat flow through a construction with an air cavity was computed and compared with experimentally

measured data. Finally, the temperature distribution in a wooden construction was studied with help of infrared thermography.

The results from experiments as well as from the numerical studies showed differences in thermal properties of modified wood and wood-based materials depending on chosen measurement method and different parameters during measuring processes. Nowadays, there is an increasing demand for low conductive materials having often heterogeneous, anisotropic and porous structure with hygroscopic character and that is why there is a call for accurate evaluation of their thermal properties. This thesis addresses the call by providing fundamental knowledge of complex heat transfer in materials and wooden structures.

Key words: thermal conductivity, thermal diffusivity, specific heat capacity, pulse-transient method, quasi-stationary method, heat-flow meter method, numerical simulation, finite element method (FEM), probabilistic analysis

Abstrakt

Troppová E. (2015) *„Sdílení tepla ve dřevě a materiálech na bázi dřeva“*, Disertační práce, Mendelova univerzita v Brně.

Hlavním cílem předkládané disertační práce bylo stanovení tepelných vlastností dřeva a materiálů na bázi dřeva pomocí různých metod měření a posouzení vlivu vybraných parametrů na procesy měření a na samotné stanovení termofyzikálních vlastností. Tato práce se dále zabývá popisem sdílení tepla, stejně jako možnostmi in-situ měření tepelných ztrát v dřevěných konstrukcích. Teze je rozdělena do tří témat: a) metody měření tepelných vlastností materiálů a jejich možná omezení; b) studium vlivu parametrů na tepelné vlastnosti materiálů; c) poměr jednotlivých složek sdílení tepla (kondukce, konvekce a radiace) na celkový tepelný tok.

Experimentální část této práce je složena z měření tepelných vlastností materiálů pomocí pulsní transientní metody, quasi-stacionární metody a metody měřidla tepelného toku. Hlavními měřenými materiály byla středně hustá dřevovláknitá deska (MDF), Lignamon (lisované bukové dřevo tepelně upravené pomocí amoniaku) a izolační dřevovláknité desky. Pro tyto materiály byla zjištěna tepelná vodivost, teplotní vodivost a měrná tepelná kapacita v závislosti na hustotě, obsahu vlhkosti a teplotě.

Pomocí parametrických numerických modelů byl zjištěn vliv a možná omezení vybraných metod měření. Numerické modelování ve výpočetním programu Ansys Mechanical APDL umožnilo sledovat pomocí citlivostní analýzy vliv vybraných parametrů na teplotní odezvu materiálů. Výsledky pravděpodobnostní analýzy zhodnotily vliv jednotlivých vstupních parametrů na měřené experimentální hodnoty. Sdružená úloha vedení tepla a proudění tekutiny byla řešena v programu ANSYS Flotran. Podíl sdílení tepla radiací na celkový tepelný tok konstrukcí se vzduchovou mezerou byl vypočten numericky a porovnán s experimentálními hodnotami.

Výsledky získané experimentálně, i pomocí numerických analýz, prokázaly rozdíly v tepelných vlastnostech modifikovaného dřeva a materiálů na bázi dřeva v závislosti na zvolené metodě měření. V současné době se upřednostňují materiály s lepšími izolačními vlastnostmi, které se často vyznačují vysokou heterogenitou a pórovitostí. Přesné stanovení

jejich tepelných vlastností není jednoduchou záležitostí, jelikož je často ovlivněno mnoha faktory. Cílem této práce bylo objasnit sdílení tepla v těchto materiálech a částech konstrukcí obsahujících studované materiály.

Klíčová slova: tepelná vodivost, teplotní vodivost, měrná tepelná kapacita, pulsní-transientní metoda, quasi-stacionární metoda, metoda měřidla tepelného toku, numerická simulace, metoda konečných prvků (MKP), pravděpodobnostní analýza

Table of Contents

List of Figures

Material and methods

Paper I.

Paper II.

Paper III.

Paper IV.

Paper IV.a

Paper V.

Paper VI.

List of Tables

Material and methods

Paper I.

Paper II.

Paper III.

Paper IV.

Paper IV.a

Paper V.

Paper VI.

List of Abbreviations

APDL	ANSYS parametric design language
BET	Brunauer-Emmett-Teller theory
CFD	computational fluid dynamics
EMC	equilibrium moisture content
FE	finite element
FEM	finite element method
FVM	finite volume method
GPH	guarded hot plate method
HAM	heat, air and moisture transfer
HFM	heat flow meter method
H-H	Hailwood Horrobin model
IR	infrared camera
LFA	laser flash method
MC	moisture content
MDF	medium density fiberboard
MTI	multilayer thermal insulation
RH	relative humidity
PDS	probabilistic design system
PMMA	polymethyl methacrylate
TPS	transient plane source method
VDP	vertical density profile

Specific symbols and Greek symbols are listed in nomenclatures of papers.

1. Introduction

Thermal properties of wood and wood based materials play an important role in variety of heat transfer phenomena. A general need exists to model heat transfer processes in such materials. The nowadays preferred materials in building industry are mostly composite materials with homogenized structure and improved mechanical and thermal properties. Many modification processes have been employed with the purpose to improve the natural properties of wood. Despite wide research in this topic, thermal properties of wood and other composite materials with fibrous structure are still affected by temperature and changes in moisture content. The heterogeneity, porosity and anisotropy together with hygroscopic character play also an important role in heat transfer through the materials.

The development of measuring methods enabled more accurate assessment of thermal parameters and verification of theoretical heat transfer models of new materials. The fundamental stationary methods compete with quick transient measurements which enable determination of a full set of thermophysical parameters within one measuring process. Those methods are validated for most isotropic stable materials. The measurement of materials with heterogeneous structure or anisotropic properties highly dependent on moisture content and density is challenging as it is influenced by variety of parameters. This dissertation thesis deal with this topic as well as with the general description of heat transferred through wood and selected wood based materials.

1.1. Aims of the study

The main aims of the thesis were as follows:

- to investigate thermal properties of wood (beech wood and Lignamon) and selected wood based materials (medium density fiberboard and low density fiberboards) based on different measuring methods (quasi-stationary, pulse transient and heat flow meter method)

- to study influence of specific parameters (e.g. density of samples, heat transfer coefficient, ambient temperature) on the measuring processes as well as on the thermal properties by using numerical methods

- to describe all heat transfer modes (conduction, convection and radiation) in a wood-based part of a construction (e.g. a structure composed of insulation fibreboards and a horizontal air cavity)

1.2. List of papers

This doctoral thesis is a summary of the following papers:

Paper I.

Troppová E, Tippner J, Hrčka R, Halachan P (2013) *Quasi-stationary measurements of Lignamon thermal properties*, BioResources 8(4): 6288-6296.

Paper II.

Troppová E, Tippner J, Hrčka R (2015) *Thermophysical properties of medium density fiberboards measured by quasi-stationary method: experimental and numerical evaluation*, Manuscript is under review in Heat and Mass Transfer.

Paper III.

Troppová E, Tippner J (2015) *The influence of specific parameters on thermal properties of medium density fiberboards by pulse transient method*, Manuscript sent to International Journal of Thermal Sciences.

Paper IV.

Troppová E, Švehlík M, Tippner J, Wimmer R (2014) *Influence of temperature and moisture content on the thermal conductivity of wood-based fibreboards*, Materials and Structures, DOI: 10.1617/s11527-014-0467-4.

Paper IV.a

Troppová E, Tippner J (2014) *Thermal conductivity and water vapour transmission properties of wood-based fiberboards*, Proceedings of the 57th International Convention of Society of Wood Science and Technology, June 23-27, 2014 - Zvolen, Slovakia

Paper V.

Troppová E, Tippner J, Švehlík M (2015) *Numerical and experimental study of conjugate heat transfer in a horizontal air cavity at different heat flow directions***,** Manuscript sent to Construction and Building Materials

Paper VI.

Troppová E, Tippner J, Klepárník J (2015) *Thermal bridges in a prefabricated wooden house: experimental and numerical characterization,* Manuscript sent to Wood Material Science & Engineering

2. Literature review

2.1. Thermal properties measurements of wood and wood-based materials

The knowledge of temperature field in a measured sample is a fundamental of all measuring methods dealing with thermal properties evaluation. The temperature distribution in a specimen is a solution of a differential equation in a shape depending on the heat source (Krempaský, 1969). Based on the exact shape of the equation, the solution may stay unchanged within time or may change in time. The measuring methods can be divided into two basic groups based on the time derivative of temperature. Stable distribution of materials´ temperature is required in steady-state techniques. The accurate measurement of the temperature difference is possible after reaching thermal equilibrium. There are some effects affecting the accuracy of steady-state measurements: the influence of heat losses from a sample to the surroundings, low accuracy in temperature measurement, and the influence of thermal contact resistance. The heat flux entering a sample must be uniaxial, thus the heat losses should be minimized in the radial direction. The heat losses to the surroundings are desirable to eliminate when specimens with higher sizes at high temperature gradients are measured. The usage of insulation around a sample or a ”guard” with a controlled identical temperature gradient minimizes the radial heat flow. Such an arrangement is utilized in guarded hot plate (GHP) and heat flow meter (HFM) measuring techniques. The GHP is an absolute measurement method which requires no calibration standards. Its principle is to reproduce the uniform, unidirectional and constant heat flux coming through a homogenous plate specimen (Dubois and Lebeau, 2013). The two samples are placed between an electrically tempered hot and a cold plate, both maintained at different temperatures. The heat dissipated by the Joule effect in the hot plate enters the sample, but it is distributed also backwards and laterally to the edges of the specimen. Therefore, rear and lateral insulations are necessary. This technique for measuring the thermal conductivities of insulation materials has been known in various forms since 1898 (Salmon, 2001). Nowadays, the GHP method is documented in the standard ISO 8302:1991. The HFM method is based on the analogous principals as the

GHP method. A specimen is placed between a hot and a cold plate and the heat flow created by the defined temperature difference is measured with a heat flux sensor. Thermal conductivity is calculated once the equilibrium criteria are met. Contrary to GHP, the HFM device has to be calibrated with a certified reference standard material of known thermal conductivity. The use of HFM method to measure the steady-state heat transfer through flat slab specimens is introduced in the standard ISO 8301:1991. The conductivity range of the HFM and the GHP methods is between 0.001-1 $W.m^{-1}.K^{-1}$. Both mentioned methods are absolute processes, as the heat flux is measured directly. Indirect heat flux measurement is termed comparative method. The comparative cut-bar technique is a widely used steady-state method for the measurement of (axial) thermal conductivity of solids (Xing et al., 2014). In this technique, the sample is placed between two reference materials of known thermal conductivity. One-dimensional Fourier´s law is applied to calculate the thermal conductivity of an unknown specimen by comparing the respective thermal gradients inversely proportional to conductivities of a reference and a measured material. Naturally, many other measuring methods exist (as e.g. the hot wire method or probe methods), but are rather limited in use for anisotropic and heterogeneous materials. Generally, many authors dealt with the thermal conductivity evaluation of wood and wood-based materials using one of the stationary techniques, as they are classical and precise methods for measuring thermal properties. Zarr et al. (1995) used the guarded hot plate method to measure thermal conductivity of fiberboards (density 380 $kg.m^{-3}$) at a temperature difference of 10°C. The effect of density, moisture content (MC) and temperature on the thermal conductivity of Scots pine, birch and larch wood measured by heat flow meter technique was determined by Yu et al. (2011). Thermal properties of wood-based panels composed of plywood and low density fiberboard were measured at heat flow meter apparatus by mean temperature of 20°C (Kawasaki and Kawai, 2006). Manohar et al. (2005) measured thermal conductivity across the wood grain on 11 wood species with different densities using the guarded hot plate method. The thermal conductivity of wood floorings strongly related to their densities was measured by Seo et al. (2011) following the guarded hot plate method. The hot wire method was used to determine the thermal conductivity of different types of wood (beech, oak, fir, Scots pine and chestnut) with

respect to the direction of grain angle (Yapici et al., 2011). The measurement precision is about 5% when using the hot wire method to establish thermal conductivity of beech, fir and pine wood (Dündar et al., 2012).

The transient (non-stationary) methods are based on recording the temperature changes occurring during the measurement. The time of each measurement is shorter compared to stationary methods, which is one of the advantages. All three thermal parameters (thermal conductivity, thermal diffusivity and specific heat capacity) are possible to calculate within one measurement when density of a sample is known. Transient techniques are obviously used to examine the sensitivity of thermal parameters on specific variables as e.g. temperature, moisture content, pressure, density, etc. As well as stationary methods, transient techniques are also affected by various factors. The ideal thermal contact between samples and the capacity of heat source should not be neglected. Temperature as a function of time is acquired and then mathematically analyzed to reach thermal parameters. During the measurement, a heat pulse passes through the measured sample and the thermal response is recorded by a sensor. Some of the transient measuring techniques enable measurement of all three thermal properties from cryogenic to high temperatures and at different ambient environments (air, vacuum or other gases). The transient plane source method (TPS) covers a thermal conductivity range of at least 0.01-500 $W.m^{-1}.K^{-1}$ to test both isotropic and anisotropic materials, in compliance with ISO 22007-2 (Gustavsson, 1991). The TPS method is based on recording the temperature increase caused by the constant heat coming through a heat source (e.g. a thin double nickel spiral sandwiched between two layers of Kapton). Two samples of the same material are located in contact with the two faces of the sensor (Almanza et al., 2004). The size of the probe has to be chosen as large as possible to obtain relevant data with minimum disturbance induced by structural heterogeneities of wood (e.g. annual growth rings, differences of densities between earlywood and latewood). Dupleix et al. (2012) studied the transverse (radial and tangential) thermal parameters of the green wood of four wood species (beech, birch, fir and spruce) at moisture content around the fiber saturation point using the TPS method.

Another transient method is the laser flash method (LFA). LFA, developed by Parker et al. (1961); it is composed of a laser which heats the specimen from the bottom side and a

sensor placed on the upper side of the specimen for detecting the temperature rise in time. Harada et al. (1998) used the LFA method to measure thermal constants of different wood species at high temperatures and under vacuum conditions to investigate thermal behavior of wood during the heating process. The thermal diffusivity of commercially available MDF with different moisture contents was investigated at a temperature range of 25-150°C using the light flash system (Zhou et al., 2013).

A special case of a transient measurement, called the quasi-stationary method, is named after a linear part of a temperature increase in time. The quasi-stationary method was developed at the Technical University in Zvolen (Požgaj et al., 1997) and utilizes knowledge from previously published methods developed by Clarke and Kingston (1950) and Kirsher and Esdorn (1954). Thermal parameters of densified ammonia-treated wood (called Lignamon) related to density values were investigated by Troppová et al. (2013), see Paper I. Hrčka and Babiak (2012) compared thermal properties of ash wood measured using a device based on the hot-wire method with a flat probe and using a device based on the quasi-stationary method.

There are still other contact transient methods to measure thermal parameters of wood-based materials. A device based on the pulse transient method was developed by the Slovak Academy of Sciences. The principle of the pulse transient method is based on the monitoring of temperature inside the specimen which is heated by heat pulse generated using the planar heat source (Kubičár et al., 2005). The thermocouple measures the temperature response. All three thermal properties are possible to investigate according to parameters of the temperature recording (a value of the maximal temperature response and time when it reaches its maximal value). Kubičár and Boháč (2002) compared the pulse transient and the stepwise transient method. The deviation was up to 10% when measuring isotropic materials.

The correct evaluation of thermal conductivity is often an object of discussion as each measuring method is limited in a principle (Asdrubali et al., 2010). Almanza et al. (2004) stated that the values of thermal conductivity obtained by the transient method are approximately 20% higher than those given by heat stationary method. The temperature gap between the HFM surfaces and those of the sample probably lead to the reduction of

the heat transferred by the conduction. When a thermal gradient is applied to a moist sample, the redistribution of moisture comes on which makes the stationary method inappropriate for the thermal measurement (TenWolde et al., 1988). Yu et al. (2011) used heat flow meter method technique to measure ovendry wood specimens and the transient plane source technique for moist samples. The heat transfer quantified by a steady-state technique includes not only equivalent conduction-convection-radiation transfer but also heat transferred via moisture movement in the material which is significant especially during the initial stages of the moisture redistribution process (Bomberg and Shirtliffe, 1978). Sonderegger et al. (2011) measured thermal conductivity of spruce and beech wood at different temperatures (10-40°C) and moisture contents (9-19% of MC) by using the HFM method. The heat transfer due to the moisture distribution is not discussed in the work. Methods based on transient heat transfer have the potential of direct determining not only thermal conductivity but also thermal diffusivity of moist material, but the accuracy is not as high as by steady-state methods applied to dry material (Mohesnin, 1980).

Thermophysical properties (thermal conductivity and diffusivity, heat capacity, thermal expansion and thermal radiative properties) are material properties affecting the transfer and storage of heat. The important factors influencing these thermophysical properties of wood and wood based materials are: wood species, density, moisture content (MC), anisotropy, grain inclination and the relation of sample thickness to moisture content (Suleiman et al., 1999). Due to the anisotropic nature of wood, there is a direction dependency of thermal conductivity in both hard and soft woods (Steinhagen 1977). Thermal conductivity in the longitudinal direction (parallel to the grain) is greater than conductivity in the transverse direction (Suleiman et al., 1999). The ratio of thermal conductivity values of longitudinal to radial direction is 2.4, longitudinal to tangential 2.6 and radial to tangential 1.1 for elm wood (Hrčka and Kurjatko, 2006). Hankalin et al. (2009) concluded that thermal conductivity of wood in the grain direction is 1.5-2.7 times the conductivity perpendicular to the grain direction. The thermal conductivity of softwoods is 2.16 times greater along the grain than in the tangential direction and 1.36 times greater than in the radial direction (Leon et al., 2000). Suleiman (2011) mentioned that measurements of wood thermal conductivity as a function of phase morphology (grain

size and orientation) indicate preferential heat conduction along the conduction chain of grains. Grønli (1996) reported that thermal conductivity is higher along the wood grain orientation and resistance to gas transport in this direction is several orders of magnitude lower. Thermal conductivity at moisture content below fiber saturation point is in the radial direction about 1.5 to 2.5 times lower than in the tangential direction for softwood species and 1.5 times lower for hardwood species (Gu, 2001). Yapici et al. (2011) stated that differences between thermal conductivities measured parallel to the grain and in the perpendicular direction are negligible in comparison with other influencing factors such as density or the chemical composition which is in contrary to the general expectations.

Specific heat capacity is as a scalar quantity independent on the anatomical direction (Hrčka and Kurjatko, 2006). Simpson and TenWolde (1999) reported that the specific heat capacity of wood depends on the temperature and moisture content, but it is practically independent on density and species. A linear relationship between wood thermal conductivity and density based on guarded hot plate measurements was found by Van Dusen (1920). The change of wood density causes a change of content of the separate anatomical and chemical components of the wood, for which the thermal conductivity is different (Deltiski, 2013). The linear relation between the conductivity and density and also between the conductivity and moisture content was proved based on an investigation of over 100 species explored by Rowley (1933). MacLean (1941) found the direct proportion between thermal conductivity and specific gravity when testing 32 wood species with different densities and moisture contents. Wangaard (1940), Siau (1984) and Rice and Shephard (2004) reported a consistent relationship between thermal conductivity and specific gravity. The effect of specific gravity may be related to the porosity of wood, as wood transfers heat by convection and conduction (Kol, 2009). Venkateswaran (1974) mentioned that the variation in the chemical components of wood results in the variation of thermal conductivities. Generally, the thermal conductivity of wood increases with increasing density, moisture content and temperature (Rowley 1933; Wangaard 1940; McLeaan 1941; Kühlmann 1962; Siau 1984, Suleiman et al. 1999; Fotsing and Takam 2004; Gu and Zink-Sharp 2005). A nearly linear dependence of thermal conductivity of wood at temperatures between 30°C and 90°C for some wood species in China was

observed by Yu et al. (2011). Linear relations of conductivity data for temperatures between -40°C and +100°C were presented by Steinhagen (1977). The conductivity of some wood species in Japan for a temperature range up to 270°C was measured by Harada et al. (1998). In the results of Ward and Skaar (1960) the thermal conductivity and specific heat of wood and wood-based materials are related linearly to temperature. Most of the linear thermal regressions were compared with the empirical relationship of temperature effect on the thermal conductivity derived by Kollmann (1951). Suleiman et al. (1999) stated that thermal conductivities of wood samples are higher at 100°C than those at 20°C which is consistent with the general expectations. The density of air decreases with a rising temperature which leads to lowering of heat conduction through voids. A possible explanation is that another mode of heat transfer occurs over the temperature of 100°C involving the microstructure of cell-wall substance (Suleiman, 2011). The relationship between thermal conductivity, temperature and density of wood was introduced by Harada et al. (1998). MacLean (1941) studied the effect of moisture content on wood thermal conductivity and established general equations for the moisture effect. Joy (1957) stated that free water increases the conductivity much more than water vapor in cell lumens. Gu and Hunt (2007) observed and also used the relationship between thermal conductivity and moisture content when modeling a heat transfer in softwood. Kol (2009) measured the thermal conductivity of pine wood at 20°C and 8%, 12% and 22% of MC. The expected linear relationship was observed in the transverse directions. Gu (2011) stated that the increased moisture content raises the amount of water molecules in the wood matrix and the greater molecular mobility enables more energy to be transported.

Various composite products are manufactured from wood, as e.g. particleboard, fiberboard or plywood. Physical properties of wood composites are different than the properties of solid wood because of the additives and the manufacture processes, esp. densification, orientation of material axes (Kamke, 1989). Xie et al. (2011) measured the thermal conductivity of ultra-low density fiberboard (56.3 $kg.m^{-3}$) and found out that the conductivity is primarily determined by the size of voids. The heat conduction through the fibers in lightweight materials seems to be negligible (Gibson and Lee, 2006) in comparison with the conduction through the air trapped within the material (Kawasaki et

al., 1998). The investigation of thermal conductivity and moisture behavior of fiberboards was carried out by Brombacher et al. (2012). The correlation between density and thermal conductivity was obvious (light material leads to low thermal conductivity). The influence of moisture content and temperature on the thermal conductivity of corkboards measured by HFM was shown by Matias et al. (1997). The relationship between thermal conductivity and density of soft fiberboards was presented in the work of Sonderegger and Niemz (2012). Another work refers to the influence of different particle sizes on thermal behavior of wood-based materials (Sonderegger and Niemz, 2009). Lewis (1967) stated that the thermal conductivity of fiberboards is on average 35 percent below that of solid wood of the same density. Zhou et al. (2013) established the relationship between thermal conductivity and temperature of thin medium density fiberboards at different moisture contents. The thermal conductivity varied in a rather double-hump shape, which is different to the linear temperature-moisture regression of wood.

2.2. Heat and mass transfer in wood-based envelopes

Low-energy and passive houses occur more widely with the increasing demand for energy consumption minimization. The optimal choice of an energy-efficient construction with the minimum influence on environment is required. Wooden or wood-based houses are a favorable alternative for building industry even in countries with no long-standing tradition of using the wood as a construction material (Desta et al., 2010). Low-energy houses are known to outperform conventional buildings in terms of energy efficiency due to the heat recovery and thermal insulation of the house (Mlakar and Štrancar, 2013). Some studies also point out that buildings with wood frames would reduce green-house gas emissions and could also be a part of the cost-effective strategy (Nässén et al., 2012).

Energetic attributes of wooden buildings are mainly influenced by thermal bridges in constructional parts. Thermal bridges are parts of a building construction where the thermal resistance changes locally and causes a change of inner temperature and an increase in the heat flow. The concern about thermal bridges is underscored by the EU legislation esp. by the European standard EN ISO 10211:2007. In addition to the heat loss that occurs at thermal bridges, condensation problems may also occur (Totten and Pazera, 2009).

Thermal bridges generally occur at the connection of walls or wall and roof systems, nearby windows and doors or between heated and heatless building parts (Šubrt, 2005).

Simplified calculation methods exist for determining heat flows through linear thermal bridges which occur at junctions of building elements (EN ISO 14683:2007). There is also an experimental method for determining thermal bridges. The infrared detection, based on the measurement of infrared radiation density from the surface, enables researchers to record the temperature scale distribution. Infrared thermography of building envelopes can be used to detect heat losses, missing or damaged thermal insulation in walls and roofs, thermal bridges, air leakage and moisture sources (Balaras and Argiriou, 2002). A thermal bridge occurs where changing the heat flux results in a change of the inner (or outer) surface temperature. Bjarløv and Vladykova (2011) calculated the thermal resistance of detached and semi-detached wooden houses by means of European standard EN ISO 6946:2005. The thermo camera was used to locate air leakages during a blower-door test and to investigate thermal bridges in the building envelope. Wood and Weber (2003) discussed the ability of infrared (IR) camera to detect moisture by imaging the different temperatures of wet versus dry building materials. The detection of thermal defects caused by fasteners in contact with metal water pipes during the construction process using infrared thermography was introduced by Wood and VanBree (2006). Rosina and Robison (2002) used thermography to locate structural members, defects and moisture diffusion in wood-framed historical buildings (nineteenth- and twentieth- century balloon frames houses). Kato et al. (2007) calculated the average heat flux through a model wall by using the infrared camera for measuring the inner temperatures. Barreira and Freitas (2007) documented the applicability of thermography to study the behavior of building materials. The IR camera experiments included the visualisation of wetting and drying process of specimens, as water evaporation is an endothermic reaction inducing local surface cooling (Chown and Burn 1983; Chew 1998). Meinlschmidt (2005) explained the method of active thermography for detection of defects in wood and wood-based materials. The material (or constructional part) is heated with radiators which lead to a rise of the surface temperature. The speed of heat dissipation into the material depends on density, heat capacity and thermal conductivity of the material. A defect (or change in the structure composition)

creates a barrier for the heat transfer which causes a change of local temperature. Ludwig et al. (2004) stated that the active thermography seems to be the most effective investigative procedure on the moisture detection in wood as the high rates of water content highly modify the thermal parameters. López (2013) claimed that despite the potential of the IR technique, only a few authors evaluated timber structures. The current studies are limited to the detection of concealed wood or significantly deteriorated areas in buildings (see e.g. Wyckhuyse and Maldague 2011; Kandemir-Yucel et al. 2007; Plescanu et al. 2008; Spencer et al. 2008). Emissivity of the surface layer depends on temperature, wavelength and direction between thermo camera and the measured construction. Over the temperature range experienced by buildings, from -10º C to 60º C, the temperature dependence of the emissivity can be ignored (Bareira et al., 2012). Hart (1991) described the usage of emissivity of some building materials which can be assumed as a constant, for a certain temperature, being quantified considering the normal to the surface and all wavelengths. The atmospheric conditions, such as ambient temperature, wind effects and the relative humidity influence the temperature of the equipment and its performance (Balaras and Argiriou, 2002).

Thermal behavior of building envelopes can be also evaluated by numerical methods, besides the experimental ones. Kosny (1995) conducted three-dimensional simulations for several wood frame walls and included the effect of thermal bridges caused by envelope structural coupling details to the calculation of resistivity values. Desta et al. (2010) reported experimental data (temperature, humidity and air pressure) for numerical validation of heat, air and moisture (HAM) transfer through a light weight building envelope under real atmospheric conditions. Steskens et al. (2009) claimed that many of simulation models to predict HAM conditions in buildings assume homogenous and constant surface transfer coefficient for convective heat and moisture transfer. Bednar and Dreyer (2003) proved that the surface transfer coefficient is strongly dependent on the local air velocity. Using homogenous and constant conditions to the HAM transfer models, the calculation of building energy demands and consumption could be underestimated (Janssen et al., 2007). Labat et al. (2013) dedicated a study to validate specific coupled transfers (coupled heat and vapor transfer in the insulation part, a bi-dimensional effect induced by

ventilated cavity and air change rate under natural conditions) by measurements of HAM transfer in an experimental house. Deru et al. (2003) presented the results of three-dimensional finite element method (FEM) heat-conduction modelling of the whole building. Mackerle (2005) stated that the finite element method has become the most prevalent method used for analysing a variety of physical phenomena in wood and wood-based materials. Numerical simulation techniques provide relatively fast estimation of the heat and moisture performance of building parts with acceptable accuracy comparing to costly and time consuming experimental studies (Zhong and Braun, 2008). Gerlich (2011) developed a three-dimensional finite element model of a building wall in numerical software Comsol Multiphysics to simulate thermal construction responses in dependence on changing boundary conditions. The main purpose was the optimization of a heating system according to the heat energy accumulation in building walls. The thermal performance of a building depends mainly on a large number of factors summarised as design variables (dimensions of walls, roof, etc.), material properties (density, thermal conductivity, transmissivity, etc.) and weather data (ambient temperature, humidity, solar radiation, etc.). The inclusion of all affecting factors is hardly possible, therefore, HAM transfer models are usually simplified in some way.

The knowledge of the fundamentals of heat transfer and solar radiation helps to understand the underlying processes that take place in a building and its interaction with the external environment (Markus and Morris, 1980). All three heat transfer processes (conduction, convection and radiation) are possible between a building and the outer environment. Kosny et al. (2014) claimed that the thermal resistivity of a building part can be increased by applying thicker insulation in wall cavity, by improving thermal resistance of insulation materials, eliminating thermal bridges or applying airtight construction. On the other hand, some authors dealt with increasing the thermal resistance of a wall by applying air cavities as insulators. Multilayer thermal insulation (MTI) products which consist of thin insulating layers (an airspace) and thin reflective layers (e.g. aluminium foil or other materials with a low emissivity value) are nowadays subjected to a scientific debate (Mavromatidis et al., 2012). The thermal performance of such materials depends notably on the infrared radiative balance between reflective layers and other surfaces.

Radiation plays an important role in heat transfer through an air cavity as well as convection transfer. The dimensions of an air cavity (mainly its thickness) are decisive for the domination of the radiative part of the heat transfer. Mavromatidis et al. (2012) developed a numerical approach to determine the influence of an air gap thickness on the overall thermal performance of a composite wall. According to the results, the thickness of an air gap higher than 3 cm caused a reduction of the material resistance because of the convective heat transfer. The critical thickness of the air layer should be determined, as it identifies the beginning of natural convection, which represents a reduction in the insulating effect of the wall (Armando et al., 2010). Mahlia and Iqbal (2010) investigated the effect of air gaps included into the wall. In that study, the energy savings were calculated for air gaps of 2 cm, 4 cm and 6 cm between insulation materials. Heat transfer by convection was ignored, which makes the survey rather limited. Xie et al. (2014) dealt with the general numerical solution of heat transfer (conduction and convection) through an insulating wall with air gaps. For the specified number of air gaps, the maximal thermal resistance per unit volume decreases with an increase in the Rayleigh number. The Rayleigh number characterized the intensity of natural convection in air gaps. The maximal thermal resistance of the wall increases with an increase in air gaps, for the specified Rayleigh number. An increase in thermal resistance is not obvious when adding more air gaps at low intensity of convection. Such statements were approved by the work of Lorente and Bejan (2002) who studied the question of how to select the size of air cavities in wall for the purpose of maximizing the global resistance to heat transfer through the wall. Also other authors proved that the air gaps placed within the wall reduce the heat flux markedly, see e.g. Al-Sanea and Zedan (2011), Al-Sanea et al. (2003) and Tsilingiris (2006).

2.3. Heat transfer modelling and optimization tasks in FEM applications

Optimization methods used in building energy modelling are useful tools for energy loss reduction (Heibati et al., 2013). Numerical models dealing with optimization of the whole building are complex and challenging tasks integrating heating, ventilation and air conditioning modeling. The computational fluid dynamics (CFD) programs are needed to provide complementary information essential for the evaluation of building thermal

performance (Zhai and Chen, 2006). Saber et al. (2011) used the finite element method (FEM) to conduct three-dimensional numerical simulation of a wall system with an airspace and low emissivity foil material. Conductive, convective and also radiative heat transfer equations (surface-to-surface radiation) were solved in the model. Results of this study showed that a wall with low emissivity foil can increase the thermal resistance of the wall remarkably. The factual value of thermal resistance improvement depends on materials used to create the wall system. In 1992, Arasteh et al. stated that the finite-element method had begun to be used within the window and building envelope industries to evaluate two-dimensional heat transfer effects. To do so, thermal behavior of building materials in a wide range of temperatures and moisture contents was needed. Labans et al. (2012) created the finite element (FE) model of a sandwich panel composed of MDF surface layers and Dendrolight core to verify its thermal properties with the experiments at hot box testing equipment. Commercially available FE software ANSYS was used for the simulation task. Authors used isotropic wood and also air properties, as the Dendrolight core is composed of glued spruce wood profiles in perpendicular angles which create air gaps. Many numerical models have been reported to help in predicting the influence of the process parameters on the final product. Heat and mass transfer models for medium density fiberboard during hot pressing process were developed by e.g. Humphrey and Bolton (1989), Carvalho and Costa (1998), Dai and Yu (2004), Kavazović et al. (2012) and others. A model for heat and mass transfer during continuous pressing of oriented strand board (OSB) was introduced by e.g. Fenton et al. (2003), Lee et al. (2006). The probabilistic and sensitivity analyses can also be applied to validate the numerical models (Domínguez-Muňos et al., 2009). As the data involved in the model are usually not known perfectly, the uncertainty of the thermophysical properties of materials should be taken into account. Due to the uncertainties in the model it is also uncertain how the numerical simulation matches reality (Čermák and Trcala, 2012). The probabilistic analysis can give an overview of e.g. the thermal response of a material within a variable range of input thermal parameters. The measuring or production process can be then optimized in respect to the probable results of the analysis.

3. Material and methods

3.1. Heat flow meter method

The heat flow meter (HFM) measuring method is based on the principles described by the following international standards: ASTM C518, ISO 8301, DIN EN 12667. A specimen (material or composed structure) is placed between two heated plates and pressed with a certain pressure to ensure the minimum and uniform contact resistance. The heat flow is created by a user-defined temperature difference between the hot and the cold plate. The plate temperatures are controlled by bidirectional Peltier systems which are coupled with a closed loop fluid flow driven by a forced air heat exchanger (see Paper IV. Fig 1). The heat flow transducers record a signal (in Volts) which is proportional to the heat flux through the sample. Thermal conductivity is calculated once the user-defined equilibrium criteria are met. By measuring the temperature difference across the thickness of the sample, thermal conductivity can be determined by the following equations:

$$q = \lambda . A . \frac{\Delta T}{\Delta x} \tag{1}$$

$$\lambda = N . \frac{\Delta x}{\Delta T} = \frac{\Delta \mathrm{x} . (q_{upper} + q_{lower})}{2 . \Delta T} \tag{2}$$

where "q" is the heat flow [W] for upper and lower plate; "λ" the thermal conductivity [$W.m^{-1}.K^{-1}$]; "A" the area [m^2]; "ΔT" the temperature difference [K]; "Δx" the thickness of the sample [m]; "N" the calibration factor [$W.m^{-2}$].

The HFM device has to be calibrated before measurement with a certified reference standard of known thermal conductivity (e.g. fiberglass board NIST 1450b). The calibration establishes the correlation between the signal output of the transducers and the actual heat flow. Equilibrium parameters are met during the measurement (maximum error of equilibrium in the averaging period is recorded). The tolerance set-up of temperature offset allows to reach an accurate mean temperature. The range of temperatures from -20°C

to +60°C can be reached at the HFM 436 Lambda by Netzsch company. The higher the mean temperatures and temperature differences, the more time is needed for reaching the equilibrium. Use of the HFM method required considering of several factors. The initial conditions has to be taken into account, therefore stable conditions in the lab environment were provided (about 35°C and 30% RH). The air lowers its temperature below zero during the measurement and reaches its saturation point. The condensation of water occurs and after some time ice covers the lateral sizes of the device. Freezing of water consequently prolongs the measurement time and negatively influences thermal conductivity evaluation. Also, the size of a sample is usually not perfectly 600 x 600 mm which allows for small air distribution across the sample.

Measurements of samples conditioned at a high relative humidity are also possible. The only problem is keeping stable moisture content of a sample until the thermal equilibrium is reached. Samples were wrapped in the foil and measured with it. The changes in moisture content were gravimetrically determined after each measurement. It was proved that the moisture losses are insignificant as well as the foil impact on the final thermal conductivity value. Redistribution of moisture inside the sample during measurement is possible in terms of Fick´s or Darcy´s law and it depends mainly on the structure of the material and the temperature difference between plates. The higher are temperature changes, the more non-uniform is MC distribution. The foil cover also provides protection against air movement within the material, e.g. when measuring some structures with air cavities.

The higher possible measured sample size (600 x 600 mm) is one of the advantages of this device as it enables measurement of composed structures. The measuring surface is the area of 300 x 300 mm at the middle of the sample. The remaining parts serve for the temperature stabilization and creation of a uniform temperature field in the samples center. It is also possible to measure a sample with just the 300 x 300 mm size, but the rest space of HFM chamber must be created by a frame from insulation material with lowest possible thermal conductivity (e.g. certified fiberglass board). Higher thickness of the sample (up to 200 mm) allows for the measurement of various building material compositions, e.g. sandwiches.

3.2. Quasi-stationary measuring method

The quasi-stationary method evolved out of principles described by Clarke and Kingston (1950) and Krisher and Esdorn (1954). Požgaj et al. (1997) developed a measuring device based on this method. Three thermal parameters (thermal conductivity, thermal diffusivity and specific heat capacity) can be calculated based on the temperature recording in time. The apparatus is composed of eight samples interspersed with a NiCr foil which produces heat. The temperature rise in the center of two middle samples is recorded with a thermocouple. The scheme of the apparatus, the theoretical background and also an analytical solution are described more widely in Paper II. Fig 2.

As other measuring processes, the quasi-stationary device is limited in a way. The temperature around samples is dependent on ambient temperature changes. The heat transfer coefficient causes the heat losses through the lateral surfaces. With an increasing thickness of the sample the influence of heat transfer through lateral parts increases (at the constant width and length). An appropriate ratio between width and thickness of a measured sample reduces those lateral heat losses. The sample size is additionally limited by the possible size of heated foil. Further, the measuring time should last ideally as long as the third (nonlinear part) occurs to allow good interpolation of temperature curve in time. The heat flow, the slope of the line and the absolute term of the line equation are needed to calculate the three parameters using the following equations:

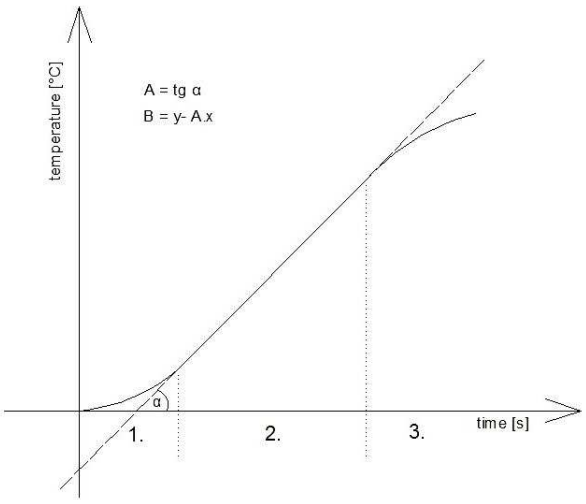

$$a = \frac{d^2.A}{6.B} \quad [\mathrm{m^2.s^{-1}}] \tag{3}$$

$$\lambda = \frac{q.d}{6.B} \quad [\mathrm{W.m^{-1}.K^{-1}}] \tag{4}$$

$$c = \frac{q}{\rho.d.A} \quad [\mathrm{J.kg^{-1}.K^{-1}}] \tag{5}$$

where "a" is the thermal diffusivity [$m^2.s^{-1}$]; "λ" the thermal conductivity [$W.m^{-1}.K^{-1}$]; "c" the specific heat capacity [$J.kg^{-1}.K^{-1}$]; "d" the thickness of the sample [m]; "q" the heat flux [$W.m^{-2}$]; "ρ" the density [$kg.m^{-3}$] and parameters of the curve "A" in [$K.s^{-1}$] and "B" in [K].

3.3. Pulse transient method

The pulse transient method is based on measuring the temperature response of a sample heated by a certain heat flow caused by an electric pulse. The thermophysical parameters (the specific heat, thermal diffusivity and thermal conductivity) are calculated from the characteristic features of the curve measured by the thermocouple (the time t_{max} at the maximal thermal response and the magnitude of the temperature response T_{max}, see equation 11 and 13). The analytical solution is described in Paper III. The heat pulse is generated by a plane heat source (thin metallic foil) placed on the lower side of a sample. A thermocouple is inserted on the upper side of the sample. The measured specimen is then sandwiched between two other samples of the same material, see Figure 1. The thermal paste can be used at all connected surfaces to ensure low thermal resistance between them.

The specimen temperature and the specimen surroundings are controlled through heat exchangers by a thermostat. A specimen characterization (thickness and density), description of experimental parameters (size and shape of the heat source) and measuring parameters (value of the electric current, heat pulse duration, stabilization time and the total time of measurement) are needed for the experiment. The values of electric voltage and the temperature in time are recorded. The measurement process runs in sequences. Each sequence is composed of the stabilization time when the temperature of the measured sample is being set up. Heat pulse is generated to the sample after the stabilization is finished. The total time of the measurement then includes the stabilization time and the time of the actual temperature response recording. A few consecutive sequences can be arranged. The right choice of these parameters depends upon the measured material and its thermal properties. Good conductors would need higher heat flux generated by the heat pulse. An example of the experimental set-up is presented in Table 1.

Table 1 Experimental set-up for some measured materials at RT-Lab device

MATERIAL	density [kg.m^{-3}]	λ [W.m^{-1}.K^{-1}]	t_{pulse} [s]	I [A]	q [W.m^{-2}]	size [mm]
cork	119	0.05	5	0.8	1399	40x40
beech wood	741	0.24	12	1.2	3270	40x40
MDF	761	0.13	30	2.5	2187	100x100

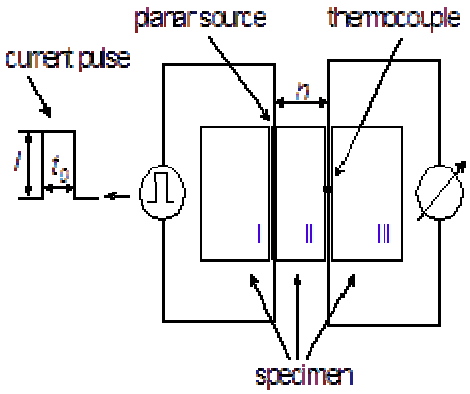

Fig 1. Scheme of the RT-Lab device based on pulse transient method (Boháč et al., 2012)

The experiment should be performed as near to an ideal model (see Figure 2) as possible to reach reliable data. Any deviation from ideal model influences the measuring process and causes data shift. Further, correction factors have to be used to obtain reliable data (Boháč et al., 2012). The ideal model assumes limited influence of heat losses from specimen surfaces and negligible heat capacity of the heat source compared to the sample. The demands for reliable data measurement are as follows:

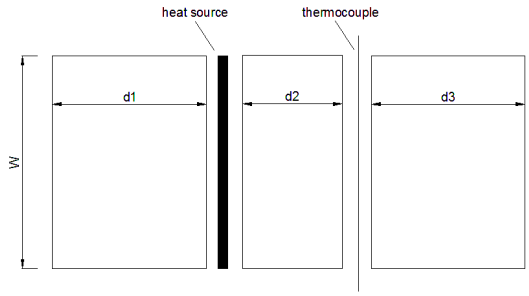

$$d_2 < 0,2W \quad (6)$$

$$d_{1,3} > 1,4d_2 \quad (7)$$

$$t_{pulse} < 0,1t_{\max} \quad (8)$$

Fig 2. Criteria of the ideal model (d – thickness [m]; W – width [m]; t_{puls} – pulse duration[s]; t_{max}-time of the measurement [s])

The ideal model accounts for infinite sample size as well as perfect thermal contacts between samples. The analytical solution for the temperature response on the heat pulse generated by the planar heat source is as follows (Štefková, 2011):

$$\Delta T(x,t) = \frac{UIt_{puls}}{2c\rho\sqrt{\pi at}} \exp(-\frac{x^2}{4at}) \tag{9}$$

The real set-up of the experiment is influenced by many factors. The deviations from the ideal model are caused by:

- the heat transfer through lateral surfaces (the heat transfer coefficient describing the heat exchange between the sample and surrounding atmosphere lowers the temperature response)

- the thermal resistance of the heat source (decreasing of the pulse total energy is caused by the real thickness of the heating foil as well as its thermophysical parameters)

- additional thermal resistances between contact surfaces (samples contacts with the platens of the heat exchanger)

The influencing factors are possible to implicate in the boundary and initial conditions of the experimental set-up. The analytical solution of the temperature field and furthermore of the thermophysical parameters including disturbing factors are as follows (Štefková, 2011):

$$T(x,y,z,t) = T_i(Q,x,y,z,t)\, f_t(Q,x,y,z,t....) \tag{10}$$

$$c = \frac{UIt_0}{\sqrt{2\pi\,\mathrm{e}}\rho d\Delta T_{\max}} f_t \tag{11}$$

$$\lambda = ac\rho \tag{12}$$

$$a = \frac{d^2}{2t_{\max}} f_t \tag{13}$$

The correction function "f_t" for temperature "T_i" describes the deformation of temperature field caused by the sum of all influencing parameters:

$$f_t = \frac{t_{\max}}{t_0 - 1} \ln\left(\frac{t_{\max}}{t_{\max} - t_0}\right) \tag{14}$$

where "a" is the thermal diffusivity [$m^2.s^{-1}$]; "λ" the thermal conductivity [$W.m^{-1}.K^{-1}$]; "c" the specific heat capacity [$J.kg^{-1}.K^{-1}$]; "d" the thickness of the sample [m]; "U" the voltage[V]; "I" the electric current [A]; "ρ" the density [$kg.m^{-3}$]; "t_0" the time of thermal impulse [s], "T_{max}" the maximum of temperature [K] and the correction function "f_t" [-].

3.4. Infrared thermography

Infrared detection is based on the measurement of infrared radiation density from the surface. The distance from the measured construction part, atmospheric temperature, relative humidity and emissivity of materials are the most influencing factors during the measurement. The larger is the distance from thermo camera to the construction, the more the emitted heat is absorbed by the surroundings. The thermogram (recording equipment) displays the temperature scale distribution of the thermal scan documented as a picture. The purpose of measuring is then the determination of the object temperature from the detected infrared radiation, which can be established using the following equation, (Barreira and Freitas, 2004):

$$R_{\text{det}} = \int_{\Delta\lambda} \rho_a(\lambda) \frac{dR(\lambda, T_a)}{d\lambda} . \mathrm{d}\lambda + \int_{\Delta\lambda} \varepsilon_0(\lambda) \frac{dR(\lambda, T_0)}{d\lambda} . \mathrm{d}\lambda \tag{15}$$

where "R_{det}" is the detected radiant exitance [$W.m^{-2}$]; "λ" the wavelength [µm]; „$\frac{dR(\lambda,T)}{d\lambda}$" the spectral radiant exitance [$W.m^{-2}.nm^{-1}$]; "ρ" the reflection factor [-] and "ε" the surface emissivity [-].

Infrared thermography (via thermocamera FLIR S65) was used to detect thermal bridges in Paper VI. The results of infrared measurements are analyzed by the Therma CAM™ Researcher software. A histogram and a diagram describing the temperature distribution of

a few lines situated on the thermal scan are required for the evaluation. The histogram is a graphical representation showing the distribution of temperatures of the thermal scan in a specific location which enable us to figure out the temperature distribution. The possibility of temperature measurement by thermo camera FLIR S65 ranges from -40° C to +120° C. Each image obtained by an IR detector gives the temperature of each pixel hit by the radiation emitted from the examined object, so defining the entire thermal field of the area is covered by the detector optic.

The thermal scan of an object depends on the heat transfer between the surface and the surroundings. If there are no external heat sources, the surface temperature of a building element is a function of temperature difference between the inside and the outside environments and the heat resistance of the various layers. Emissivity of the surface layer depends on temperature, wavelength and direction between thermo camera and the measured construction. The atmospheric conditions, such as ambient temperature, wind effects and the relative humidity influence the temperature of the equipment and its performance. To avoid all influencing factors during measurement, the night scanning in the inner side of building is recommended. The surrounding temperature and emissivity of scanned surfaces is needed.

3.5. Numerical modeling in ANSYS software

Numerical modeling widely uses engineering simulation software based on some variational methods which allow solutions of a variety of multiphysics phenomena in complicated domains. Those programs use discretization methods to find an approximate solution of the calculated problem. The finite element method (FEM) is used in ANSYS Mechanical APDL and ANSYS Workbench platform. FEM is a generalized Ritz-Galerkin method which consists in sequential discretization of the solved task (Kolář and Němec, 1997). The finite volume method (FVM) enables very effective solving of partial differential equations in ANSYS CFX program dealing mostly with fluid flow problems.

FEM relies on the decomposition of the domain into a finite number of subdomains - elements for which the approximate solution is constructed by applying the variational or weighted residual method (Madenci and Guven, 2006). The general procedure of the

thermal analysis in ANSYS software consists of 1) pre-processing (creating geometry, material description and assignment, meshing and applying boundary conditions), 2) solution (solving selection of equations at defined nodes) and 3) post processing phase (evaluation of the heat flux and temperature fields), (Moaveni 2008). On the contrary, FVD uses the decomposition of the domain into the finite number of control volumes in which the differential equations are assigned. As the ANSYS CFX preprocessor does not enable creation of geometry or the FE model, the solver environment uses a previously created node database which is then transferred onto a finite volume mesh. The accuracy of calculated results is generally influenced by the mesh size. On the other hand, mesh refining requires higher hardware capacity of the computer and prolongs computational time significantly. With increasing mesh refinement (increasing number of nodes) in the fluid part of the model, the numerical solutions converge more probably. Convergence of the solved task is a significant factor in numerical modeling, as it points out the ability to find a solution at given parameters. Modeling usually implies approximating of the geometry, material properties and heat transfer equations (Martínez, 1988). Simplification of material properties (e.g. isotropic, independent on temperature or moisture content) introduces uncertainties in the model. An optimal choice of the solution method, mesh size and simplification of the solved task is always needed. The ANSYS CFX software was used for comparative study of heat transfer in horizontal air cavity, see Paper V.

The ANSYS FLOTRAN finite element package enables to compute conjugate heat transfer problems dealing mainly with two-dimensional or three-dimensional fluid flow fields. This part of the ANSYS Mechanical APDL software was used to calculate heat flow in an air enclosure subjected to all three heat transfer modes. In the fluid, the conservation equations for viscous fluid flow and energy are solved. The interaction between solid and fluid part is also possible. The same element (FLUID 141 for 2-D analysis or FLUID 142 for 3-D analysis) is assigned to the fluid and also to the non-fluid parts, which differ only by the material number. The connected mesh then enables mutual interaction between parts. In the non-fluid region, only the energy equation is solved. A segregated sequential solver algorithm is used meaning that each of the governing equation for each degree of freedom is solved separately and then coupled together in sequences.

Parametric models were introduced where iterative approach was necessary. The Ansys Parametric Design Language (APDL) was used to create the parameterized macro files, which contain the APDL commands for whole the modeling process from preprocessing to postprocessing. Stationary and transient conduction, convection and radiation tasks were solved using the FEM. Macro files are listed in the attachment of the thesis (Annex 1 to Annex 4). The Probabilistic Design System (PDS) was used for the sensitivity analyses. The relations between input and output variables are possible to calculate based on the probabilistic analysis. The input parameters (material properties, geometry or parameters of the analysis as the time step or mesh cize) are randomly sampled according to the Monte Carlo method. The range of these input parameters is described by Gaussian distribution. The range of distribution is defined by average value of the parameter and the standard deviation. The whole analysis (creating models with randomly sampled parameters, solving the problem in high count of cycles, evaluation of results) is repeating in the PDS file according to the repetition rate. The correlation matrix with the relations between input and output parameters is one of the main results of the probabilistic analysis. Values of Spearman´s correlation coefficient close to number “1” show high correlation between parameters in a positive or a negative way. The correlation between randomly sampled input variables is convenient in some cases (e.g. for description of the dependence of thermal conductivity on density or the relation between thermal conductivity parallel and perpendicular to the grain).

4. Paper I.

Quasi-Stationary Measurements of Lignamon Thermal Properties

Eva Troppová,[a] Jan Tippner,[a] Richard Hrčka,[b] and Pavol Halachan[b]

BioResources 8(4), pp. 6288-6296

a: Department of Wood Science, Mendel University in Brno, Czech Republic
b: Department of Wood Science, Technical University in Zvolen, Slovakia

Abstract

Thermal properties of wood and modified wood-based materials are important parameters that influence the manufacturing process and final industrial utilization. The aim of this work was to investigate three main thermal properties (thermal conductivity, thermal diffusivity, and specific heat capacity) of ammonia-treated compressed beech wood (Lignamon material) and natural beech wood (*Fagus sylvatica*).These properties were measured based on the quasi-stationary method developed at the Department of Wood Science at the Technical University in Zvolen. The influence of increased density (caused by ammonium treatment and compression) of four different types of Lignamon material on the thermal properties was discovered, and the results were compared with those from untreated beech wood. The results confirmed a dependency on the density of the material. With increasing Lignamon compression rate (increasing density value), the thermal conductivity increases and the thermal diffusivity decreases. The maximum value of thermal conductivity reached Lignamon 6k (0.26 $W.m^{-1}.K^{-1}$ by 1070 $kg.m^{-3}$) and 7n (0.26 $W.m^{-1}.K^{-1}$ by 950 $kg.m^{-3}$).

Keywords: Lignamon; Thermal conductivity; Specific heat capacity; Thermal diffusivity; Quasi-stationary method

4.1. Introduction

The substitution of improved domestic species for unavailable high-grade tropical wooden species has led to progress in modification processes. The current state of applied wood modifications is described in the work of Hill (2006) and Rowell (2006). Modifications of wood from local sources are still very topical (Hill 2011, Esteves and Pereira 2009), and the use of modern technologies enables outdated ideas to become more prevalent, efficient, and environment-friendly. Wood modification has been viewed as the right approach to achieve the desired properties of wood with a minimum of expended energy and materials.

Interestingly, ammonia-treated wood was developed in Czech lands in the early 1960s (Czerny and Valasek 1974, Berzins 1972, Davidson and Baumgardt 1970, Kalnins et al. 1967, Pandey et al. 1991). This material is called Lignamon, a compressed beech wood modified by ammonium. The technological process is composed of four basic steps. First, untreated beech wood with a high moisture content (18 ± 3%) is heated to a maximum of 103 °C. Second, the sample is plasticized using ammonia steam. The process of modification is discontinuous. Then, the sample is compressed within the range of 0.8 to 1.3 MPa. The higher the pressure is, the denser the final Lignamon sample is. After disposing of the spare nitrogen from the modified sample, the drying and stabilization procedures are performed. Lignamon exhibited higher durability and density and darker colour, as recently reported by Weigl et al. (2009, 2012). Lignamon has been used in mechanical engineering, furniture, and musical instrument production. Lignamon can also be used for many other purposes: it can be used as a substitute for imported tropical wood, alloys, and plastics, and as material for handgrips, shafts, flooring, and bearing surfaces (Sedliačik 1998).

The properties of Lignamon are primarily based on the properties of raw wood material (*Fagus sylvatica* L.) and its technological processing. The process of transforming the native material into Lignamon influences the density, mechanical properties, and appearance (Stojčev 1979). The least mentioned and examined properties of Lignamon are thermal conductivity, thermal diffusivity, and specific heat capacity.

There are two different methods (stationary and non-stationary) for measuring the thermal properties of materials; these methods have been described by many authors. The thermal conductivity measurements of beech wood with the stationary method (guarded hot plate) were carried out by Niemz et al. (2010), MacLean (1941), Skaar (1988), and others. The wood species itself has no important effect on thermal conductivity, which means that data from other sources for almost any species with a known specific gravity can be compared (Steinhagen 1977). The unsteady state method was used to obtain all three thermal properties of different wooden species. Hrčka (2010) employed a method that contacted air at the beech wood surface to establish the thermal properties. Transient measurements of thermal conductivity and thermal diffusivity using the plane source technique on hardwood samples were introduced by Suleiman et al. (1999). Kühlmann (1962) investigated the thermal properties of spruce, oak, and beech with the Krischer and Esdorn apparatus. A nonsteady-state heating device was used to determine the thermal properties of larch (Chudinov and Stepanov 1971).

The quasi-stationary method employed in this work was developed at the Department of Wood Science at the Technical University in Zvolen (Požgaj et al. 1997). The method is based on two principles described by Clarke and Kingston (1950) and Krisher and Esdorn (1954). Quasi-stationary is defined as resembling stationary conditions resulting from the linear part of temperature measurement needed for the evaluation of thermal properties.

The main goal of this article was to establish the thermal properties (thermal conductivity, thermal diffusivity, and specific heat capacity) of Lignamon material and untreated beech wood (UB) using the quasi-stationary method. The specific objectives were as follows: a) to investigate the influence of increased density (measured by X-ray densitometer) of Lignamon on the thermal properties, and b) to establish the accuracy of the measuring method and compare the results for native beech wood with the available literature sources.

4.2. Material and Methods

There are two main parts to our research: a) material preparation, evaluation of density profiles, air conditioning of samples, and experimental measurements of thermal properties;

and b) the processing of data according to the least squares method using a macro written in Excel (Hrčka and Babiak 2012).

Four different types of Lignamon samples were cut from massive blocks (Lignamon 6k and 7n) or thin planks (Lignamon 24 and 25) with approximate dimensions of 50 x 50 x 8 mm (width x length x thickness). The wood fiber directions are longitudinal in width, radial in length, and radial-tangential in thickness. Thermal properties were measured in the direction of heat flow, which is the radial-tangential direction for all samples. Samples of Lignamon 6k and 7n were highly pressed (compression rate of 38 %) during the modification process and therefore reached higher densities and darker colors. Lignamon 24 and 25 were made of varnished floor parquets and have brighter colors. Eight samples were made from each type of Lignamon. Next, eight samples of untreated beech (UB) wood were prepared to compare the thermal properties of Lignamon with unmodified wood samples. An X-ray densitometer (X-RAY Dense-Lab, Germany) was used to scan all samples with a scanning step length of 0.01 mm. An average density profile from each type of sample was established. All 40 samples were conditioned under 20 °C and a relative humidity of 65% in a Sanyo MTH 2400 air chamber to reach the equilibrium moisture content.

The non-stationary method (quasi-stationary) is based on the evaluation of temperature changes in measured samples. The theory's background lies in solving the heat transfer equation with specific boundary conditions (constant heat flux on the upper surface of the measured sample, zero heat flow in the middle of the apparatus reached due to the sample's symmetry, and a constant temperature in the whole sample) (Fig. 1). The apparatus is composed of eight samples that are alternately interspersed with NiCr thin foil (0.01 mm) to produce heat. The block of samples is insulated by polystyrene and pertinax on both sides of the apparatus. A rise in temperature was measured in the middle of the samples and was recorded with a thermocouple and a computer (Požgaj et al. 1997; Hrčka and Babiak 2012). The average heat flux generated by the heat source and entering the samples through the thin foil was in the range of 957 to 1052 W/m^2 at different measurements. Together, 13 different sample arrangements of each material type were measured. Thermal properties were established as approximate values of two samples placed in the center of the

apparatus, between which the temperature sensor was placed. After each measurement, the two middle samples were changed and their average densities and thermal properties evaluated.

The data from the measurements are illustrated as a curve and describe the temperature increase in time in the center of the middle sample (Fig. 2). There are two nonlinear parts of the curve. One is at the beginning (caused by the sum of infinite series), and the other is at the end of the measurement (caused by heat loss through lateral surfaces). The middle part is linear, as is the temperature increase with time. The thermal properties were calculated by interpolation of the curve using the theoretical line (programmed in Visual Basic for Applications).

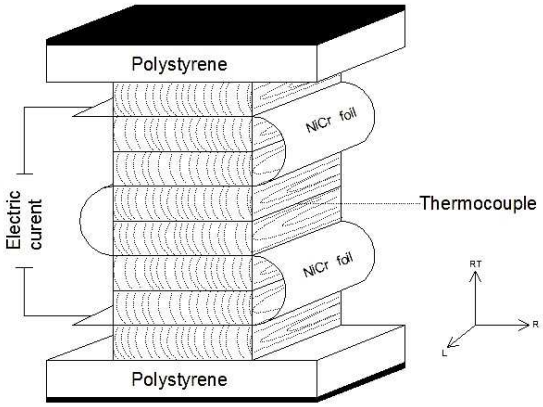

Paper I. Fig 1 Scheme of the apparatus

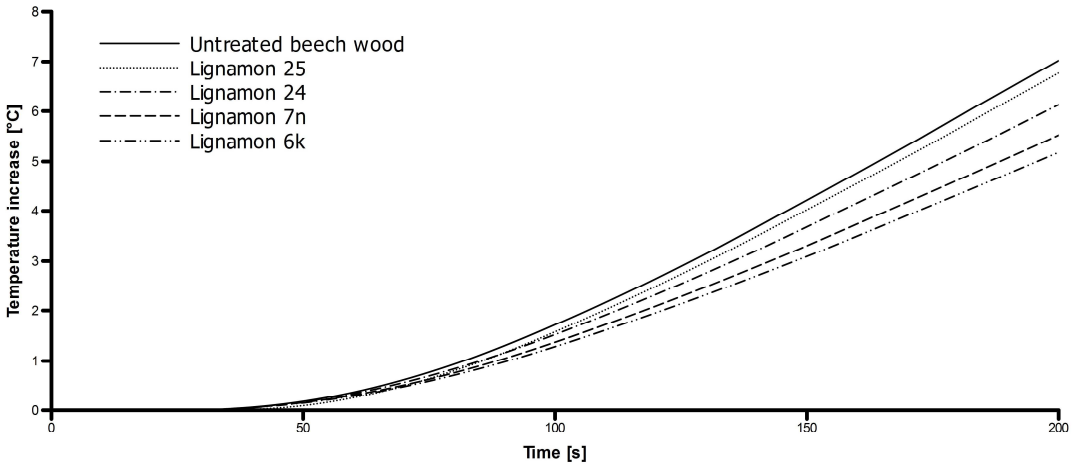

Paper I. Fig 2 The temperature increase between central samples recorded by a thermocouple

4.3. Results and Discussion

Density profiles of all samples reached almost uniform distribution, with no large fluctuations. Only Lignamon 25 exhibited a slight decrease in density in the middle of the samples. X-ray densitometry results are shown in Fig. 3. The lower density values from surface layers with depth of 0.1 mm are caused by the roughness and non-flatness of surfaces. This so called edge effect originates during preparation of samples and influences the scanning process. The differences between microstructure of untreated beech wood and compressed Lignamon are shown in Fig. 4. The densification process causes deformation of the wood structure, especially buckling from fibers and change in growth rings orientation.

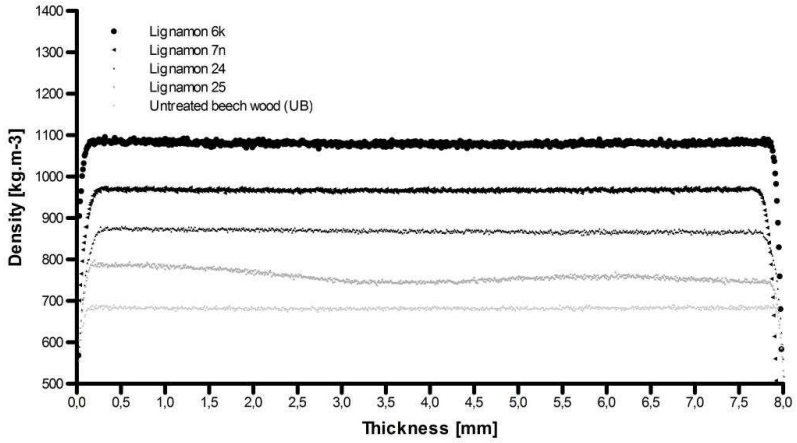

Paper I. Fig 3 Average density profiles of all samples (mean coefficients of variation in %: Lignamon 6k- 1.8; Lignamon 7n- 3.4; Lignamon 24- 2.0; Lignamon 25- 2.8; UB- 1.6)

Paper I. Fig 4 Microstructure pictures of untreated beech wood (on the left side) and Lignamon (on the right side); magnification of approximately 100x

The thermal conductivity, thermal diffusivity, and specific heat capacity were derived from the measurements based on the quasi-stationary method. The results are presented in Table 1. The measured data confirm the dependence on density (compression rate of ammonium-treated samples), see Fig. 5. In general, thermal conductivity increases as the density, moisture content, or temperature of the wood increases (see Kühlmann 1962). The more the Lignamon samples were pressed (Lignamon 6k and 7n), the higher the density and thermal conductivity value were. However, the dependence of thermal diffusivity on the density value follows an inverted trend. The specific heat capacity of wood is practically independent of density, which is confirmed by our measurement. The average equilibrium moisture content (7.8 % with standard deviation 0.5) of all measured samples was established according to the gravimetric method.

Paper I. Table 1 Mean Properties of Samples Measured in the Radial-Tangential Direction

Property	**UB (untreated beech wood)**	**Lignamon 25**	**Lignamon 24**	**Lignamon 7n**	**Lignamon 6k**
ρ [kg.m^{-3}]	675 (4.5)	753 (11.7)	857 (8.0)	950 (18.9)	1070 (9.4)
λ [W.m^{-1}.K^{-1}]	0.21 (0.05)	0.21 (0.07)	0.25 (0.04)	0.26 (0.06)	0.26 (0.05)
a [10^{7} m^{2}.s^{-1}]	1.2 (0.2)	1.2 (0.2)	1.2 (0.2)	1.1 (0.2)	1.1 (0.1)
c [J.kg^{-1}.K^{-1}]	2632 (272)	2350 (395)	2397 (212)	2519 (314)	2244 (234)
Mean: density (ρ), thermal conductivity (λ), thermal diffusivity (a), and specific heat capacity (c) for 7.8% of EMC; the values in parentheses describe the standard deviation of measurement					

The results for untreated beech wood exhibit the lowest value of thermal conductivity (0.21 W.m^{-1}.K^{-1}) and the highest value of specific heat capacity (2632 J.kg^{-1}.K^{-1}). Lexa et al. (1952) published a thermal conductivity value of 0.19 W.m^{-1}.K^{-1} of *Fagus sylvatica* within the density range of 700 to 1000 kg.m^{-3}. The thermal conductivity (0.18 W.m^{-1}.K^{-1}) of American beech at 12% moisture content with a density of 680 kg.m^{-3} is published also in Simpson and TenWolde (1999). The value of 0.173 W.m^{-1}.K^{-1} in the radial direction and 0.170 W.m^{-1}.K^{-1} in the tangential direction for *Fagus* with a density of 684 kg.m^{-3} was reported by Požgaj et al. (1997). The differences between thermal conductivity values available in the literature and our measured data can be caused by the relatively high

variation coefficient (21%) (Fig. 5), primarily resulting from the variability of the density between samples, as well as by the measurement method itself (the influence of heat loss through the lateral surfaces and of a leak between central samples where the sensor was placed), sample preparation methods, or technological process deviations.

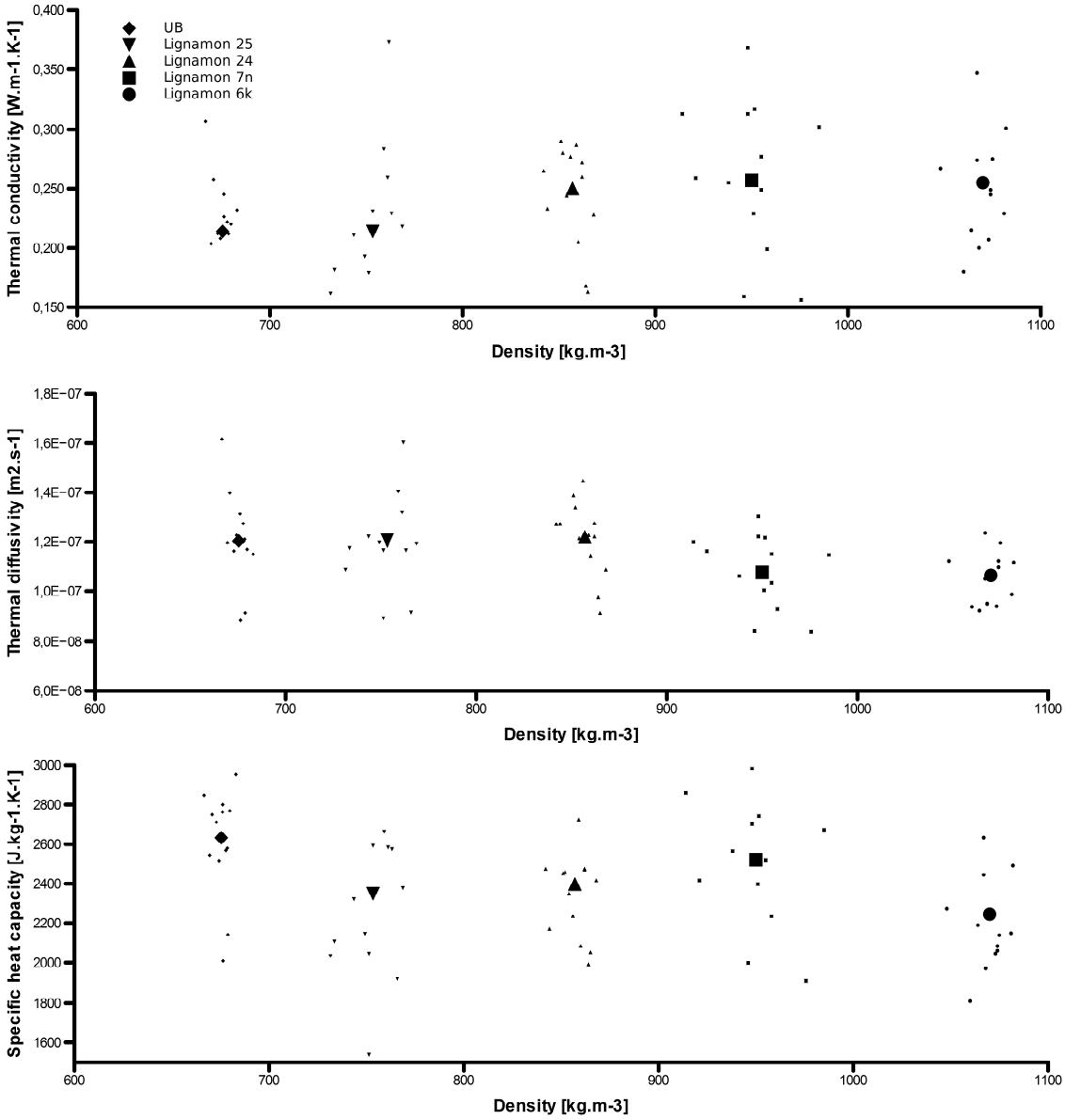

Paper I. Fig 5 Dependence of thermal properties on material densities: top: thermal conductivity dependence (λ [W.m^{-1}.K^{-1}]); middle: thermal diffusivity dependence (a [m^2.s^{-1}]); bottom: specific heat capacity dependence (c [J.kg^{-1}.K^{-1}]

4.4. Conclusions

The test analysis proved that there are statistically significant differences between the results of all the measured properties of modified and native beech wood. For instance, the thermal conductivity of Lignamon 6k (density 1070 kg.m^{-3}) and 7n (density 950 kg.m^{-3}) was 23.8% higher on average than that of UB (density 675 kg.m^{-3}), which should have a practical impact on the use of modified material, *e.g.*, in the case of flooring and heating.

The results indicate that the well-known ascending character of thermal conductivity and a descending one for diffusivity are dependent on the density in a moist environment, see Požgaj et al. (1997).

The maximum value of thermal conductivity was found in Lignamon 6k (0.26 W.m^{-1}.K^{-1} by 1070 kg.m^{-3}) and 7n (0.26 W.m^{-1}.K^{-1} by 950 kg.m^{-3}). The thermal conductivity of the samples increased with increasing density (increasing compression rate of Lignamon).

The minimum value of specific heat capacity (2244 J.kg^{-1}.K^{-1}) was found in Lignamon 6k with the highest thermal conductivity value (0.26 W.m^{-1}.K^{-1} by 1070 kg.m^{-3}). Our measurement proved the independency of specific heat capacity on density.

A higher value of a measured data variation coefficient (ranging from 8.7 to 31%) was caused by the natural variability of the wood material increased by the modification processes as well as by the measuring method itself.

Acknowledgements

This article is supported by the project “The Establishment of an International Research Team for the Development of New Wood-based Materials” Reg. No. CZ/1.07/2.3.00/20.0269. This work was also supported by the Slovak Research and Development Agency under contract No. SK-CZ-0045-11 and by the Ministry of Education, Youth, and Sports of the Czech Republic under contract No. 7AMB12SK077.

4.5. References

Berzins GV (1972) *Wood plastic coating as a way of increasing quality, material substitution*, Holztechnologie 13(2): 103-109.

Chudinov BS, Stepanov VI (1971) *Experimental investigation for determination of the thermal properties of wood and wood-based materials*, Holztechnologie 12(3): 154-159.

Czerny R, Valasek V (1974) *Lignamon a new pattern material*, RussCastProd 12(1): 506-507.

Clarke LN, Kingston RST (1950) *Equipment for the simultaneous determination of thermal conductivity and diffusivity of insulating materials using a variable state method*, Austr. J. of Appl. Science 1(2): 172-187.

Davidson RW, Baumgardt WG (1970) *Plasticizing wood with ammonia – A progress report*, Forest Prod. J. 20(3): 20-24.

Esteves BM, Pereira HM (2009) *Wood modification by heat treatment: A review*, BioResources 4(1): 370-404.

Hill CAS (2006) *Wood Modification: Chemical, Thermal and Other Processes*, Wiley, Bangor, Wales.

Hill CAS (2011) *Wood modification: An update*, BioResources 6(2): 918-919.

Hrčka R (2010) *Wood Structure and Properties*, J. Kúdela and R. Lagaňa (eds.), Arbora Publishers, Slovakia.

Hrčka R, Babiak M (2012) *Some non-traditional factors influencing thermal properties of wood*, Wood Research 57(3): 367-374.

Kalnins AJ, Darzins TA, Jukna, AD, Berzins GV (1967) *Physical mechanical properties with ammonia chemically plasticized wood*, Holztechnologie 8(1): 23-28.

Krischer O, Esdorn H (1955) *Simple short-term method for the simultaneous determination of thermal conductivity, heat capacity and thermal effusivity of solids*, VDI-Forsch.-*H.* 450.

Kühlmann G (1962) *Investigation of the thermal properties of wood and particleboard in dependency from moisture content and temperature in hygroscopic range*, Holz als Roh- und Werkstoff 20(7): 259-270.

Lexa J, Nečesavý V, Paclt J, Tesařová M, Štafko J (1952) *Mechanical and Physical Properties of Wood*, Wood Technology, Práca, Bratislava.

MacLean JD (1941) *Thermal conductivity of wood*, Heating, Piping and Air Conditioning 13(6): 380-391.

Niemz P, Sonderegger W, Hering S (2010) *Thermal conductivity of Norway spruce and European beech in the anatomical directions*, Annals of Warsaw Agricultural University – S.G.G.W. 72(1): 66-72.

Pandey CN, Kanoh HC, Mani R (1991) *Trials on bending of vapour phase ammonia plasticized wood II*, Journal Timb. Dev. Assoc. 37(4): 512.

Požgaj A, Chovanec D, Kurjatko S, Babiak M (1997) *Wood Structure and Properties*, Priroda, Bratislava.

Rowell RM (2006) *Chemical modification of wood: A short review*, Wood Material Science and Engineering 1(1): 29-33.

Sedliačik M (1998) *The issue of Lignamon manufacturing*, Drevárska Súčasnosť 5(9): 1365.

Simpson W, TenWolde A (1999) *Physical properties and moisture relations*, Forest Product Laboratory, Wood Handbook-Wood as an engineering material, General Technical Report FPL-GTR-190, U.S. Department of Agriculture, Forest Service, Forest Products Laboratory, Madison, WI, pp. 4.1-4.19.

Skaar C (1988) *Wood Water Relations*, Springer, New York.

Stojčev A (1979) *Lignamon-improved wood: Manufacturing, properties and using*, SNTL/ Papers of Research and Development Institute of Wood Technology in Prague, 98.

Steinhagen HP (1977) *Thermal conductive properties of wood, green or dry, from -40 °C to +100 °C: A literature review*, U.S. Department of Agriculture Forest Service, Forest Products Laboratory, Madison, WI.

Suleiman BM, Larfeldt J, Leckner B, Gustavsson M (1999) *Thermal conductivity and diffusivity of wood*, Wood Science and Technology 33(6): 465-473.

Weigl M, Pöckl J, Grabner M (2009) *Selected properties of gas phase ammonia treated wood*, European Journal of Wood and Wood Products 67(1): 103-109.

Weigl M, Müller U, Wimmer R, Hansmann C (2012) *Ammonia vs. thermally modified timber– Comparison of physical and mechanical properties*, Journal of Wood and Wood Products 70(1-3): 233-239.

5. Paper II.

Thermophysical properties of medium density fiberboards measured by quasi-stationary method: experimental and numerical evaluation

Eva Troppová [1*], Jan Tippner [1], Richard Hrčka [2]

Manuscript is under review in Heat and Mass Transfer

[1] Department of Wood Science, Faculty of Forestry and Wood Technology, Mendel University in Brno
[2] Department of Wood Science, Faculty of Wood Sciences and Technology, Technical University in Zvolen

Abstract

This paper presents an experimental measurement of thermal properties of medium density fibreboards with different thicknesses (12, 18 and 25 mm) and sample sizes (50 x 50 mm and 100 x 100 mm) by quasi-stationary method. The experimentally gained values were used to verify a numerical model and furthermore served as input parameters in the numerical probabilistic analysis. The sensitivity of measured outputs (time course of temperature) to influential factors (density, heat transfer coefficient and thermal conductivities) was established and described by the Spearman's rank correlation coefficients. The dependence of thermal properties on density was confirmed by measured data. Density was also proved to be an important factor for sensitivity analyses as it highly correlated with all output parameters. The relevancy of the experiment is mainly influenced by the choice of proper ratio between thickness and width of samples and elimination of heat losses through lateral surfaces caused by convective heat transfer.

Keywords: Medium density fiberboard; Quasi-stationary measurement; Thermal conductivity; Thermal diffusivity; Specific heat capacity; Finite Element Method

5.1. Introduction

Medium density fiberboard (MDF) is a widely used composite material made of wood fibers. Its´ favorable physical and mechanical properties enable usage mainly in furniture and construction production. Many authors described mechanical properties of MDF (Bodig and Jayne, 1993; Cai and Ross, 2010; Ganev et al., 2005; Wilczyński and Kociszewski, 2007; Schulte and Frühwald, 1996), but there are only limited studies on the thermal properties of wood-based materials. The knowledge of thermal properties is important especially in the process of drying, thermal modification, hot pressing or general in processes where heat transfer occurs. Thermal properties of wood-based materials as well as wood itself are mainly affected by density, temperature and moisture content (MacLean 1941; Steinhagen 1977; Suleiman et al., 1999) and vary within each type due to heterogeneity of the material. Measurements of thermal properties of MDF with different moisture contents were held by (Zhou et al., 2013). Thermal conductivity, thermal diffusivity and volume heat capacity of untreated, thermally modified and densified MDF were compared in the work of (Grześkiewicz et al., 2012).

Different methods can be used to establish thermal properties of MDF. The stationary method performs a measurement when the temperature of the measured material does not change with time, as for example guarded hot plate (Salmon 2001; Xamán et al., 2009) or heat flow meter methods (Yu et al., 2011). Thermal conductivity is then determined by the heat flow, the mean temperature difference between the sample surfaces and the dimensions of samples. Transient methods, as for example hot strip method (Gobbé et al., 2004; Ladovie et al., 2000; Jannot 2011), transient plane source technique (Gustafsson 1991) or pulse transient method (Boháč et al., 2003; Boháč et al., 2004) enable measurement of a full set of thermo physical parameters within a single measurement. Temperature development is a function of time in the transient dynamic techniques. A non-stationary method based on principles described by Clarke and Kingston (1950) and Krischer and Esdorn (1955) was developed at the Technical University in Zvolen (Požgaj et al., 1997). Quasi-stationary apparatus is based on the monitoring of temperature changes in the middle of samples and enables simultaneous determination of thermal conductivity, thermal diffusivity and specific heat capacity. Measurements of thermal properties are

generally influenced by variety of parameters. The main factors that significantly affect accuracy of results include material properties (dimensions of samples, heterogeneities), conditions during measurement (temperature, heat transfer coefficient) and parameters of the measuring device (sensor placement, heat supply). The comparison of the hot-wire and the quasi-stationary method for measurement of wood thermal properties was introduced by Hrčka and Babiak (2012). The results illustrated the influence of thickness or dimensions of the sample in the direction of heat flow on the final thermal properties.

Numerical simulations of heat transfer were performed to find the influence of various physical parameters on thermal response of wood-based materials in this article. Parametric studies predict the significance of each parameter. A simulation of heat and mass transfer in wood was carried out by Younsi et al. (2006), Gu (2001) and Hunt and Gu (2004). One of the challenging issues remains the description of heat transfer in wood-based materials during the measuring process and the evaluation of parameters that influence the final temperature rise in time. Data such as geometry of samples, material properties, or loads are usually not known perfectly (Čermák and Trcala, 2012). Therefore, the verification of a numerical solution with experimental data and analytical calculations is needed.

The main goal of this article was to establish the thermal properties (thermal conductivity, thermal diffusivity and specific heat capacity) of MDFs using the quasi-stationary method. To extend knowledge about this method, a numerical simulation of heat transfer in MDF samples was done and compared with the analytical solution. A probabilistic numerical study was conducted to quantify the influence of specific parameters on the accuracy of measurement.

5.2. Material and Methods

Commercially available MDFs with three different thicknesses (12, 18 and 25 mm) were cut to approximate dimensions (width x length) of 50 x 50 mm and 100 x 100 mm. All 60 samples (10 samples of each thickness and sample size) were conditioned at 20 °C and a relative humidity of 65% in a Sanyo MTH 2400 climatic chamber to reach the equilibrium moisture content. Mean density from each type of sample was evaluated by the gravimetric method. Small blocks of dry MDF sample were cut with sledge microtome in order to

obtain a smooth surface. Reflected light microscopy images were prepared with laboratory microscope Leica DM2000. All images show homogeneous structure of the middle layer in 25 mm thick MDF board, see Figure 1. Wood fibers are oriented mainly in samples´ plane direction.

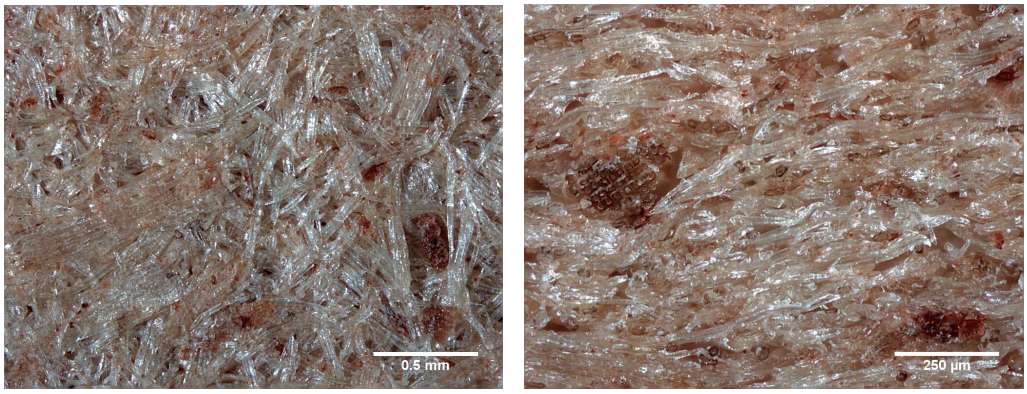

Paper II. Fig 1 Microstructure pictures of MDF surfaces in the direction parallel to the plane (left image) and perpendicular to the plane (right image)

5.2.1. Experimental measurement of thermal properties using the quasi-stationary method

The apparatus consists of a block of eight samples alternately interspersed with NiCr thin foil (0.01 mm) to produce heat, see Figure 2. Both sides of the block of samples are insulated by polystyrene (20 mm) and thin pertinax boards (several layers of paper coated with phenol resin) to avoid heat losses to the surrounding. The heat source generates constant heat flux which enters samples through the NiCr foil and warms them up (Požgaj et al., 1997). The average heat flux ranged from 590 to 640 $W.m^{-2}$ at different measurements. The rise in temperature was recorded with a thermocouple placed in the center of the two middle samples (in x,y,z=[0,0,0]). Those two samples were changed after each measurement and their averaged thermal properties evaluated. Second thermocouple was placed closer to the edge of samples (in x,y,z=[0.0183,0,0.0123] for a sample with 100x100 mm and x,y,z=[0.0125,0,0.0124] for a sample with 50x50 mm) to gain other thermal response for more accurate verification of the numerical model.

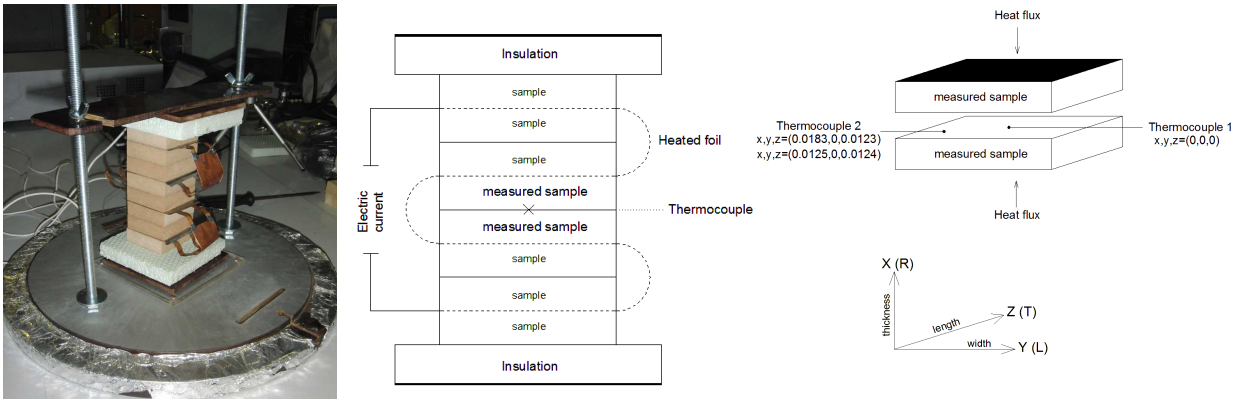

Paper II. Fig 2 Scheme of the experimental device with flow direction (adopted from Hrčka 2010; Troppová et al., 2013)

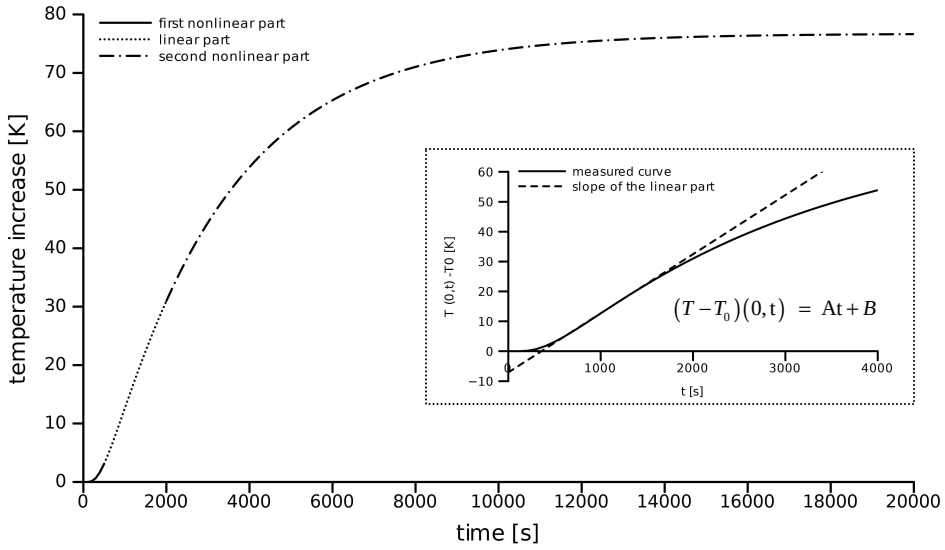

Paper II. Fig 3 The temperature response recorded between middle samples by a thermocouple in the center with a detailed linear part of the curve

The data from the measurements are illustrated in Figure 3 as a curve and describe the temperature increase in time in the center of the middle samples. There are three different parts of the curve. The first nonlinear part at the beginning of the experiment is mainly influenced by thermal diffusivity perpendicular to the sample´s plane direction. The second part influenced by heat capacity is linear as is the temperature increased with time. The method is called quasi-stationary as it is defined as resembling stationary conditions resulting from the linear part of the temperature measurement needed for the evaluation of thermal properties (Troppová et al., 2013). The last nonlinear part of the temperature curve

is influenced by thermal diffusivity in-plane direction and by heat loss through lateral surfaces. All three parts of the temperature response are necessary for evaluation of thermal parameters. The accuracy of the quasi-stationary method depends on the precision of measurement and on fulfilling the boundary conditions used in the solution of heat the conduction equation (Yapici et al., 2011). Without the middle linear part, the exact calculation of thermal conductivities in both directions (perpendicular to plane and along with plane directions) is impossible. The linear relation between temperature and time is described as follows (Požgaj et al., 1997):

$$T(0,t)-T_0=\frac{qd}{\lambda}\left(\frac{\alpha_x t}{d^2}-\frac{1}{6}\right) \tag{2.1}$$

The non-stationary method (quasi-stationary) is based on the evaluation of temperature changes in measured samples [30]. The analytical solution is based on solving the heat transfer equation with specific boundary conditions: constant heat flux on the upper surface of the measured sample (eq. 2.2), zero heat flow in the middle of the apparatus reached due to the sample´s symmetry (eq. 2.3), and a constant temperature in the whole sample at the beginning of experiment (eq. 2.4):

$$\left(\frac{\partial(T-T_0)}{\partial x}\right)_{x=d}=-\frac{q}{\lambda} \tag{2.2}$$

$$\left(\frac{\partial(T-T_0)}{\partial x}\right)_{x=0}=0 \tag{2.3}$$

$$(\mathrm{T}-\mathrm{T}_0)_{(x,0)}=0 \tag{2.4}$$

The interpolation of the measured curve according the least square method is needed for evaluation of the thermal properties. The three-dimensional model with accounted heat losses is used for interpolation of the whole nonlinear curve (Hrčka and Babiak, 2012):

$$T(\mathrm{x,y,z,t})-T_0=\frac{8\mathrm{q}}{c\rho R}\sum_{r=1}^{\infty}\sum_{p=1}^{\infty}\sum_{m=1}^{\infty}\frac{(-1)^{r+1}\cos\left((2\mathrm{r}-1)\frac{\pi}{2}\frac{z}{L}\right)}{(2\mathrm{r}-1)\frac{\pi}{2}}\frac{(-1)^{p+1}\cos\left((2\mathrm{p}-1)\frac{\pi}{2}\frac{y}{T}\right)}{(2\mathrm{p}-1)\frac{\pi}{2}}\cos\left((m-1)\pi\frac{\mathrm{R\text{-}x}}{R}\right)$$
$$\left(\frac{1-e^{-\left(((m-1)\pi)^2\frac{\alpha_R}{R^2}+\left((2\mathrm{p}-1)\frac{\pi}{2}\right)^2\frac{\alpha_T}{T^2}+\left((2\mathrm{r}-1)\frac{\pi}{2}\right)^2\frac{\alpha_L}{L^2}\right)t}}{\left((m-1)\pi\right)^2\frac{\alpha_R}{R^2}+\left((2\mathrm{p}-1)\frac{\pi}{2}\right)^2\frac{\alpha_T}{T^2}+\left((2\mathrm{r}-1)\frac{\pi}{2}\right)^2\frac{\alpha_L}{L^2}}\right) \tag{2.5}$$

Thermal diffusivities α_L and α_T are equal as MDF is assumed to be a plane isotropic material. Let us consider the slope of the linear part of the curve as parameter A and intercept as parameter B. The thermal diffusivity perpendicular to plane is than calculated according:

$$\alpha = \frac{d^2 A}{6B} \tag{2.6}$$

The thickness of boards must be known. The heat flux value is needed to calculate thermal conductivity:

$$\lambda = \frac{qd}{6B} \tag{2.7}$$

Moreover, if MDF density is known, specific heat can be determined:

$$c = \frac{q}{\rho d A} \tag{2.8}$$

The determination of parameters in parallel to the plane direction utilizes the relationship (2.5) and the non-linear technique employed in the least square method. The thickness d is equal to dimension R. The nonlinear technique provides both thermal diffusivities in perpendicular and parallel directions and heat capacity. Then thermal conductivities in both directions are calculated according to:

$$\lambda = \alpha.c.\rho \tag{2.9}$$

5.2.2. Numerical simulation and parametric study

Two finite element numerical models have been developed for the simulation of the quasi-stationary apparatus using Ansys Mechanical APDL 14.5 software. Parametric scripts were created in Ansys Parametric Design Language. The numerical model consists of two MDF samples (blocks with dimensions 49.87 x 49.60 x 18.10 mm for the first case and 101.4 x 98.2 x 18.3 mm for the second case) perfectly bonded with no interaction between them. Quadratic hexahedral thermal solid elements (SOLID279) created regular mesh in the model. Experimentally obtained values of density, specific heat capacity and thermal conductivity in both directions (longitudinal and transverse) were specified and assigned to the geometry. Heat transfer is caused by the heat flow (0.73 W) applied to the upper and

lower surface of samples. Heat transfer coefficient (25 $W.m^{-2}.K^{-1}$) was assigned to lateral surfaces. A thermal transient analysis with the end time (max 5500 s) was performed. A number of substeps (also 5500 s, then time step is 1 s) enabled to calculate the temperature in both thermocouple points every second which is comparable with experimental recordings. Four different parameters describing the nonlinear curve were computed, see Table. 2.1. Parameters *t_der_lin1* and *t_der_lin2* describe the beginning and the end of the linear part of the curve essential for evaluation of thermal properties. Parameters *t_1der_max* and *t_2der_max* describe time at maximal first and second derivation dealing with the speed of change in the temperature response. Those parameters were than used as output parameters in the probabilistic analysis.

After verification of numerical results, the probabilistic analysis was performed to find which parameters influence the temperature response and furthermore the evaluation of thermal properties in both cases (for 50 x 50 mm and 100 x 100 mm samples). The Ansys Probabilistic Design System enabled description of the relationship between the input parameters (longitudinal and transverse thermal conductivity, density and heat transfer coefficient) and output parameters (described in Table 1) based on many calculated cycles. The main results of the probabilistic analysis are Spearman's rank correlation coefficients showing relation and sensitivity between all mentioned parameters. The input parameters were sampled based on the Direct Monte Carlo method. This technique randomly samples the variables according to input range defined with Gaussian distribution. The range for sampling the parameters was set up using the average value of the parameter (gained from experiments) and the standard deviation (established in accordance to 10% variance). Output parameters were calculated in 100 cycles of simulations.

Paper II. Table 1 Description of the computed output parameters

OUTPUT PARAMETERS	DESCRIPTION	CONDITION
t_*der_lin1*	*time at beginning of the linear part*	$\frac{der(i+2)-der(i+1)}{der(i+1)-der(i)}<1$
t_*der_lin2*	*time at the end of the linear part*	$\frac{der(i+2)-der(i+1)}{der(i+1)-der(i)}<0.99$
t_*1der_max*	*time at maximal first derivation*	$der1=\max\_der1$
t_*2der_max*	*time at maximal second derivation*	$der2=\max\_der2$

5.3. Results and Discussion

The thermal conductivity, thermal diffusivity and specific heat capacity were derived from the measured temperature response while using analytical solution of the quasi-stationary method (see equations 2.5-2.9). The measured data differ notably, as shown in Table 2. The results proved that the thermal measurements of MDF samples with dimensions 100 x 100 mm and thicknesses 12 and 18 mm are reliable only. The standard deviation of measurements is higher for samples with dimensions 100 x 100 mm. This can be caused by the higher variability of samples, but does not predicate on accuracy of the measuring method. The irrelevancy of measured data at higher thicknesses (cases with 25 mm thickness) and smaller dimensions (all samples with 50 x 50 mm) is caused by the missing linear part of the output curve, which strongly influences the data evaluation. The higher the thickness of MDF sample, the higher heat losses to the surrounding from lateral surfaces. The proper ratio between thickness and width of the sample lowers the influence of the heat transfer coefficient on the heat losses through lateral surfaces (Požgaj et al., 1997). Even the ratio 0.24 (samples with widths 50 mm and thickness 12 mm) was not sufficient for relevant measurement. Thermal conductivity increases with increasing density of samples, as stated by e.g. Kühlmann (1962). The positive correlation between thermal conductivity and density was confirmed by measured data (valid only for reliable results).

Paper II. Table 2 Mean thermal properties of MDF samples measured in the direction perpendicular (across) the plane

DIMENSIONS [mm]	**THICKNESS** [mm]	**DENSITY** [kg.m^{-3}]	**λ_X** [W.m^{-1}.K^{-1}]	**α_X** [10^7 m^2.s^{-1}]	**HEAT CAPACITY** [J.kg^{-1}.K^{-1}]
50 x 50	12	767 *(10.7)*	0.21 *(0.01)*	1.14 *(0.04)*	2426 *(56)*
	18	778 *(12.4)*	0.22 *(0.02)*	1.16 *(0.06)*	2476 *(161)*
	25	753 *(4.5)*	0.24 *(0.02)*	1.27 *(0.04)*	2500 *(105)*
100 x 100	12	721 *(1.8)*	0.12 *(0.02)*	1.08 *(0.06)*	1514 *(81)*
	18	741 *(3.3)*	0.12 *(0.02)*	1.10 *(0.08)*	1538 *(119)*
	25	715 *(30.7)*	0.17 *(0.01)*	1.14 *(0.05)*	2132 *(79)*

** values in parentheses describe the standard deviation of measurements*

Yapici et al. (2011) published a thermal conductivity value of 0.192 W.m^{-1}.K^{-1} at 7.2% moisture content and 20 Celsius degrees for MDF with a density of 640 kg.m^{-3} measured by the hot-wire method. The thermal conductivity (0.195 W.m^{-1}.K^{-1}) at 25 Celsius degrees for oven-dried MDF with a density of 765 kg.m^{-3} established according to the light flash system was published by Zhou et al. (2013). A variety of factors strongly influence the thermal conductivity values (density, moisture content, temperature, measuring method, technological process, sample preparation), as seen from the difference between data available in literature and our measured values. The variability in data obtained according to the quasi-stationary method primarily results from the variability between samples and from the influence of heat losses from lateral surfaces. Thermal parameters were obtained at 20 Celsius degrees and at average equilibrium moisture content 7.6% of all samples.

Paper II. Table 3 Mean values of MDF thermal properties

DIMENSIONS [mm]	**THICKNESS** [mm]	**λ_Y** [W.m^{-1}.K^{-1}]	**λ_X** [W.m^{-1}.K^{-1}]	**α_X** [10^7 m^2.s^{-1}]	**α_Y** [10^7 m^2.s^{-1}]	**HEAT CAPACITY** [J.kg^{-1}.K^{-1}]
100 x 100	12	0.12	0.29	1.1	2.6	1514
100 x 100	18	0.24	0.24	1.1	2.2	1538

The thermal conductivity and thermal diffusivity in both directions (perpendicular and parallel to the plane) may be calculated following the quasi-stationary method. Those averaged values are presented in Table 3 for two types of MDF samples. The duration of the measurement was prolonged to reach all three parts of the thermal curve. There are only limited experiments on wood-based materials dealing with thermal parameters in the direction parallel to the plane, as for practical building applications, the heat flow is primarily across the plane. On the other hand, the in-plane thermal conductivity is one of the important parameters during edge banding. The in-plane thermal conductivity and also thermal diffusivity is 2 to 2.4 times greater than in the perpendicular direction, see Table 4. The microstructure picture shows the orientation of wood fibers mainly parallel to the plane of the MDF board (Figure 1.). TenWolde et al. (1988) published wood thermal conductivity values along the wood grain 1.5 to 2.8 times higher than the conductivity across the grain, which also described our data.

The comparison between the experimental recordings in both thermocouple locations and numerical calculations is obvious in Figure 4. for the case of 100 x 100 x 18 mm and in Figure 5. for the case of 50 x 50 x 18 mm. The numerical and experimental data were in close agreement with each other (differences between temperatures were lower than 0.3 °C in all parts). Testing of mesh density at a large range as well as using different ANSYS element types did not influence the results perceptibly. On the contrary, a time step of transient analysis influences the shape of the curve considerably, especially in the first and the second part of the curve. The comparisons show a good agreement between the calculated numerical and the measured data; especially at solution with time step 1 second (temperature is calculated every second). Such a well fitted model can consequently be used for sensitivity analyses.

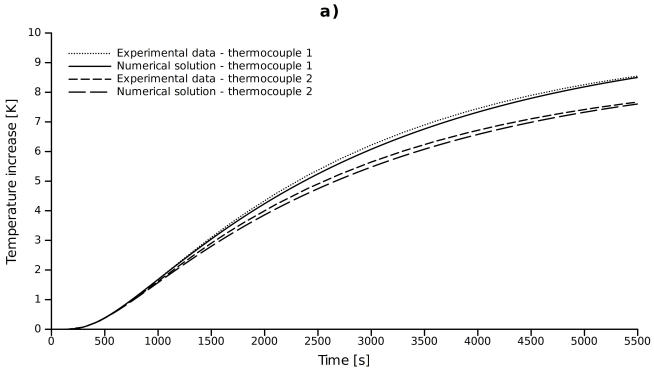

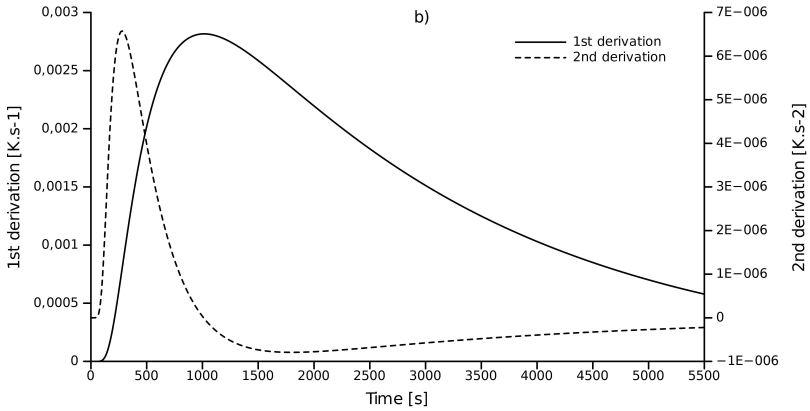

Paper II. Fig 4 Results of numerical solution for the case of 100 x 100 x 18 mm specimens; a) comparison of numerical and experimental temperature increase in time for both thermocouples, b) first and second derivation of the temperature curve

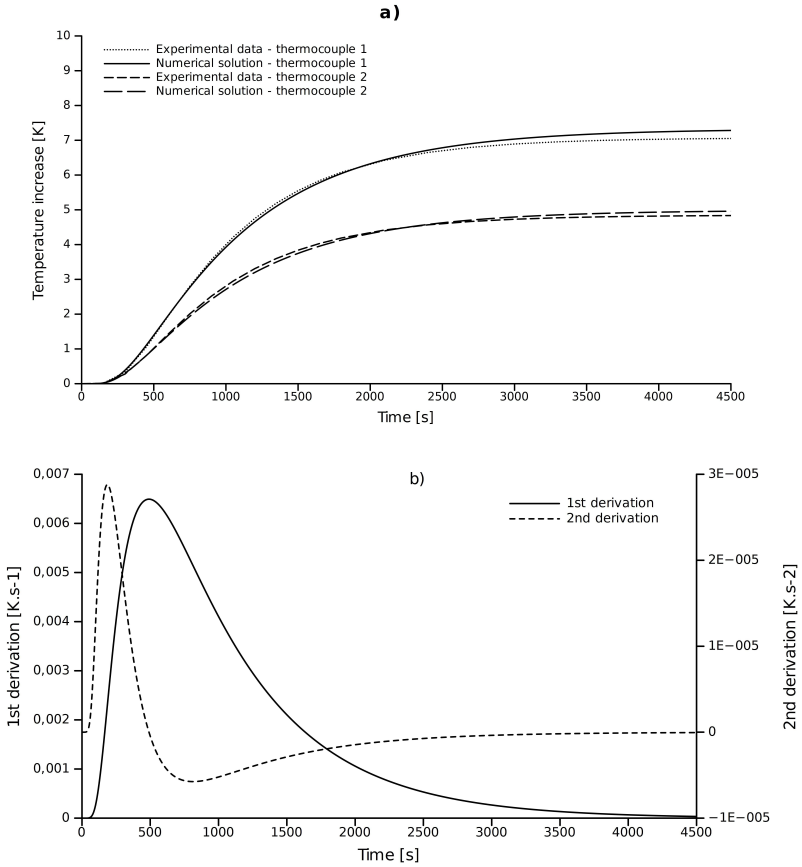

Paper II. Fig 5 Results of numerical solution for the case of 50 x 50 x 18 mm specimens; a) comparison of numerical and experimental temperature increase in time for both thermocouples, b) first and second derivation of the temperature curve

The same amount of heat was applied on MDF samples in both computed cases (50 x 50 mm and 100 x 100 mm). The faster change of temperature described by the first derivation (see Figure 4b. and Figure 5b.) is obvious in samples with smaller dimensions. Even the last nonlinear part of the curve occurs earlier in the case of 50 x 50 mm samples. The deformation of the temperature field caused by heat losses through lateral surfaces (see Figure 6.) is much more evident at smaller dimensions.

Verified numerical models were used for probabilistic analysis based on variable solutions with randomized input variables (density, heat capacity, longitudinal and transverse thermal conductivity, heat transfer coefficient). The output parameters (see Table 2.1) are instrumental towards describing the modeled curve from the quasi-stationary measurements (Hrčka and Babiak, 2012). The evaluation of the probabilistic sensitivities is based on the correlation coefficients between all random input variables and particular random output variables. Spearman´s rank order correlation coefficients are shown for cases with 50 x 50 mm and 100 x 100 mm samples in Table 5. (the two variables are weakly correlated with each other for values closer to zero; the two variables are highly correlated either in a positive or negative sense for values closer to 1 or -1, respectively).

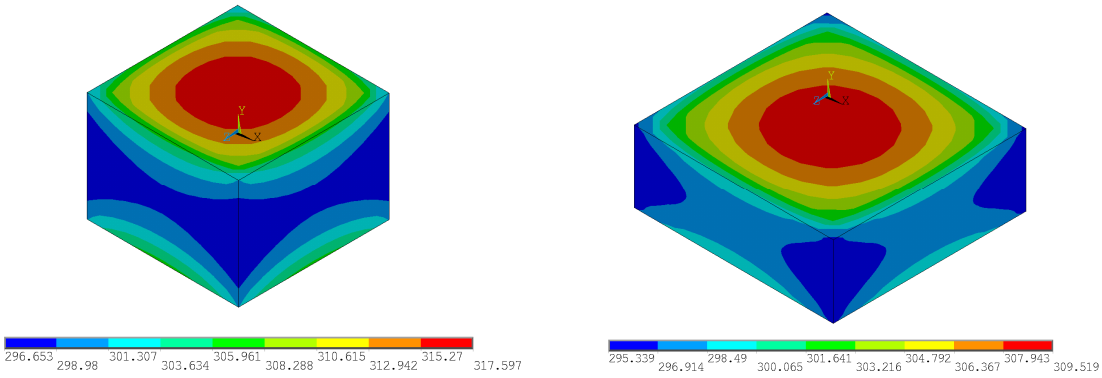

Paper II. Fig 6 Numerical results of the temperature field at the end of the measurement for MDF samples with dimensions 50 x 50 mm (left) and 100 x 100 mm (right)

Density proved to be an important factor in sensitivity analyses as it highly correlated with all output parameters in a positive way, see Table 4. The analysis showed also the significant correlation between transverse conductivity and all output parameters. The

higher transverse conductivity is, the quicker will be the temperature response on the applied heat. The thermal conductivity perpendicular to the plane influences also the end of the first nonlinear part (described by parameter *t_der_lin1)* as well as the linear part of the curve (*t_der_lin2*). The value of the heat transfer coefficient and the in-plane thermal conductivity influences mainly the last part of the nonlinear curve. The higher heat losses are from lateral surfaces, the faster will appear the second nonlinear part of the curve. The in-plane thermal conductivity of 50 x 50 mm samples is an insignificant parameter for the linear part of the curve as it is short compared to the other nonlinear parts. The short linear part then causes shifts in data evaluation.

Paper II. Table 4 Matrix of correlation coefficients based on ANSYS probabilistic analyses

DIMENSIONS	PARAMETER	λ_X	λ_Y	DENSITY	HEAT TRANSFER COEFFICIENT
50 x 50 mm	t_1der_max	-0.491	(-0.141)	0.821	(-0.070)
	t_2der_max	-0.599	(-0.077)	0.777	(0.044)
	t_der_lin1	-0.461	(-0.144)	0.831	(-0.093)
	t_der_lin2	-0.461	(-0.144)	0.832	(-0.093)
100 x 100 mm	t_1der_max	-0.480	-0.225	0.820	(0.033)
	t_2der_max	-0.651	(-0.015)	0.743	(0.086)
	t_der_lin1	-0.434	-0.290	0.819	(0.030)
	t_der_lin2	-0.423	-0.294	0.822	(0.022)

** values in brackets indicate not significant correlation coefficient (a significance level of 2.5% has been used).*

5.4. Conclusions

The experimental measurement of MDF thermal properties by quasi-stationary method and subsequently the numerical probabilistic analysis dealing with impact of selected parameters on the reliability of measurement was presented in this work. The thermal conductivity and thermal diffusivity in both directions (perpendicular and parallel to the plane) was assessed. The in-plane thermal conductivity (λ_y=0.24 $W.m^{-1}.K^{-1}$ by 721 $kg.m^{-3}$) is 2 to 2.4 times greater than in the perpendicular direction (λ_x=0.12 $W.m^{-1}.K^{-1}$). The positive correlation between thermal conductivity and density was confirmed by our measured data. Thermal measurements of MDF with different thicknesses (12, 18 and 25

mm) and sample sizes (50 x 50 mm and 100 x 100 mm) were held. The results proved that the thermal measurements of MDF samples with dimensions 100 x 100 mm and thicknesses 12 and 18 mm are reliable only. The irrelevancy of measured data is caused by the missing linear part of the output curve as well as by the increased heat losses from lateral surfaces.

The valid experimental results were used for verification of the numerical model and furthermore as the input variables in the probabilistic analysis. Numerical results give information about correlation between selected input and output parameters describing mainly the measured temperature response. The analysis showed a high impact of the sample's density. The future incorporation of realistic density profiles into the numerical model will improve the results of the sensitivity analysis. The extensive experimental evaluation of the relationship between density and thermal properties will be needed. The heat transfer coefficient decelerates the temperature increase in time, mainly in the second and the third part of the measurement process. The relevancy of the measurement is also influenced by the choice of the proper ratio between thickness and width of the sample. The accuracy of the quasi-stationary method depends on the precision of measurement and fulfillment of conditions during measurement, especially the test duration resulting in all three needed parts of the temperature curve. The reliability of experiments can be increased by avoiding heat losses (insulating all lateral parts of samples) so that the size of samples would not affect the determination of thermal parameters.

Nomenclature

x, y, z	coordinates	[m]
d	thickness	[m]
R, L, T	dimensions	[m]
c	specific heat capacity	[$J.kg^{-1}.K^{-1}$]
α_R and $\alpha_T (=\alpha_X)$, $\alpha_L (=\alpha_Y)$,	thermal diffusivities	[$m^2.s^{-1}$]
T	temperature	[K]
T_0	constant initial temperature	[K]

λ_X	thermal conductivity perpendicular to the plane	[W.m^{-1}.K^{-1}]
λ_Y	in-plane thermal conductivity	[W.m^{-1}.K^{-1}]
ρ	density	[kg.m^{-3}]
q	heat flux	[W.m^{-2}]
t	time	[s]

Acknowledgement

This article is supported by the project "The Establishment of an International Research Team for the Development of New Wood-based Materials" Reg. No. CZ/1.07/2.3.00/20.0269 and by the Internal Grant Agency of the Mendel University (project no. 8/2011). This work was also supported by the Slovak Research and Development Agency under the contract No. SK-CZ-0045-11 and by the Ministry of Education Youth and Sports of the Czech Republic under the contract No. 7AMB12SK077.

5.5. References

Babiak M (1976) *Some thermal properties of spruce wood and its wood based materials*, Drevárska fakulta VŠLD Zvolen 114.

Bodig J, Jayne BA (1993) *Mechanics of Wood and Wood Composites*, Malabar: Krieger Publish. Comp. r. 21.

Boháč V, Gustavsson M, Kubičár L´, Vretenár V (2003) *Measurements of building materials by transient methods*, in Thermophysics 2003, Proc. of the Meeting of the Thermophysical Society - Working Group of the Slovak Physical Society 58-66.

Boháč V, Kubičár L', Vretenár V (2004) *Use of transient method to investigate the thermal properties of two porous materials*, High Temperature-High Pressure 35/36: 67-74.

Cai Z, Ross RJ (2010) *Mechanical properties of wood-based composite materials, Wood Handbook: Wood as an engineering material: Chapter 12*. Centennial ed. General technical report FPL; GTR-190. Madison, WI. U.S. Dept. of Agriculture, Forest Service, Forest Products Laboratory 12.1-12.12.

Clarke LN, Kingston RST (1950) *Equipment for the simultaneous determination of thermal conductivity and diffusivity of insulating materials using a variable state method*, Australian Journal of Applied Science 1: 172-187.

Čermák P, Trcala M (2012) *Influence of uncertainty in diffusion coefficients on moisture field during wood drying*, International Journal of Heat and Mass Transfer, http://dx.doi.org/10.1016/j.ijheatmasstransfer.2012.07.070.

Ganev S, Gendron G, Cloutier A, Beauregard R (2005) *Mechanical Properties of MDF as a Function of Density and Moisture Content*, Wood and Fiber Science 37(2): 314-326.

Gobbé C, Iserna S, Ladevie B (2004) *Hot strip method: application to thermal characterization of orthotropic media*, International Journal of Thermal Sciences 23: 951-958.

Grześkiewicz M, Borysiuk P, Kramarz K (2012) *Physical and mechanical properties of thermally modified and densified MDF*, International Wood Products Journal 3(1): 21-25.

Gu HM (2001) *Structure based, two-dimensional anisotropic, transient heat conduction model for wood*, Ph.D. dissertation, Dept. of Wood Sci. & Forest Prods., Virginia Tech. Blacksburg, 1-242.

Gustafsson SE (1991*) Transient plane source technique for thermal conductivity and thermal diffusivity measurements of solid materials*, Review of Scientific Instruments 62: 797-804.

Hrčka R (2010) *Variation of thermal properties of beech wood in the radial direction with moisture content and density*, Wood Structure and Properties, J. Kúdela and R. Lagaňa (eds.), Arbora Publishers, Slovakia.

Hrčka R, Babiak M (2012) *Some non-traditional factors influencing thermal properties of wood*, Wood Research 57(3): 367-374.

Hrčka R, Halachan P, Babiak M, Lagaňa R, Tippner J, Troppová E, Trcala M (2014) *Transverse isotropic material thermal properties measurement*, Proceedings of the 57th International Convention of Society of Wood Science and Technology, Zvolen, Slovakia, 622-629.

Hunt JF, Gu HM (2004) *Finite element analyses of two dimensional, anisotropic heat transfer in wood*, International Ansys Conference 1-13.

Jannot Y, Deiovanni A, Félix V, Bal H (2011) *Measurement of the thermal conductivity of thin insulating anisotropic material with a stationary hot strip method*, Measurement Science and Technology 22.

Krischer O, Esdorn H (1955) *Simple short-term method for the simultaneous determination of thermal conductivity, heat capacity and thermal effusivity of solids*, VDI-Forsch.-H. 450, (in German).

Kühlmann G (1962) *Investigation of the thermal properties of wood and particleboard in dependency from moisture content and temperature in hygroscopic range*, Holz als Roh- und Werkstoff 20 (7) 259-270.

Ladevie B, Fudym O, Batsale JC (2000) *A new simple device to estimate thermophysical properties of insulating materials*, International Communications in Heat and Mass Transfer 17: 473-484.

MacLean JD (1941) *Thermal conductivity of wood*, Heating, Piping and Air Conditioning 13(6): 380-391.

Požgaj A, Chovanec D, Kurjatko S, Babiak M (1997*) Wood structure and properties*, Priroda, 1- 486 (in Slovak).

Salmon D (2001) *Thermal conductivity of insulations using guarded hot plates, including recent developments and source of reference materials*, Measurement Science and Technology 12: 89-98.

Schulte M, Frühwald A (1996) *Shear modulus, internal bond and density profile of medium density fibre board (MDF)*, European Journal of Wood and Wood Products 54(1): 49-55.

Steinhagen HP (1977) *Thermal conductive properties of wood, green or dry, from -40 °C to +100°C: a literature review*, U.S. Department of Agriculture forest service, Forest products laboratory Madison.

Suleiman BM, Larfeldt J, Leckner B, Gustavson M (1999) *Thermal conductivity and diffusivity of wood*, Wood Science and Technology 33: 465-473.

TenWolde A, McNatt JD, Krahn L (1988) *Thermal properties of wood and wood panel products for use in buildings*, U.S. Department of Energy 1-57.

Troppová E, Tippner J, Hrčka R, Halachan P (2013) *Quasi-stationary measurements of Lignamon thermal properties*, BioResources 8(4): 6288-6296.

Wilczyński A, Kociszewski M (2007) *Bending properties of particleboard and MDF layers*, Holzforschung 61(11): 717-722.

Xamán J, Lira L, Arce J (2009) *Analysis of the temperature distribution in a guarded hot plate apparatus for measuring thermal conductivity*, Applied Thermal Engineering 29: 617-623.

Yapici F, Ozcifci A, Nemli G, Gencer A, Kurt S (2011) *The effect of expanded perlite on thermal conductivity of medium density fiberboard (MDF) panel*, Technology 14 (2): 47-51.

Younsi R, Kocaefe D., Kocaefe Y (2006) *Three-Dimensional Simulation of Heat and Moisture Transfer in Wood*, Applied Thermal Engineering 26 (11): 274-285.

Zhou J, Zhou H, Hu C, Hu S (2013) *Measurements of Thermal and Dielectric Properties of Medium Density Fiberboard with Different Moisture Contents*, BioResources 8(3): 4185-4192.

Zi-Tao Yu, Xu Xu, Li-Wu Fan, Ya-Cai Hu, Ke.Fa Cen (2011) *Experimental Measurements of Thermal Conductivity of Wood Species in China: Effects of Density, Temperature, and Moisture Content*, Forest Product Journal 61(2): 130-135.

6. Paper III.

The influence of specific parameters on thermal properties of medium density fiberboards by pulse transient method

Eva Troppová[1], Jan Tippner[1]

Manuscript sent to International Journal of Thermal Sciences

a: Department of Wood Science, Mendel University in Brno, Czech Republic

Abstract

The usage of low conductive heterogeneous materials led to demands for accurate measurements of their thermal properties. The aim of this work was to investigate the various effects influencing the accuracy of the pulse transient method when measuring wood-based materials. Thermal properties (thermal conductivity, thermal diffusivity, and specific heat capacity) of medium density fibreboards with different thicknesses (12 and 18 mm) measured at the thermal pulse transient device are presented in this paper. The polymethyl methacrylate was used as a standard reference material for further investigation of the influence of specific parameters on the thermal response to a heat pulse. The numerical probabilistic analysis showed significant factors influencing the measured thermophysical parameters. Density, thermal conductivity of the outer samples as well as the ambient temperature proved to be important in the measuring process. Suggestions for further improvements in the method are made based on results from sensitivity analyses.

Keywords: Medium density fiberboard (MDF); Pulse transient method; Polymethyl methacrylate (PMMA); Thermophysical properties; Finite element method (FEM); Probabilistic analysis

6.1. Introduction

A contemporary preference of using low conductive materials especially in building industry leads to need for more accurate measuring methods of its thermophysical parameters. Modern materials of this kind possess significant heterogeneity and porosity that is the reason for their good thermal insulation properties (Boháč et al., 2003). Classical stationary measuring methods, such as guarded hot plate method or heat flow meters have a limitation regarding number of evaluated parameters. On the contrary, transient measuring methods can give a full set of thermophysical parameters within one measurement, namely thermal conductivity, thermal diffusivity and specific heat.

Despite the chosen method, the effects that influence the process of heat transfer through the measured material have to be known. The moisture content proved to be an important influencing factor as the changing moisture content in pores changes the equilibrium thermodynamic state in the material (Boháč et al., 2003). Many authors dealt with the influence of moisture content on the thermal conductivity of building materials, as e.g. Matias et al. (1997), Brombacher et al. (2012) or Zhou et al. (2013). The heterogeneity of wood-based composite materials is created by the orientation of fibers and distribution of pore sizes. The knowledge of porosity in the material structure permits the evaluation of thermal conductivity (Thunman and Leckner, 2002). Kubičár et al. (2005) examined the thermal conductivity values for heterogeneous porous materials at the surrounding air and vacuum atmosphere. They stated that the gas in pores significantly influences the heat transport through porous materials. As many authors experienced, also density is another highly influencing factor, because it is related to the porosity of the material. Sonderegger and Niemz (2009 and 2012) described relationships between thermal conductivity and density for wood-based composites. Further work refers to Xie et al. (2011) for ultra-low density fibreboards and Chen et al. (2010) for medium density fibreboards properties related to density profiles. Both proved the positive correlation between thermal conductivity and density.

Kubičár et al. (2005) described the main advantages of transient measuring methods. The pulse-transient method is based on generation of a non-stationary temperature field by a pulse of heat inside the specimen. The stabilized temperature of samples is interrupted by

the small heat disturbance. The thermophysical parameters are possible to calculate based on the temperature response. The temperature distribution is a solution of the partial differential equation considering appropriate boundary and initial conditions (Štofanik et al., 2007). The heat losses from lateral surface together with the thermal contacts and source heat capacity influence the measurement. The specimen thickness influences the penetration of the deformed temperature field which results in data shifts (Boháč et al., 2002). The sensitivity of those factors on the thermal response (mainly on the maximum of temperature and time at this maximum temperature value) is possible to calculate based on numerical probabilistic analysis. The correlation coefficients describe the close or week correlations between input and output parameters in a positive or a negative way. The ideal analytical model neglecting all the influence parameters is not feasible at real measuring conditions (Štefková, 2011). Therefore the numerical analysis can establish the potential most important factors influencing the thermal response.

6.2. Material and Methods

The purpose of this study was to investigate the influence of specific parameters on measured thermophysical properties of medium density fibreboards (MDF). The numerical model based on Finite element method (FEM) describing the heat transfer and temperature field in the measured sample was analyzed and compared with experimentally obtained values for samples with thickness 12 mm. The energy equation (Fourier´s law) is solved in the numerical analysis. The probabilistic numerical analysis was used to reach parameters influencing the thermal response to a short heat pulse. Those calculated parameters were compared with parameters of polymethyl methacrylate (PMMA) which was used as a standard reference material. Such comparison enabled to discover specific factors influencing the measurement process of wood-based materials. The thermal properties of MDFs with thicknesses 12 and 18 mm were calculated from experimental data. Furthermore, the X-Ray densitometer was used to measure the density distribution of both types/thicknesses of MDF specimens.

6.2.1. The pulse-transient method

Commercially available MDFs with thicknesses of 12 and 18 mm were cut to approximate dimensions 100 x 100 mm. All 20 samples (10 samples of each thickness - type) were conditioned under 20 °C and a relative humidity of 65% in a Sanyo MTH 2400 climatic chamber to reach the average equilibrium moisture content (7.6 %). Mean density of all samples was evaluated by gravimetric method. Those samples were used for measurements of thermal parameters. Additionally, other 10 + 10 samples from the same MDF plate were cut to dimensions 50 x 50 mm for the X-Ray densitometry (X-RAY DENSE LAB working with resolution 0.01 mm).

The experimental set-up consists of three MDF samples with approximate dimensions 100x100 mm (width x length) to ensure symmetrical conditions, see Figure 1. The planar heat source (heating foil) is placed between the first and the second sample. Heat is generated by electric current pulse at certain duration. The thermocouple is inserted between the second and the third sample. All three samples have to be made from the same material, a three parts of one specimen ideally. The experiment should be performed as near to the ideal model as possible to avoid deviations in measurement accuracy (Boháč et al., 2005). Criteria of the ideal model and parameters of specimen set up should be fulfilled to reach high measurement precision (Boháč et al., 2005). Therefore, first and third MDF samples could be at least 1.4 thicker than the measured second one to ensure the thermal balance. The thickness of the first and third sample was 18 mm when measuring the second sample with 12 mm thickness and 25 mm for cases with the 18 mm measured second samples. The ratio between thickness and width of the measured sample should be lower than 0.2 (Boháč et al., 2002 and 2005). Also this criterion was fulfilled in all cases All MDF samples are connected to each other with thin layer of heat sink paste ensuring ideal thermal contacts. An electrical current coming through the metallic foil generates the heat pulse and furthermore the non-stationary temperature field within the specimen (Kubičár et al., 2005). The temperature response is measured by a thermocouple placed in the center of the upper surface of the middle sample, see Figure 1. The specific heat, thermal diffusivity and thermal conductivity are calculated from the parameters of the temperature response - the time and the magnitude of the maximal temperature increase. Typical temperature

increases are between 0.5-2 °C (Boháč et al., 2002). The samples arrangement is pressed between platens kept at stable temperature by two heat exchangers, see Figure 2. The temperature of the heat exchangers is controlled by a liquid medium from a thermostat. An isothermal cover of chamber is used to suppress any temperature gradients along the specimen set.

Measuring process is controlled by electronic unit RT-Lab (developed at Institute of Physics Slovak Academy of Science). RT-Lab is an autonomous control unit that realizes all operations needed for realization of the experiment. Each measurement is organized in sequences and consists of stabilization time and proper time of the measurement. The temperature of specimen set and also of the surrounding atmosphere is stabilized at certain temperature (20 °C at our measurements). After stabilization time (from 3 to 6 hours at average in our case), the heat pulse is generated with a short delay which is instrumental towards better control of temperature stabilization. Duration of the heat pulse was set to 20s (see section 2.2).

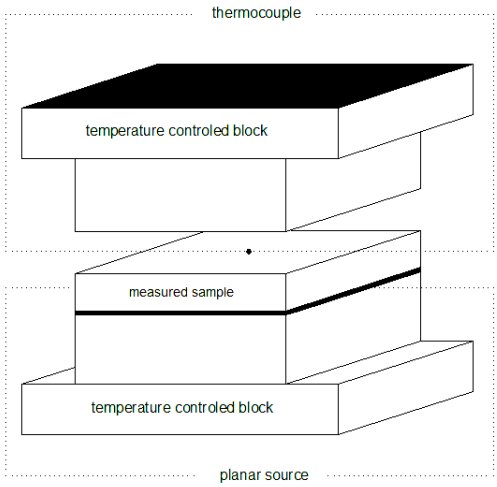

Paper III. Figure 1 Scheme of the measured set-up composed of three MDF specimens with different thicknesses

Paper III. Figure 2 Opened chamber of RT-Lab device based on pulse-transient method

The analytical solution for the temperature response on the heat pulse generated by the planar heat source is as follows (Štefková, 2011):

$$\Delta T(d,t) = \frac{UIt_0}{2c\rho\sqrt{\pi at}} \exp(-\frac{d^2}{4at}) \tag{1}$$

The approximate solution valid for the maximum of temperature response gives simple formulas for the calculation of thermal parameters (Boháč et al., 2002; Štefková, 2011):

$$a = d^2 / 2t_{\_\max} \tag{2}$$

$$c = \frac{UIt_0}{\sqrt{2\pi e}\rho dT_{\_\max}} \tag{3}$$

$$\lambda = a\,\rho\,c \tag{4}$$

Additional measurements were held on a block of MDF samples with dimensions 50x50x12 mm and cylindrical PMMA samples with radius 20 mm and thickness 6 mm for validation of the numerical results and furthermore for the reference parameters of the sensitivity analysis.

6.2.2. Numerical simulation and probabilistic study

Parametric three-dimension finite-element model was created in ANSYS Mechanical APDL 14 software. The model consists of three MDF blocks with assigned orthotropic thermal properties given by experiments. The central measured MDF block has 12 mm thickness. The outer blocks have 18 mm thicknesses to ensure the requirements of the ideal model. Quadratic thermal solid elements (SOLID90) were used for mapped meshing. A heat pulse with certain power and duration was assigned as the planar source on area placed between the first and the second block. The heat pulse was applied as average heat (9.03 W at 100 x 100 mm and 8.77 W at 50 x 50 mm) at certain time pulse duration (20 s) preceded by 15 seconds delay. The convection boundary conditions with heat transfer coefficient of 10 $W.m^{-2}.K^{-1}$ was assigned to the lateral surfaces. The temperature of 293.15 K was assigned as the uniform surrounding (bulk) temperature as well as the stable boundary temperature on top and bottom sides of the outer blocks. The temperature response at the center point (node) on the upper surface of the middle block was calculated and compared with the experimental curve. The end time of the transient thermal analysis as well as the total time of the experimental measurement was 1300 s. Ideal thermal contacts at each contacting surface enabled perfect heat transfer through samples. The sensitivity analysis proved that the thermal resistance between surfaces does not influence heat transport significantly. Therefore all the volumes were bonded perfectly with no interaction between them.

The second numerical model consists of three cylinders of PMMA material. The thicknesses of samples were as followed: 6 mm the measured middle sample and 15 mm the outer cylinders. Isotropic thermal conductivity and other physical properties were assigned to the geometry. All boundary conditions were assigned to the model in the same way as in the previous simulation, including: the heat transfer coefficient (10 $W.m^{-2}.K^{-1}$); average heat (4.85 W) at time interval (10 s) after 10 seconds delay and the stable temperature (294.42 K). The temperature response at the center point on the upper surface of the middle cylinder was computed.

After verification of the numerical model by comparing the temperature response given by experiments and by the numerical solution, the probabilistic analysis (performed by

ANSYS Probabilistic Design System) was used to find the most influencing factors on the temperature response. The results of the probabilistic analysis are correlation coefficients. The Spearman´s rank order correlation coefficients describe the relation between the input and output parameters. Thermal conductivity, heat capacity, density and heat transfer coefficient were chosen as the input parameters. The maximum temperature value (*T_max*) and the time at the maximum temperature value (*t_max*) were assigned as the output parameters since these two parameters describe the temperature response of the material, see Figure 3. The input parameters were randomly sampled based on the Direct Monte Carlo method. This method samples the input parameters in range according to the Gaussian distribution defined by average value and standard deviation. The correlation coefficients were calculated from input and output parameters of 100 cycles of simulations.

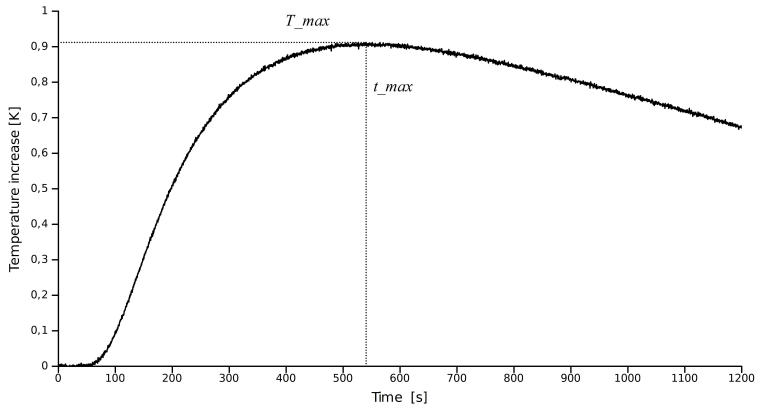

Paper III. Figure 3 Description of the typical temperature response of the material on the heat pulse

6.3. Results

The thermal properties of MDF samples with dimensions 100 x 100 mm and thicknesses 12 and 18 mm were measured at 20°C. The results are shown in Table 1. Mean thermal conductivity data measured by pulse-transient method are relatively lower compared to values reached by other methods. The thermal conductivity (0.192 $W.m^{-1}.K^{-1}$) at 7.2% moisture content and 20°C for MDF with a density of 640 $kg.m^{-3}$ measured by the hot-wire method was published by Yapici et al. (2011). Zhou et al. (2013) used light flash method to establish thermal conductivity (0.195 $W.m^{-1}.K^{-1}$) at 25 Celsius degrees for oven-dried MDF

with a density 765 kg.m^{-3}. All published works varied in used measuring method as well as in properties of samples (density, moisture content and temperature) which could explain the differences between our measured data and those gained by other authors.

Paper III. Table 1 Mean thermal properties of MDF samples measured at 20°C (values in brackets mean variation coefficient [%])

Size of samples	**d** [mm]	**ρ** [kg.m^{-3}]	**λ** [W.m^{-1}.K^{-1}]	**a** [10^{7} m^{2}.s^{-1}]	**c** [J.kg^{-1}.K^{-1}]
100 x 100 mm	12	745 (1.1)	0.123 (1.2)	0.976 (1.2)	1625.4 (1.3)
	18	765 (1.7)	0.171 (4.9)	1.261 (2.5)	1772.1 (5.6)

Only a week positive correlation between density and thermal conductivity was found on measured data. This could be caused by small variations between density values which are proved by the low coefficients of variation in density data (lower than 1.7%). The overall density of specimens was calculated gravimetrically, but the real material densities vary within the thickness of the sample. The variation of density in the thickness direction referred to the vertical density profile (VDP) profoundly affects the mechanical and physical properties of MDF. Therefore an X-ray densitometer was used to scan all samples. Results of the densitometry are presented in Fig. 4. All density profiles are symmetrical with high-density faces and slight decrease in density at depth of 2 mm from surface layers. A parabolic density profile describes density distribution in MDF with thickness of 12 mm. There are high differences between the high-density faces with mean density of 890 kg.m^{-3} and the core values of 665 kg.m^{-3}. On the contrary, a flat and almost homogeneous densification of fibers in the core of samples is present in MDF with thickness of 18 mm.

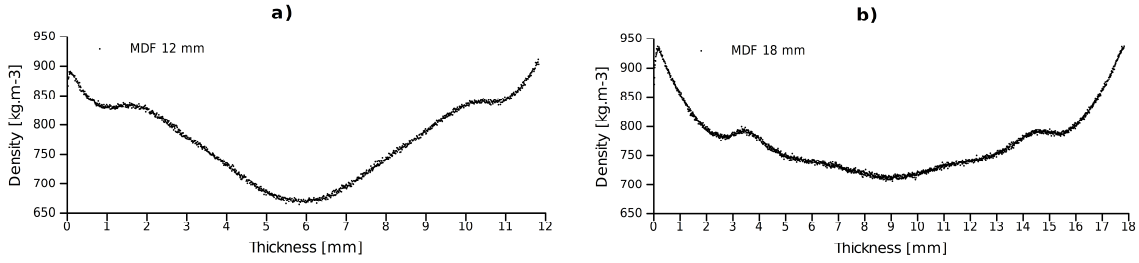

Paper III. Figure 4 Average density profiles of all MDF samples with: a) 12 mm thickness; b) 18 mm thickness

The measurement of the reference isotropic and homogenenous material PMMA was held and the temperature response recorded. The temperature increase in time was compared with the numerical results. The data were in a close agreement between each other, see Figure 5. The thermal properties of PMMA (thermal conductivity, density, thermal diffusivity, specific heat capacity) and the boundary conditions (temperature and heat transfer coefficient) were used as input parameters for the probabilistic analysis. The maximum of the temperature response as well as the time at the temperature maximum were used as output parameters. The correlation between all input and output parameters is described by Spearman´s rank order correlation coefficients, see Table 2. The input and output parameter is weakly correlated with each other when the correlation coefficient is close to zero. Two parameters are highly correlated either in a positive or negative sense for coefficients closer to 1 or -1, respectively. The coefficients in brackets mean negligible influence of the parameter.

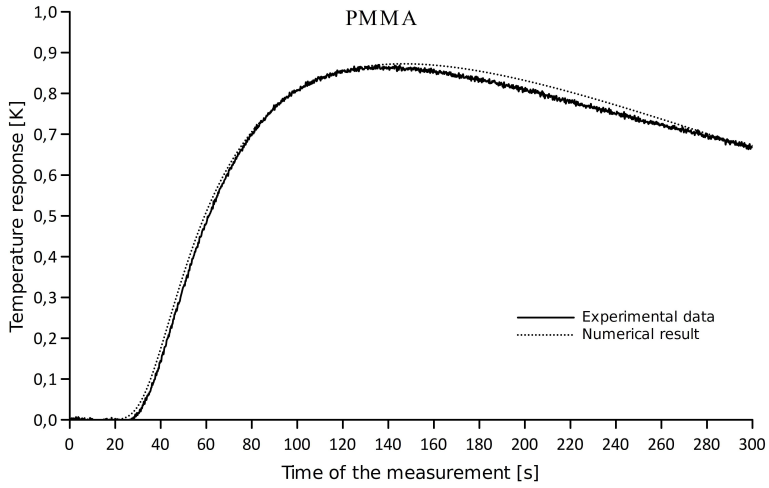

Paper III. Figure 5 Experimental and numerical data showing the agreement of both methods in description of the temperature response of PMMA on the heat pulse

The same procedure was held experimentally and numerically on orthotropic and heterogeneous MDF samples at each sample size (100 x 100 mm and 50 x 50 mm). A reasonable agreement between experimental and numerical data was found for both cases. The maximum deviation from the experimentally gained values does not exceed 0.3 °C. These relatively small differences can be caused by the simplified boundary conditions in

the numerical model, e.g. the heat at certain duration applied in the model is the time-dependent heat flux function in real conditions. The mesh refinement defining the number of solved equations as well as the time step (each second in the model, but 0.1 second in experiment) can influence the temperature response as well. All these factors significantly prolong the calculation time and increase demands for hardware capacity especially in case of probabilistic analyzes. That is why the compromise resolution was used.

As seen from the Figure 6, there are differences between thermal response of MDF with the same thickness 12 mm and different sizes 50 x 50 mm and 100 x 100 mm. The maximal thermal response and therefore the calculated thermal diffusivities for both samples vary notably (1.37×10^{-7} $m^2.s^{-1}$ at 50 x 50 mm specimen and 1.05×10^{-7} $m^2.s^{-1}$ at 100 x 100 mm).

The heat flow through the test sample is three-dimensional because of the convection heat transfer from lateral surfaces. The surrounding temperature is stable, but the heat pulse causes temperature gradient in the sample and therefore enables the heat losses to the surroundings. The heat transfer coefficient influences mainly the decreasing part of the curve as it causes cooling of the sample. The sensitivity analysis showed the negligible influence of the heat transfer coefficient on the maximum temperature response.

The differences in results of thermal parameters at two different sample sizes are explained by the increased heat transfer in direction perpendicular to the heat pulse. This problem could result from different temperatures assigned to heated platens between which the samples are pressed and the real surrounding temperature. Although the samples are covered by the isothermal cover, the room temperature influences the inner conditions. The bigger are the differences between the assigned temperature of platens and the room temperature, the more is deformed the temperature field (due the fibrous anisotropic character) within the measured specimen, especially at small dimensions. Such a problem is possible to solve by insulating the lateral surfaces of the sample so that the dimensions of samples would not affect the determination of thermal parameters.

Paper III. Table 2 Correlation coefficients between parameters

Material	Parameter	λ_1	c_1	ρ_1	λ_2	α
PMMA	*T_max*	(0.132)	-0.705	-0.614	(-0.160)	(-0.096)
	t_max	-0.547	0.599	0.516	-0.491	(0.161)
MDF 50x50 mm	*T_max*	0.359	-0.401	-0.443	-0.442	(-0.110)
	t_max	-0.448	0.637	0.613	(-0.029)	(0.089)
MDF 100x100 mm	*T_max*	(0.126)	-0.710	-0.619	(-0.147)	(-0.088)
	t_max	-0.578	0.600	0.508	-0.427	(0.190)

Density of the sample was proved to be the most important parameter that influences the temperature response, see Table 2. The MDF samples have high-density faces which possibly add a higher resistance to the heat transfer at the surface in comparison to the heat transfer through the material. As the density correlates with moisture content positively, it is appreciated to measure dried samples so that the changing moisture content could not cause density fluctuations. The differences between correlation coefficients of the homogeneous material PMMA and the heterogeneous MDF samples showed the significant influence of the thermal conductivity of first and third samples. The increased thermal conductivity of surrounding samples causes decrease in maximum of the temperature response and furthermore negatively influences the heat capacity evaluation of the measured sample. This problem occurs mainly when using materials with high variability in structure and properties.

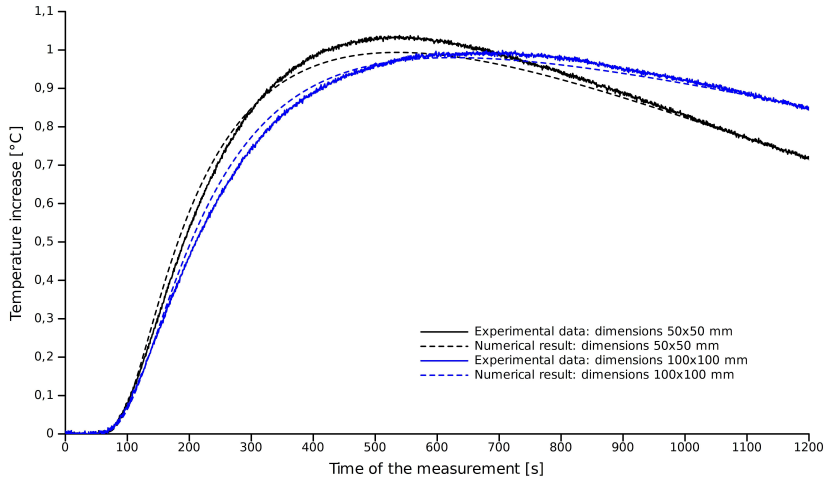

Paper III. Figure 6 Temperature response of MDF samples with dimensions 50 x 50 mm and 100 x 100 mm

6.4. Conclusion

A major motivation for this research was to investigate various effects influencing the accuracy of the pulse transient method when measuring heterogeneous fibrous orthotropic wood-based composites. The method was successfully applied in case of medium density fiberboards with different thicknesses (12 and 18 mm); thermal properties (thermal conductivity, thermal diffusivity, and specific heat capacity) were measured and compared with other published data. The numerical analysis was held to further investigate significant factors influencing the measured thermal parameters. The experimental and numerical results let to following conclusions:

- A week positive correlation between experimentally determined density and thermal conductivity was found. This is probably caused by small variations between samples densities (coefficient of variation is lower than 1.7%). The thermal conductivity of MDF samples is 0.123 $W.m^{-1}.K^{-1}$ at mean density 745 $kg.m^{-3}$ and 0.171 $W.m^{-1}.K^{-1}$ at mean density 765 $kg.m^{-3}$. Mean thermal conductivity data measured by pulse-transient method are relatively lower compared to values reached by other methods.

The numerical analysis was held to further investigate significant factors influencing the measured thermal parameters. The experimental and numerical results let to following conclusions:

- Density of the sample was proved to be the most important parameter that influences the temperature response. The variation in vertical density profile profoundly affects thermal properties of MDF. The high-density faces of MDFs possibly add higher resistance to the heat transfer at the surface of samples. A more accurate numerical model with heterogeneous properties including relation between density and thermal properties should help to quantify this phenomenon.
- Changes in samples moisture content during measurement can influence evaluation of thermal diffusivity value.

- The dimension of the measured sample affects the determination of thermal parameters. The differences in results of thermal parameters at two different sample sizes are explained by the increased heat transfer in direction perpendicular to the thickness of the sample. The surrounding temperature is a decisive factor on the heat response of the material, especially at small dimensions.
- The differences between correlation coefficients of the homogeneous material PMMA and the heterogeneous MDF samples showed the significant influence of the thermal conductivity of first and third samples on the thermal response.

The numerical analysis proved the overvaluation of specific heat capacity data (not higher than 5%) caused by the increased thermal conductivity of surrounding samples. This problem occurs when materials with very variable properties are used so that all three samples in set-up differ notably.

To further improve measurements at heat pulse method, the following suggestions are made:

- to insulate the lateral surfaces of samples, so that the dimensions would not noticeably affect the determination of thermal parameters. The proper ratio between thickness and width of samples has to be established for each measured material.
- to use first and third samples with the same thermal conductivity as the measured second sample, so that the variation in properties would not influence the accuracy of the measurement.
- to protect samples from changes in moisture content e.g. by wrapping them into thin foil or measure dry samples

Nomenclature

a	thermal diffusivity	$[m^2.s^{-1}]$
c	specific heat capacity	$[J.kg^{-1}.K^{-1}]$
λ	thermal conductivity	$[W.m^{-1}.K^{-1}]$
d	thickness of the measured sample	[m]

t_{max}	time at the maximum temperature	[s]
T_{max}	maximum temperature	[K]
U	voltage	[V]
I	electric current	[A]
ρ	density	[kg.m^{-3}]
t_0	duration of the heat pulse	[s]

Acknowledgement

The authors are grateful for the support of Internal Grant Agency (IGA) of Faculty of Forestry and Wood Technology, Mendel University in Brno, Czech Republic (project no. IGA 5/2014 "Elasto-plastic material model of wood-based composite").

6.5. References

Boháč V, Gustavsson M, Kubičár L´, Vretenár V (2003) *Measurements of building materials by transient methods*, in: Thermophysics 2003, Proc. of the Meeting of the Thermophysical Society - Working Group of the Slovak Physical Society, pp. 58-66.

Boháč V, Kubičár L´, Dieška P, Némethy L (2009) *Investigation of moisture influence on thermophysical parameters of Porfix aerated concrete*, in: Thermophysics 2009, Proc. of the Meeting of the Thermophysical Society - Working Group of the Slovak Physical Society, pp. 13-19.

Boháč V, Kubičár L´, Vretenár V (2002) *Investigation of Heat Transport in Calcium Silicate Boards by Pulse Transient Method*, in: Thermophysics 2002, Proc. of the Meeting of the Thermophysical Society - Working Group of the Slovak Physical Society, Slovak Academy of Science, pp. 87-94.

Boháč V, Kubičár L´, Vretenár V (2005) *Methodology of the testing of model for contact pulse transient method and influence of the disturbance effects on evaluating thermophysical parameters of the PMMA*, Measurement science review 5(3): 98-103.

Brombacher V, Michel F, Niemz P, Volkmer T (2012) *Investigation of thermal conductivity and moisture behaviour of fiberboards and material combinations*, Bauphysik 34: 157-169.

Chen S, Liu X, Fang L, Wellwood R (2010) *Digital X-ray analysis of density distribution characteristics of wood-based panels*, Wood Science and Technology 44: 85-93.

Kubičár L´, Boháč V, Vretenár V, Barta Š, Neuer G, Brandt R (2005) *Thermophysical properties of heterogeneous structures measured by pulse transient method*, International Journal of Thermophysics 26(6): 1949-1962.

Matias L, Santos C, Reis M, Gil L (1997) *Declared value for the thermal conductivity coefficient of insulation corkboard*, Wood Science and Technology 31: 355-365.

Miller RA, Kuczmarski MA (2009) *Method for measuring thermal conductivity of small samples having very low thermal conductivity*, National Aeronautics and Space Administration, Glenn Research Center, Ohio, NASA/TM-2009-215460, pp.1-31.

Sonderegger W, Niemz P (2009) *Thermal conductivity and water vapour transmission properties of wood-based materials*, European Journal of Wood and Wood Products 67: 13-321.

Sonderegger W, Niemz P (2012) *Thermal and moisture flux in soft fibreboards*, European Journal of Wood and Wood Products 70: 25-35.

Štefková P (2011) *Study of Thermal Properties of Materials*, Ph.D. thesis, Brno University of Technology, Institute of Physical and Applied Chemistry, pp. 1-133.

Štofanik V, Markovič M, Boháč V, Dieška P, Kubičár L´ (2007) *RT-Lab – the Equipment for Measuring Thermophysical Properties by Transient Methods*, Measurement Science Review 7(3): 15-18.

Thunman H, Leckner B (2002) *Thermal conductivity of Wood- Models for different stages of combustion*, Biomass and Bioenergy 23(1): 47-54.

Xie Y, Tong Q, Chen Y, Liu J, Lin M (2011) *Manufacture and properties of ultra-low density fibreboard from wood fibre*, BioResources 6(4): 4055-4066.

Yapici F, Ozcifci A, Esen R, Kurt S (2011) *The effect of grain angle and species on thermal conductivity of some selected wood species*, BioResources 6(3): 2757-2762.

Zhou J, Zhou H, Hu C, Hu S. (2013) *Measurement of thermal and dielectric properties of medium density fiberboard with different moisture contents*, BioResources 8(3): 4185-4192.

7. Paper IV.

Influence of temperature and moisture content on the thermal conductivity of wood-based fibreboards

Eva Troppová[1], Matěj Švehlík[1], Jan Tippner[1], Rupert Wimmer[1,2]

Materials and Structures, DOI: 10.1617/s11527-014-0467-4

a: Department of Wood Science, Mendel University in Brno, Czech Republic

b: Institute for Natural Materials Technology, IFA Tulln, University of Natural Resources and Life Sciences

Abstract

Temperature and moisture content are important parameters affecting thermal properties of wood and wood-based materials. Quantitative data are required to better characterize the thermal performance of fibreboards. The aim of this work was to assess thermal conductivity of insulation fibreboards at different temperatures (ranging from -10°C to +60°C at 10°C increments) and moisture contents (gravimetrically determined after conditioning at 15%, 50%, 85% RH). Thermal measurements were done conducted with at stationary boundary conditions. The relationship between thermal conductivity, temperature and MC of samples was found by fitting data to a second order polynomial function. Moisture behavior was characterized by applying the Hailwood-Horrobin (H-H) sorption model. The single-hydrate model was used with the equilibrium moisture data at each conditioned climate step, starting at 10% RH, up to 90% RH, at 10% RH increments. Total sorption as a composite of hydrated and dissolved water sorption was quantified for adsorption as well as desorption. Modelled data were in close agreement with the experimental data. Accurate datasets on the thermal behaviour of insulation materials are crucial in numerical modelling approaches, which will improve the proper design of building envelopes.

Keywords: Thermal conductivity; Heatflow meter (HFM); Adsorption isotherm; Hailwood-Horrobin model

7.1. Introduction

According to DIN EN 316 standard low-density fibreboards are porous panels having a density between 230 kg/m^3 and 400 kg/m^3. They are usually wet-laid, with very low additions of adhesives and sizing agents (Maloney 1993 and Youngquist 1999). Nowadays, different new dry-processes are used to manufacture very low density fibreboards (about 50 kg/m^3) with better thermal insulation parameters (Barbu 2012 and Xie 2011). Low-density fibreboards usually refer to insulation boards as they are mainly used as thermal insulation materials in civil engineering. They are often subject of strong temperature and humidity changes especially when installed as facade insulation. The expressed changes of environmental conditions cause alterations of physical properties. One of the negative consequences due to varying moisture contents are unwanted dimensional changes. Because of shrinking and swelling of the material visual and structural problems occur, including splitting, development of decay and stain fungi, and loss of mechanical strength. Along with the moisture changes, the thermal conductivity may also alter (Steinhagen 1977).

To combat unwanted changes of moisture in wood-based panels, hydrophobic additives might get added (Jiřičková et al. 2006). These additives, however, may also lead to changed thermal characteristics (Sonderegger and Niemz 2012). The transportation of heat through the panel is driven by the proportion of voids (Smith 1997 and Bekhta and Dobrowolska 2006). Herein, the positive dependency of thermal conductivity on temperature plays an important role, and becomes decisive in the case of e.g. sun exposed facades (Gur'ev and Khainer 1999). Thermal conductivity of fibreboards increases with increasing temperature linearly about 0.45% per Kelvin in the range of 10°C to 30°C (Sonderegger and Niemz 2010). Thermal conductivity depends also on the manufacturing method of the boards, mainly on the orientation of fibres, the porosity distribution and the glue fraction (Sonderegger 2011).

There is a number of ways to measure thermal conductivity. The steady-state technique measures conductivity when the material is in complete equilibrium (Salmon 2001). The heatflow meter technique uses two calibrated heatflux transducers with the specimen placed in between. A steady-state heatflux is maintained by applying a given thermal gradient

across the specimen. Thermal conductivity is then evaluated according to Fourier´s law (Siau 1984). Yu et al. (2011) used a guarded heatflux method to establish thermal conductivity of commercially produced wood-based panels. The influence of moisture content and temperature on the thermal conductivity of insulation fibreboards by heatflow measurements was shown by Matias et al. (1997). The investigation of thermal conductivity and moisture behavior of fibreboards including sorption and desorption curves was carried out by Brombacher et al. (2012) at temperatures between 10°C and 30°C. Further work refers to relationships between thermal conductivity of wood-based composites and density, as well as different particle sizes (Sonderegger and Niemz 2012) and (Sonderegger and Niemz 2009).

The vapor sorption behavior of wood fibres is comparable to solid wood, as shown before (Scheiding 1998). The Hailwood-Horrobin (H-H) model or Dent model has been frequently applied to fit the experimental data related to vapor sorption of wood. With the H-H model, sorption isotherms of wood and other natural fibres can be assessed (Hill et al. 2009).

The purpose of this work was to assess and quantify the influence of temperature and moisture on the thermal conductivity of insulation fibreboards. To comply with European standards, insulation board manufacturers usually provide thermal conductivity data measured at 23°C and 0% moisture content. As thermal conductivity is changing with temperature and moisture content, data and relationships addressing these dependencies are required, to better quantify insulation performance. The specific research objectives are therefore as followed: a) characterize the influence of temperature and moisture content on thermal conductivity of fibreboards, and b) evaluate the moisture behavior of the material using the sorption and desorption isotherms using the Hailwood-Horrobin model. The aim of the present study was also to obtain accurate parameters suitable for a wider range of temperatures and moisture contents, to numerically model coupled moisture and heat transfer processes in wooden buildings.

7.2. Material and Methods

Commercially available, wet-processed insulation fibreboards with a thickness of 35 mm were provided by the Hofatex® company. Spruce and fir chips were used as a raw material for the fibreboard production. No adhesives were added to the mixture of water and fibres. Hydrophobicity of the boards was improved by the addition of 1.5% paraffin. Aluminium sulphate (7-8%) was added to accelerate curing and hardening. Final fibreboards were glued by using the starch adhesive. The insulation fibreboards are commonly used as thermal roof insulation, outer building sheathing or ceiling facing. The thermal conductivity was 0.049 $W.m^{-1}.K^{-1}$, based on ISO 8301:1991, determined at oven-dry conditions. Ten samples sized 600 mm x 600 mm were cut, and dried in a Sanyo MTH 2400 chamber at 60°C until weight constancy (< 0.1%). Constancy of the density was checked after the heatflow measurements. For this, four small samples (50x50x35 mm) were cut from the middle part of each board. Mean gravimetric density was 243 $kg.m^{-3}$, with the coefficient of variation being as low as 0.58%.

Thermal conductivity was measured across the thickness of the board using the heatflow meter HFM 436 Lambda by Netzsch®. The fibreboard samples were placed between the two heated platens with the heatflux sensors installed (Figure 1). Thermal conductivity was determined as soon thermal heatflow equilibrium has been reached at the defined temperature difference. The heatflow meter was calibrated with the standard fiberglass board NIST 1450b, having a thickness of 25 mm. Heatflow was detected in the midpoint of the sample, representing an area of 300 mm by 300 mm. The full size of 600 mm x 600 mm was needed to ensure steady-state thermal conditions for the measured area. The temperature difference between the hot and a cold plate was set to 10°C. We have used a set of eight temperature points, ranging from -10°C to +60°C, at 10°C increments. All samples were conditioned at 20°C, and 15%, 50%, 85% relative humidity (RH) in a Sanyo MTH 2400 air chamber, respectively. Samples were wrapped in thin and transparent foils (thickness 0.01 mm) to keep moisture losses at a minimum. Samples were weighed before and after the heatflow measurement to ensure stable moisture contents. Moisture losses were recorded, and the foil-effect on thermal conductivity was also assessed.

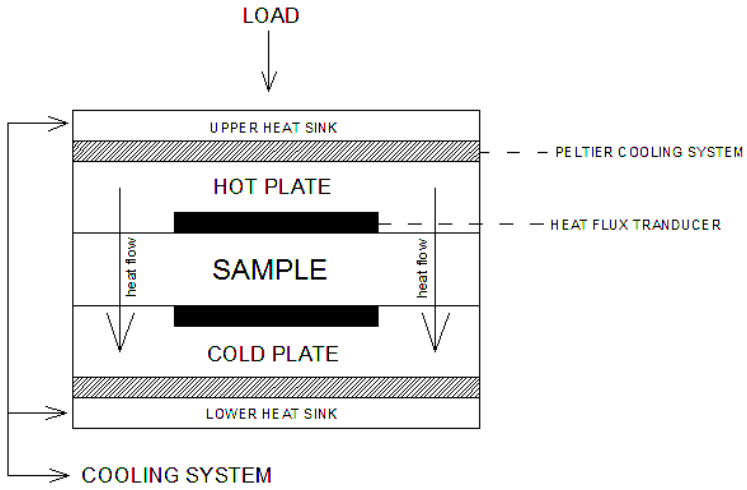

Paper IV. Fig 1 Heatflow measurement setup for the tested insulation fibreboards

Adsorption and desorption isotherms were obtained by testing 50 samples with the approximate dimensions of 50 mm x 50 mm x 35 mm. Equilibrium moisture contents (EMC) were measured (after reaching weight constancy < 0.1%) at 20°C, starting at 10% up to 90% RH, with 10% RH increments (conditioned also in the air chamber). Prior to the sorption tests the samples were dried at 60°C. Desorption measurements started from 90% RH reached by adsorption. Therefore, desorption isotherm represents rather a scanning curve than actual desorption boundary curve.

The Hailwood-Horrobin (H-H) model (Simpson 1980) as the most used model for the prediction of EMC in wood was applied. Here, the single-hydrate model was used with the equilibrium moisture data at each conditioned climate step. The constants A, B, C (1) and coefficients of the H-H model (2) were obtained through fitting a second order polynomial function to the experimental data, following (Skaar 1988). Goodness of fit was indicated by the coefficient of determination (R^2). The total sorption isotherm (3) was determined from the sum of hydrated (4), and the dissolved (5) water,

$$\mu = \frac{\varphi}{A + B.\varphi - C.\varphi^2} \tag{1}$$

$$K_1 = \frac{-B + \sqrt{B^2 + 4.A.C}}{2.A} \qquad K_2 = 1 + \frac{B}{A.K_1} \tag{2}$$

$$M_{total} = M_{hyd} + M_{dis} \tag{3}$$

$$M_{hyd} = \left(\frac{100}{\sqrt{(B^2 + 4.A.C)}}\right).\left(\frac{K_1.K_2.h}{1 + K_1.K_2.h}\right) \tag{4}$$

$$M_{dis} = \left(\frac{100}{\sqrt{(B^2 + 4.A.C)}}\right).\left(\frac{K_1.h}{1 - K_1.h}\right) \tag{5}$$

with μ being the moisture content [-]; φ the relative humidity [-]; A,B,C the regression fitting constants, K_1, K_2 the coefficients calculated for the Hailwood-Horrobin model, M_{hyd} the moisture content of hydrated water [%], M_{dis} the moisture content of dissolved water [%], and finally M_{total} as the total moisture content [%].

7.3. Results and Discussion

Thermal conductivity data of the measured insulation fibreboards at different moisture contents, for the temperature range of -10°C to 60°C, are shown in Figure 2. The average equilibrium moisture contents after conditioning at 15%, 50%, 85% of RH were gravimetrically determined. Thermal conductivity increased as temperature and moisture content of the wood went up, as previously reported (Kühlmann 1962). Yu et al. (2011) reported that the thermal conductivity is linearly proportional to the temperature, which confirms the own data.

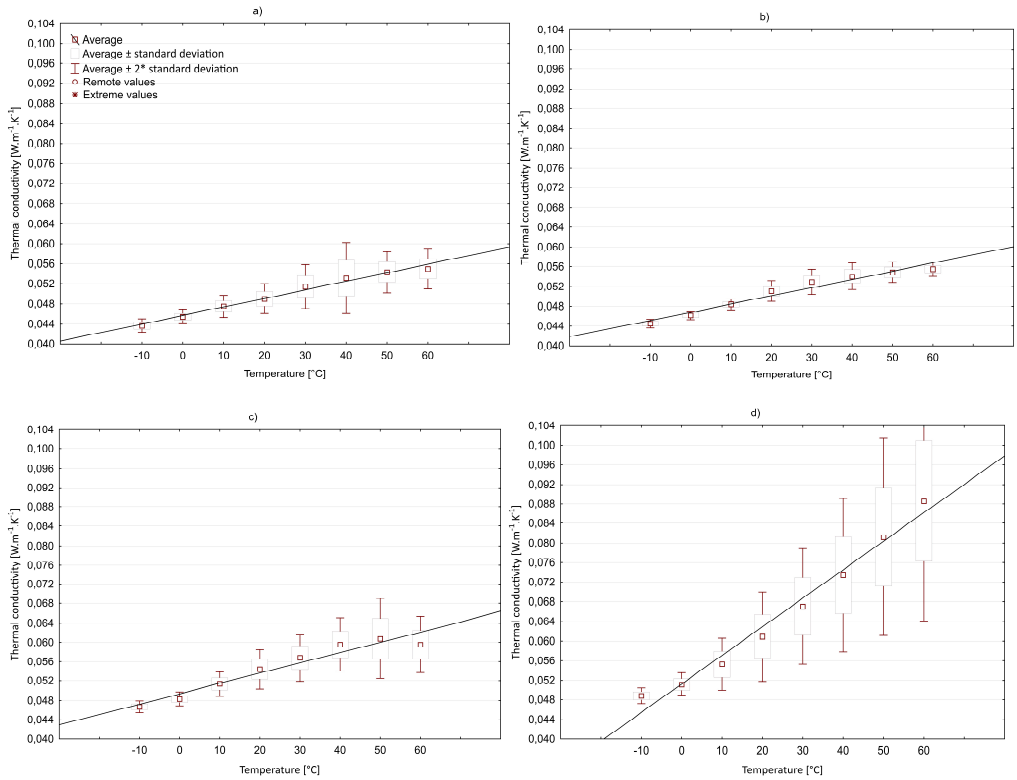

Paper IV. Fig 2 Insulation fibreboard thermal conductivity as related to temperature, at different moisture contents of the boards: a) oven dry, b) 2.58%, c) 7.41%, d) 14.29%

Accuracy of the heatflow measurement was ±3%. The influence of the thin protective foils on thermal properties proofed to be negligible (<1%). A greater variability can be seen at higher temperatures and moisture contents, which may be caused by inner moisture transfer. Even though the overall change of MC is less than 0.3% during measurement, an inner translocation of moisture seems to be possible (Avramidis and Siau 1987). This assumption is supported by the increased time at higher temperatures and moisture contents required to complete a single heatflow measurement. The heat transfer quantified by steady-state technique includes not only equivalent conduction-convection-radiation transfer but also latent heat transferred via moisture movement in the material. Application of the thermal gradient to a previously homogeneously moist fiberboard leads to a vapor pressure gradient in the material and hence to vapor diffusion and furthermore the transfer of vapor enthalpy during measurement. The heat flow due to moisture gradient is

significant especially during the initial stages of the moisture redistribution process (Bomberg and Shirtliffe 1978). Condensation occurred at the colder surfaces when conditioned at 85 % of RH leading to higher variability in measured thermal conductivity data. Increasing the MC increases the time required to reach steady-state conditions (Bomberg and Shirtliffe 1978), which confirms our assumption. The final heat flow depends on the distribution of moisture in the material in a closed system (Rudtsch 2000). The water content distribution is dependent on the temperature gradient. With lower temperature differences becomes the MC distribution rather uniform (Ikeda et al. 1980).

The conductivity values varied with moisture content, which is caused by water conduction. The higher the moisture content, the higher the thermal conductivity (Zhou et al. 2013). Thermal conductivity increased almost linearly with moisture content at a given temperature. Further, the higher the temperature, the bigger the differences were between conductivity values at oven-dry condition (increase of 12%) and at 14.2% of MC (increase of 61%). The relationship between thermal conductivity, temperature and MC of samples was established. The regression equation was found by fitting the data with a second order polynomial function (R^2= 0.958, formula 6).

$$\lambda = 0.0474 + 5.895e^{-4}w + 1.117e^{-4}T + 6.743e^{-5}w^2 - 1.226e^{-7}T^2 + 2.922e^{-5}wT \quad (6)$$

Mean moisture contents calculated for each RH during adsorption and desorption are shown in Table 1. Sorption hysteresis was observed as expected (Siau 1984, Skaar 1988 and Požgaj et al. 1997); the hysteresis coefficient describing the ratio of measured EMCs in adsorption and desorption for every RH (mean values of 8 determinations) was as high as 0.77.

The experimental data allowed representing the hysteresis for the total RH range. Parameters describing the polynomial fitting curve are listed in Table 2. The goodness of fit (R^2) was 0.94 for adsorption, and 0.97 for desorption when using the H-H model. K_1 and K_2 are equilibrium constants representing fitting parameters of measured EMC values. The K_2 value was 0.75 for adsorption, and 0.59 for desorption, which indicates that the dissolved water shows lower activity than the liquid water. Total sorption as a composite of

hydrated and dissolved water sorption is shown for adsorption as well as desorption (Figure 3). The H-H model separates the total moisture sorbed into its monomolecular (expressed in hydrated water) and polymolecular component (dissolved water) (Mantanis and Papadopoulos, 2010). Moisture content corresponding to the complete hydration was 5.56% for adsorption and 8.11% for desorption

Paper IV. Table 1 Mean values for experimentally derived EMC at various levels of RH for insulation fibreboards (coefficient of variation in parentheses)

Relative air humidity [%]	10	20	30	40	50	60	70	80
	Equilibrium moisture content [%]							
adsorption	3.0 (8.97)	4.1 (6.24)	5.2 (3.74)	6.7 (3.52)	7.8 (3.19)	9.2 (2.48)	10.4 (2.67)	14.1 (2.88)
desorption	5.3 (3.88)	6.2 (4.58)	7.6 (3.28)	8.9 (2.57)	10.2 (2.20)	11.6 (5.26)	13.2 (5.07)	15.2 (14.12)

Paper IV. Table 2 Constants calculated for the H-H adsorption isotherms

parameters	**A**	**B**	**C**	**K_1**	**K_2**	**R^2**
adsorption	2.28	14.56	12.23	9.49	0.75	0.94
desorption	1.10	11.03	6.89	17.93	0.59	0.97

Except of the H-H model, the Brunauer-Emmett-Teller (BET) theory or Dent model are often applied theories for sorption. These models use a multi-layered sorption concept, but they do not taking account partial cycles in terms of RH variations (Merakeb et al. 2009).

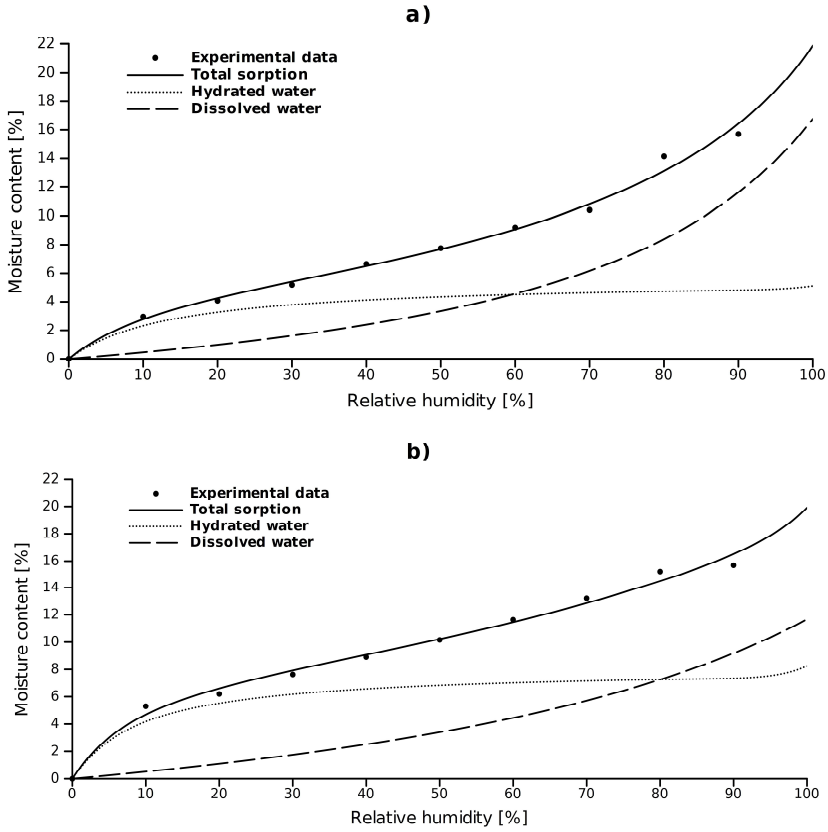

Paper IV. Fig 3 Sorption isotherms [(a) adsorption and (b) desorption] according to the H-H model at 20°C

7.4. Conclusions

A major motivation for this research was to obtain accurate parameters needed for numerical modeling of coupled moisture and heat transfer processes of insulation materials used in wooden buildings. A relationship between thermal conductivity, temperature and MC of samples was established, based on second order polynomial function fitting of experimental data. Increasing conductivity along with raising temperature and moisture content was again notified. The differences between conductivity values at oven-dry conditions and at 85% RH increased remarkably as temperature went up.

Mean values for experimentally derived EMC at various levels of RH for wood-based fibreboards were evaluated. Using the Haiwood-Horrobin (H-H) equation it was possible to separate total sorption into the hydrated and dissolved water sorption components.

Increasing humidity leads to increased moisture contents. The thermal behavior of fibreboards when installed as building façade insulation is remarkably affected by changes in temperature and moisture content. This finding is insufficiently known to manufacturers and builders. Accurate data on the thermal behaviour of insulation materials are needed, also to improve numerical modelling approaches to better optimize building envelopes.

Acknowledgement

This article is supported by the project "The Establishment of an International Research Team for the Development of New Wood-based Materials" Reg. No. CZ/1.07/2.3.00/20.0269. This work was also supported by the Internal Grant Agency of the Mendel University (project no. 25/2013).

7.5. References

Avramidis S, Siau JF (1987) *An investigation of the external and internal resistance to moisture diffusion in wood*, Wood Science and Technology 21: 249-256.

Barbu MC (2012) *Developments of wood markets- resizing of timber industry*, Proceedings of the 55th International Convention of Society of Wood Science and Technology, Beijing, China: 1-11.

Bekhta P, Dobrowolska E (2006) *Thermal properties of wood-gypsum boards*, Holz Als Roh - Und Werkstoff 64: 427-428.

Bomberg M, Shirtliffe CJ (1978) *Influence of moisture and moisture gradients on heat transfer through porous building materials*, in: Thermal Transmission Measurements of Insulation, ASTM International 211-234.

Brombacher V, Michel F, Niemz P, Volkmer T (2012) *Investigation of thermal conductivity and moisture behaviour of fiberboards and material combinations*, Bauphysik 34: 157-169.

Gur'ev V, Khainer S (1999) *Correlation of structure and thermal conductivity of highly disperse porous-fiber materials under variations of temperature and moisture*, Glass & Ceramics 56: 364-368.

Hill CAS, Norton A, Newman G (2009) *The water vapour sorption behaviour of natural fibers*, Journal of Applied Polymer Science 112: 1524-1537.

Ikeda T, Horie G, Hokoi S (1980) *Heat and moisture transfer in porous building material under condensation*, IABSE Congress report 11: 553-562.

Jiřičková M, Pavlík Z, Fiala L, Černý R (2006) *Thermal Conductivity of Mineral Wool Materials Partially Saturated by Water,* International Journal of Thermophysics 27:1214-1227.

Kühlmann G (1962) *Investigation of the thermal properties of wood and particleboard in dependency from moisture content and temperature in hygroscopic range*. Holz als Roh- und Werkstoff 20(7): 259-270.

Maloney TM (1993) *Modern particleboard and dry-process fiberboard manufacturing*, San Francisco, CA: Miller Freeman Publications.

Mantanis GI, Papadopoulos AN (2010) *The sorption of water vapour of wood treated with a nanotechnology compound*, Wood Science and Technology 44(3): 515-522.

Matias L, Santos C, Reis M, Gil L (1997) *Declared value for the thermal conductivity coefficient of insulation corkboard*, Wood Science and Technology 31: 355-365.

Merakeb S, Dubois F, Petit Ch (2009) *Modeling of the sorption hysteresis for wood*, Wood Science and Technology 43: 575-589.

Požgaj A, Chovanec D, Kurjatko S, Babiak M (1997) *Wood Structure and Properties. Priroda*, Bratislava.

Rudtsch S (2000) *Thermal conductivity measurements for the separation of heat and mass diffusion in moist porous materials*, High Temperatures - High Pressures 32(4): 487 – 491

Salmon D (2001) *Thermal conductivity of insulations using guarded hot plates, including recent developments and source of reference materials*, Measurement Science and Technology 12: 89-98.

Scheiding W (1998) *Development, production and investigation of major characteristics of water-glass-bonded fiberboards made of spruce*, Dissertation, TU Dresden.

Siau JF (1984) *Transport processes in wood*, Berlin, Springer-Verlag.

Simpson W (1980) *Sorption theories applied to wood*, Wood and Fiber 12: 183-195.

Skaar C (1988) *Wood-water relations*, Springer, Berlin.

Smith D (1997) *Thermal conductivity of fibrous glass board by guarded hot plates and heat flow meters: An international round-robin*, International Journal of Thermophysics 18: 1557-1573.

Sonderegger W (2011) *Experimental and theoretical investigations on the heat and water transport in wood and wood-based materials*, Dissertation, ETH Zurich.

Sonderegger W, Niemz P (2009) *Thermal conductivity and water vapour transmission properties of wood-based materials*, European Journal of Wood and Wood Products 67: 313-321.

Sonderegger W, Niemz P (2010) Thermal and moisture flux in soft fibreboards. European Journal of Wood and Wood Products 70 (1): 25-35.

Sonderegger W, Niemz P (2012) *Thermal and moisture flux in soft fibreboards*, European Journal of Wood and Wood Products 70: 25-35.

Steinhagen HP (1977) *Thermal conductive properties of wood, green or dry, from -40 °C to +100°C: a literature review*, U.S. Department of Agriculture Forest Service, Forest Products Laboratory, Madison, WI.

Xie Y, Tong Q, Chen Y, Liu J, Lin M (2011) *Manufacture and properties of ultra-low density fibreboard from wood fibre*, BioResources 6(4): 4055-4066.

Youngquist JA (1999) *Wood-based composites and panel products (Chapter 10). In: Wood handbook—Wood as an engineering material*, Gen. Tech. Rep. FPL–GTR–113. Madison, Wisconsin, USA; U.S. Department of Agriculture, Forest Service.

Yu ZT, Xu X, Fan LW, Hu YC, Cen KF (2011) *Experimental measurements of thermal conductivity of wood species in China: effects of density, temperature and moisture content*. Forest Product Journal 61(2): 130-135.

Zhou J, Zhou H, Hu Ch, Hu S (2013) *Measurement of thermal and dielectric properties of medium density fiberboard with different moisture contents*, BioResources 8(3):4185-4192.

8. Paper IV.a

Thermal conductivity and water vapour transmission properties of wood-based fiberboards

Eva Troppová[1], Jan Tippner[1]

Proceedings of the 57th International Convention of Society of Wood Science and Technology, June 23-27, 2014 - Zvolen, Slovakia

a: Department of Wood Science, Mendel University in Brno, Czech Republic

Additional measurements of water vapor transmission properties of different fiberboards was held and afterwards presented at the international SWST conference. Selected parts of the article are presented below:

8.1. Material and Methods

The sorption of six commercially available insulation fiberboards varying in thickness and density from three different companies were investigated. An overview of differences between the investigated boards is in Table 1. Adsorption and desorption isotherms were obtained by testing 20 samples with dimensions of 50mm x 50mm x board thickness per type. Equilibrium moisture contents (EMC) were measured at 20 °C, starting at 10 % up to 90% RH, with 10% RH increments. The specimens were dried at 60 °C before the adsorption tests. The single-hydrate Hailwood-Horrobin (H-H) model (Simpson 1980) comparable with Dent model was used with the equilibrium moisture data at each conditioned climate step. The parameters A, B, C (1) and coefficients of the H-H and Dent model (2) were obtained through fitting a second order polynomial function to the experimental data, following Skaar (1988). The total sorption isotherm (3) was determined from the sum of hydrated (4), and the dissolved (5) water which is equal to the sum of primary (6) and the secondary (7) sorbed water of the Dent model.

$$\frac{RH}{MC} = A + B(RH) - C(RH)^2 \quad (1)$$

$$K_1 = b_2 = \frac{-B+\sqrt{B^2+4AC}}{2A} \qquad K_2 = 1 + \frac{B}{AK_1} \qquad b_1 = \frac{B}{A} + 2b_2 \quad (2)$$

$$M_{total} = M_{hyd} + M_{dis} = M_1 + M_2 \quad (3)$$

$$M_{hyd} = M_0 \left(\frac{K_1 K_2 h}{1+K_1 K_2 h}\right) \qquad M_{dis} = M_0 \left(\frac{K_1 h}{1-K_1 h}\right) \quad (4, 5)$$

$$M_1 = M_0 \left(\frac{b_1 h}{1-b_2 h+b_1 h}\right) \qquad M_2 = M_0 \left(\frac{b_1 b_2 h^2}{(1-b_2 h)(1-b_2 h+b_1 h)}\right) \quad (6, 7)$$

$$M_0 = \frac{100}{\sqrt{B^2+4AC}} \quad (8)$$

with MC being the moisture content [-], RH the relative humidity [-], A,B,C the regression fitting constants, K_1, K_2 the coefficients calculated for the Hailwood-Horrobin model, b_1, b_2 the coefficients calculated for the Dent model, M_{hyd} the moisture content of hydrated water [%], M_{dis} the moisture content of dissolved water [%], M_1 the moisture content of primary sorbed water [%], M_2 the moisture content of secondary sorbed water [%] and finally M_{total} as the total moisture content [%].

Paper IV.a Table 1 Description of measured insulation fiberboards

Material	**Producer**	**Manufacturing method**	**Thickness** [mm]	**Additives**	**Density** [kg.m^{-3}]	**Thermal conductivity*** [W.m^{-1}.K^{-1}]
1	A	dry process	40	aluminium sulfate	265	0.048
2	A	dry process	40	aluminium sulfate	160	0.039
3	B	wet process	40	paraffin	210	0.044
4	C	dry process	32	PUR + paraffin	270	0.063
5	C	dry process	60	PUR adhesive	230	0.047
6	B	wet process	35	paraffin	260	0.049

*Values given by producers, determined according to EN ISO 10456

8.2. Results and Discussion

The sorption models (H-H model and Dent model) allowed representing the hysteresis for the total RH range. The total sorption of material 6 is shown for adsorption and desorption (Figure 1). The H-H model separates the total moisture sorbed into its monomolecular (expressed in hydrated water) and polymolecular components (dissolved water) (Mantanis and Papadopoulos 2010), which is comparable to primary and secondary sorbed water of the Dent model. The primary water (M_1) of the Dent model is slightly higher than the hydrated water (M_{hyd}) of the H-H model, see Figure 1. The secondary water of the Dent model (M_2) is slightly lower than the dissolved water (M_{dis}) of the H-H model, which is also confirmed by Sonderegger and Niemz (2012). However, the total sorption isotherm (M_{total}) is equal in both models. Complete monolayer coverage of all available sorption sites is represented by MC 5.56 % corresponding to complete hydration for adsorption and MC 8.11% for desorption. As seen from Figure 1, the values at 100 % RH were lower for desorption than for adsorption. This was caused by the fact that the measurements start and end at 90 % of RH instead of 100 % of RH.

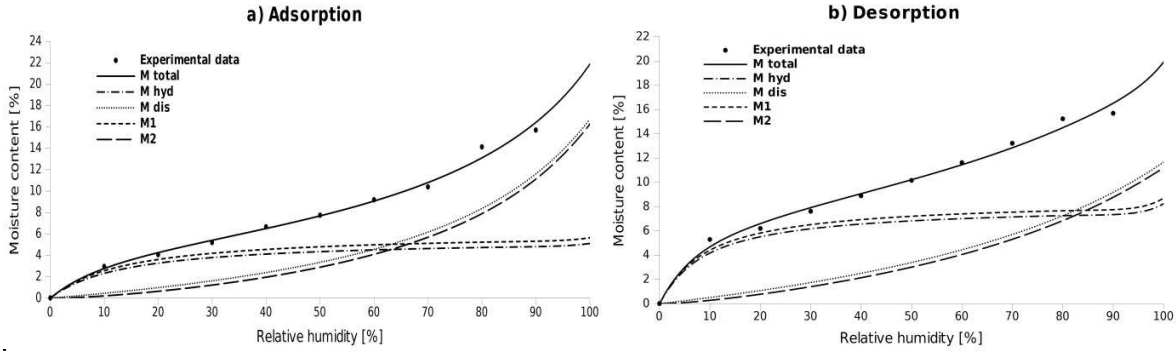

Paper IV.a Figure 1 Sorption isotherms of material 6 ((a) adsorption, (b) desorption) according to the single-hydrate H-H model and Dent model

Figure 2 shows the total adsorption and desorption curves of materials 1-5. Sorption isotherm of selected fiberboards (material 1, 2 and 5) rapidly increases above about 80% RH. This effect can be caused due to the absence of additives which are in some cases added during the manufacturing process to improve the water resistance properties. Additives probably change the saturation of water vapor in the air, as discussed by Sonderegger and Niemz (2012), Lesar et al. (2009) or Seifert (1972).

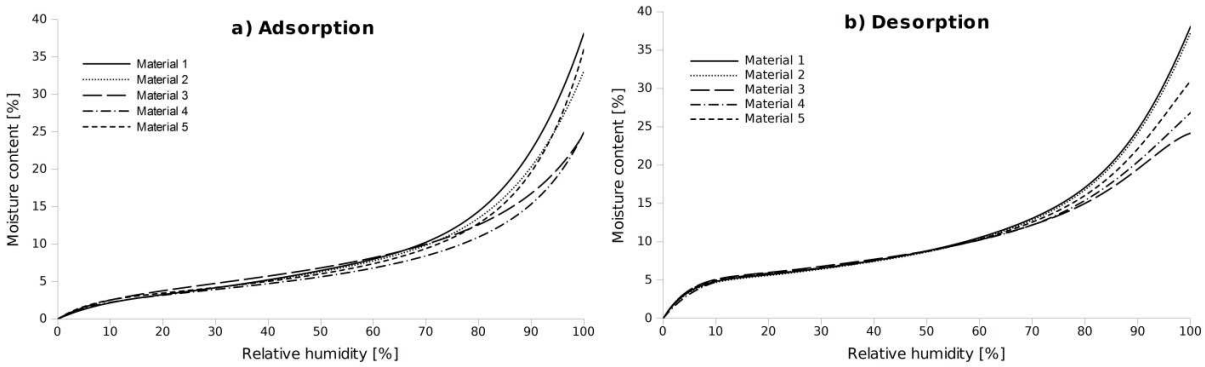

Paper IV.a Figure 2 Adsorption (a) and desorption (b) isotherms of the total sorption (material 1-5) according to the H-H and Dent model

8.3. Conclusions

Mean values for experimentally derived EMC at various levels of RH were evaluated. The H-H model and Dent model were used to investigate the water vapor sorption. The expected sorption hysteresis was observed. The manufacturing process and the lack of additives probably lead to increase in sorption of selected fiberboards above 80 % RH.

8.4. References

Lesar B., Gorisek Z., Humar M. (2009) *Sorption properties of wood impregnated with boron compounds, sodium choride and glucose*, Dry Technology 27(1) : 94-102.

Mantanis G.I., Papadopoulos A.N. (2010) *The sorption of water vapour of wood treated with a nanotechnology compound*, Wood Science and Technology 44(3): 515-522.

Simpson W. (1980) *Sorption theories applied to wood*, Wood Fiber 12(3) : 183-195.

Skaar C (1988) *Wood-water relations*, Springer, Berlin.

Sonderegger W., Niemz P. (2012) *Thermal and moisture flux in soft fibreboards*, European Journal of Wood and Wood Products 70 : 25-35.

Seifert J. (1972) *Zur Sorption und Quellung von Holz un Holzwerkstoffen. Erste Mitteilung: Einflusse auf das Sorptionsverhalten der Hlzwerkstoffe*, Holz Roh-Werkst 30(3) : 99-11

9. Paper V.

Numerical and experimental study of conjugate heat transfer in a horizontal air cavity

Eva Troppová [1*], Jan Tippner [1], Matěj Švehlík[1]

[1] Department of Wood Science, Faculty of Forestry and Wood Technology, Mendel University in Brno

Manuscript sent to Construction and Building Materials

Abstract

The demand for general reduction of the energy consumption in civil engineering leads to more frequent use of insulating materials with air gaps or cavities. Heat transfer through a constructional part can be decreased by adding an air gap and low emissivity reflective foils to the structure. In the first part of this paper, the impacts of cavity thickness and inner surface emissivity on combined conduction, convection and radiation heat transfer was experimentally explored in the case of constructional part with a horizontal cavity subjected to constant downward heat flux. The heat flow meter Netzsch HFM 436 Lambda was used for steady-state measurements. Results suggest that the studied parameters seriously affect the combined heat transfer in the composed structure. In the second part the paper reports the numerical study of two-dimensional conjugate heat transfer in closed horizontal cavity having air as the intervening medium. Numerical models validated by related experimental results were performed to further investigate the effect of radiation heat transfer. It was found that in general, the total heat flux through the composed structure decreases with increasing air cavity thickness, which is significant especially when low emissivity inner surfaces are taking into account. The direction of heat flow (downward or upward heat flow) has a significant impact on the convection heat transfer. An important contribution from the present work is the analysis of the optimal thickness of the cavity at different boundary conditions. The optimal thickness of the enclosure with low emissivity surfaces is 16 mm when subjected to upward heat flux.

Keywords: horizontal air cavity, conjugate heat transfer, Rayleigh-Bénard convection, numerical models, insulation fibreboard, reflective foil

9.1. Introduction

The demand for reduction of the energy consumption in building industry leads to more frequent use of environmentally friendly building materials such as wood or wood-based composites. There are various kinds of exterior wall systems which can be well optimised by varying the insulation material (Kosnya et al., 2014). However, there are also other possibilities to optimize the thermal performance of building. Probably the best insulating materials nowadays derive benefit from low thermal conductivity of air or low-conductive gasses. A vacuum insulation panel is an example of such a material (Baetensa et al., 2010). However, there is still the hazard of losing inner vacuum or gas (Xie at al., 2010). Simple adding of non-ventilated air gap into a structure composition is more frequently used solution.

The experimental and numerical methods exist to study the thermal performance of constructional parts including an air layer. The numerical model for determining an influence of the air gap thickness on the thermal resistance of a whole construction is included in the work of Mavromatidis et al. (2012). The thicker the air layer, the more the inner gas flux affects the overall thermal conductivity. Many authors dealt with the optimal air gap thickness as with increasing dimensions the convection heat transfer occurs (Xie et al., 2014; Armando et al, 2010; Mahlia and Iqbal, 2010). The dimension of an air cavity (mainly its thickness) is also decisive for domination of radiative part of the heat transfer. Another way how to improve thermal properties of a construction without using additional insulation and therefore escalate the thickness is to insert a reflective foil to the wall composition. Numerical heat transfer analysis of combined conduction and radiation in transparent insulation material is performed by Kessentinia et al. (2014). The thermal resistivity of an enclosed air cavity with reflective surfaces was investigated by Saber (2012) at different inclinations and directions of a heat flow. Pelzers and Schijndel (2013) studied also an influence of reflective insulation material enclosed by air cavities on the overall thermal performance. They stated that the highest thermal resistance values are

obtained when reflective materials are applied in building components in which upward heat flow occurs.

Multi-layer insulation material consisting of plywood, aluminium reflective foil and air gaps was investigated by Pasztory et al. (2013). The heat transfer was theoretically determined by finite element method and then compared with results of steady state heat flow measurement. A guarded hot box was used by Mavromatidis et al. (2012) to determine the heat transfer through different layers of fibrous materials and aluminium foils, placed between one or two air gaps. The impact of cavity thickness on a block of exterior wall`s thermal conductivity researched Aviram et al. (2001) by the means of a guarded hot box. All experimental studies respect the fact that the radiant thermal insulation is the most effective when installed as a boundary surface of an air chamber. The effective thermal resistance depends then on the emissivity of the radiant barrier and the thickness of the air cavity (Escudero et al., 2013).

The presented investigation deals with the combined effect of natural convection and surface radiation in air filled cavities surrounded by uniformly heated plates of wood-based fibreboards. Both experimental and numerical validation is performed. The average heat flux passing through the construction with different air gap thicknesses was measured using the heat-flow meter. The possibility of increasing the thermal resistance by using low emissivity aluminium foils was investigated. Numerical models describing the heat propagation and air movement in the cavity were performed at different directions of a heat flow.

9.2. Material and methods

9.2.1. Experimental measurement

Dry-processed insulation fibreboards provided by Agepan® company were cut to a size 600 mm x 600 mm. Hydrophobic, diffusion-open fibreboards with a thickness of 32 mm were conditioned in a Sanyo MTH 2400 chamber at 20°C and 65% relative humidity until weight constancy (weight changes < 0.1%). The structure with horizontal air gap was created from fibreboards. A frame from the same material was placed between two fibreboards to create an air cavity, see Figure 1. The thickness of the frame determined the

thickness of the horizontal air gap which varied from 5 mm to 20 mm at 5 mm increments. Additionally, inner surfaces of fibreboards creating the air cavity were covered by aluminium foils.

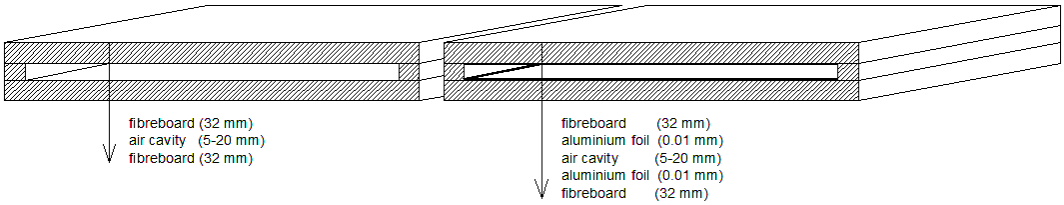

Paper V. Figure 1 The composition of measured samples; left: without aluminium foils (ε=0.9), right: with aluminium foils on inner surfaces (ε=0.3)

The effective thermal conductivity of the construction was measured across the thickness using the heat flow meter Netzsch® HFM 436 Lambda. Measured samples were placed between two platens with thermal sensors and pressed with certain pressure to ensure minimum thermal resistance. Stationary measurements were held at mean temperature of 20°C. The temperature difference between the hot and a cold plate was set to 10°C. The hot plate is at the top during all measurements, see Figure 2. Samples were wrapped in thin transparent foils (thickness 0.01 mm) to avoid moisture changes during the measuring process. Five different measurements at each air gap thickness were held to study variation in data. Afterwards, the low-emissivity reflective foils were placed at each inner side of fibreboards to enclose the air cavity. Heat flow was detected as soon thermal equilibrium has been reached. Effective thermal conductivity of the whole composed sample is then calculated based on the following equation:

$$\lambda_{eff} = N\frac{\Delta x}{\Delta T} = \frac{\Delta x(q_{upper}+q_{lower})}{2\Delta T} \quad (1)$$

with λ_{eff} the effective thermal conductivity [$W.m^{-1}.K^{-1}$]; q is the heat flow [W]; λ the thermal conductivity [$W.m^{-1}.K^{-1}$]; ΔT the temperature difference [K]; Δx the thickness of the sample [m]; N the calibration factor [$W.m^{-2}$].

Firstly, solely fiberboards were measured to compare thermal conductivity values with the normative ones. Afterwards, measurements with different air gap thicknesses were held. Finally, reflective foils with aluminium cover were placed on both inner sides of fibreboards to enclose the air cavity. Thermal measurements were then repeated for all selected cavity dimensions (5, 10 15 and 20 mm).

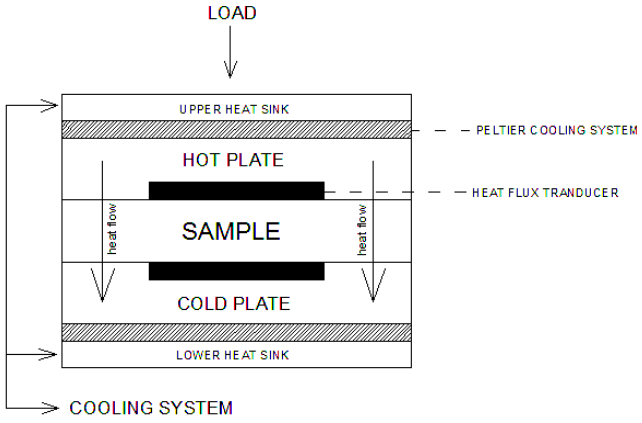

Paper V. Figure 2 Setup of the heat flow meter measurement (adopted from Troppová et al., 2014)

The heat transfer through the composed samples consists of all heat transfer modes: heat conduction in the solid materials, convection and radiation in the air cavity. The ratio of change in transferred heat via radiation depends on the temperature difference between surrounding plates and the emissivity of surfaces. The presumption is therefore that the low emissivity surfaces decrease the total heat flow through the structure based on decreased radiation heat transfer. The optimal thicknesses of the air gap together with the direction of the heat flow are the most influencing factors.

9.2.2. Numerical analysis

Ansys Parametric Design Language (APDL) was used to develop finite element numerical models describing the heat transfer through the structure. Two-dimensional analyses were performed using the Ansys FLOTRAN element Fluid 141 in quadrilateral form. Geometry consists of a solid/non-fluid and a fluid part. The two non-fluid parts represent fibreboards layers. The fluid part is defined as incompressible air layer with

enabled buoyancy driven flow. Physical properties of both materials (see Table 1.) were assigned to the geometry. The fluid-structure interaction was created by the connection of adjacent finite element meshes with different material properties. Dirichlet´s (first type) boundary conditions were used. Different temperatures were assigned to the top and the bottom line of the model which creates temperature difference 10 K. The fluid flow in the air cavity is caused only by the temperature gradient as the pressure value is uniform at the beginning of the analysis. The boundary conditions applied to the model are described in Figure 3.

Paper V. Table 1 Physical properties of non-fluid and fluid materials used in the model

Material property	Solid (fibreboards)	Fluid (air)
λ_0 [W.m^{-1}.K^{-1}]	0.0530	0.0242*
ρ [kg.m^{-3}]	195	1.125
c [J.kg^{-1}.K^{-1}]	2100	1006.43
μ_0 [kg.m^{-1}.s^{-1}]	-	1.7894e^{-5}*

* Thermal conductivity and dynamic viscosity vary with temperature based on Sutherland's formulas (Ansys, 1998): see eq. 2 and eq. 3

$$\lambda = \lambda_0 \left(\frac{T}{c_1}\right)^{1,5} . \left(\frac{c_1 + c_2}{T + c_2}\right) \qquad (2)$$

with λ_0 the initial thermal conductivity [W.m^{-1}.K^{-1}]; c_1 the temperature when $\lambda = \lambda_0$: 293.15 [K]; c_2 the Sutherland coefficient: 194.44 [K].

$$\mu = \mu_0 \left(\frac{T}{c_1^{\mu}}\right)^{1,5} . \left(\frac{c_1^{\mu} + c_2^{\mu}}{T + c_2^{\mu}}\right) \qquad (3)$$

with λ_0 the initial dynamic viscosity [W.m^{-1}.K^{-1}]; c_1^{μ} the temperature when $\mu = \mu_0$: 293.15 [K]; c_2^{μ} the Sutherland coefficient: 110.56 [K].

The governing equations solved by Ansys FLOTRAN in fluid environment of the model are the Navier-Stokes equations. Following assumptions in the solved simulation of closed air domain are valid: the flow is laminar, the fluid is nonparticipating in radiation transfer,

and the Boussinesq approximation is performed in the steady-state calculation. This approach is valid as the temperature differences in the domain are small. The conservation equations for viscous fluid flow and energy are solved in the fluid region, while only the energy equation (Fourier´s law) is solved in the solid/non-fluid region. For the fluid element, the velocities (in X and Y direction) are obtained from the conservation of momentum principle, the pressure is obtained from the conservation of mass principle and the temperature is obtained from the law of conservation of energy (Anderson, 1995). The Boussinesq model treats density as a constant value in all solved equations, except for the buoyancy term in the momentum equation:

$$(\rho - \rho_0)g \approx -\rho_0 \beta (T - T_0)g \qquad (4)$$

with ρ is the density [kg.m^{-3}]; g the gravitational acceleration [m.s^{-2}]; ρ_0 the constant density of the flow [kg.m^{-3}]; β the thermal expansion coefficient [K^{-1}] and T_0 the operating temperature [K].

The solution of air velocity and also the heat transfer in the air layer is strongly dependent on the mesh distribution. A fine mesh (a quadrilateral element) with 20 divisions along the cavity thickness was created. The stationary analyses with high number of iterations (1000 iterations) were performed. The number of global iterations required to achieve a converged solution vary depending on the size of the problem. The smaller the cavity and therefore the element size, the higher iteration number is needed.

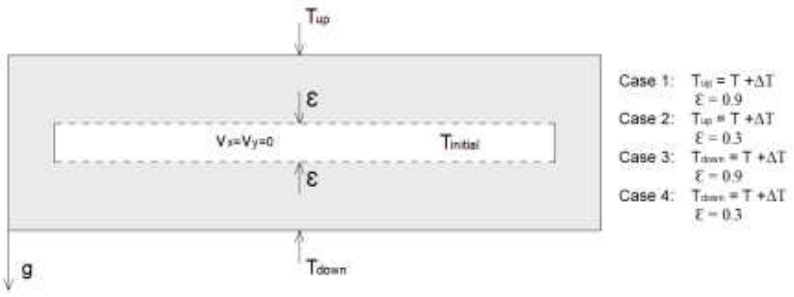

Paper V. Figure 3 Boundary conditions applied to the model

There were four different cases calculated for four various thicknesses of the air cavity (5, 10, 15 and 20 mm). The cases differ in the emissivity value assigned to inner surfaces (0.3 or 0.9) and the direction of the heat flow (upwards and downwards). The differences between boundary conditions of all cases are described in detail in the Table 2. The experimental data were used for validation of case 1 (without reflective foils) and case 2 (with reflective foils).

Paper V. Table 2 Differences between computed cases

Cases	**Air cavity thickness** [mm]	**Emissivity coefficient of inner surfaces** [-]	**Temperature T_{up}** [°C]	**Temperature T_{down}** [°C]	**Direction of heat flow**
Case 1	5, 10, 15, 20	0.9	25	15	downwards
Case 2	5, 10, 15, 20	0.3	25	15	downwards
Case 3	5, 10, 15, 20	0.9	15	25	upwards
Case 4	5, 10, 15, 20	0.3	15	25	upwards

9.3. Results

The average thermal conductivity of conditioned fibreboards determined at mean moisture content 4.6% and 20°C by heat flow meter is 0.053 $W.m^{-1}.K^{-1}$, based on ISO 8301:199. The measured thermal conductivity value was further used in numerical simulations. Effective thermal conductivity data of the measured composed samples with and without reflective foils, at the mean temperature 20°C, are shown in Table 3. Accuracy of the heatflow measurement was ±3%. Effective thermal conductivity increases with increasing thickness of the air cavity, for both cases. The emissivity coefficient was proved to be the most influential factor contributing to the decrease of total heat flow. The significance of radiation transfer increases with increase in the air gap thickness. The effective thermal conductivity of the sample with reflective foils decreased to 13.7% compared to the sample without reflective foils at 20 mm thick air gap. There is almost no difference between both cases at 5 mm air gap. This is caused by low temperature gradient within the small cavity, therefore low impact of radiation transfer. Therefore, the thicker is the air enclosure, the more efficient is the usage of low effective reflective foils.

Paper V. Table 3 Experimental effective thermal conductivity values for system with air gaps

Effective thermal conductivity λ [W.m^{-1}.K^{-1}]	**Thickness of the air gap [mm]**			
	5	**10**	**15**	**20**
without reflective foils	0.0537 (0.24)	0.0557 (1.62)	0.0588 (1.92)	0.0617 (2.13)
with reflective foils	0.0531 (0.22)	0.0508 (1.08)	0.0517 (1.19)	0.0532 (0.35)

Thermal transmittance, described as the rate of heat transfer through one square meter of a structure divided by the temperature difference (in W.m^{-2}.K^{-1}), is common concept in building design. It is a benchmark for the comparative efficiency of materials or whole building elements. Therefore, thermal transmittances of structures with and without low emissivity foils for different air gap thicknesses were calculated based on the experimental data. As seen from Figure 4, the thermal transmittance decreases with increasing air gap thickness. The low thermal conductivity of air decreases the total heat transferred through the whole structure. The high impact of emissivity of inner surfaces is apparent. The thicker is air gap, the bigger are differences between transmittance values for cases with and without reflective foils.

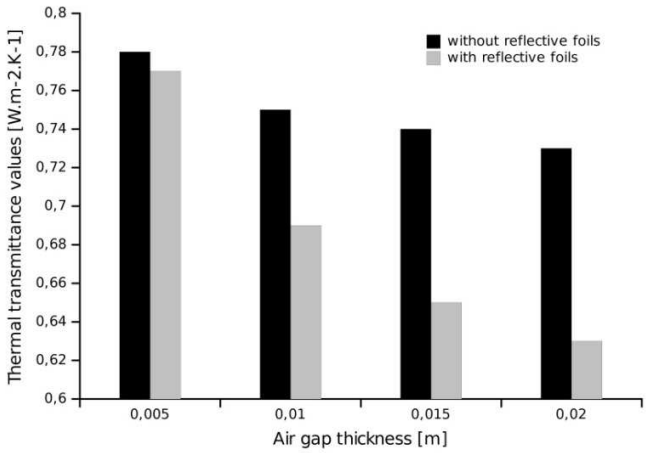

Paper V. Figure 4 Experimentally obtained thermal transmittance values for a structure with different air gap thicknesses at downward heat flux

Cases 1 and 2 (see Table 2) were computed using Ansys FLOTRAN to reach the heat flux values caused by all heat transfer modes. The total heat flux values computed numerically were compared with the experimental ones and they were in a close agreement between each other, see Figure 5. The numerical results differ from the experimental values by less than <4% over the range 6 $W.m^{-2}$ to 8 $W.m^{-2}$. It was found that the radiative heat transfer is dominant at high emissivity coefficient of inner cavity surfaces (Figure 5, Case 1). Pelzers and Schijndel (2013) stated that the convective heat transfer is dominant when low emission coefficient materials are applied to structure, which confirm the own data (Figure 5, Case 2).

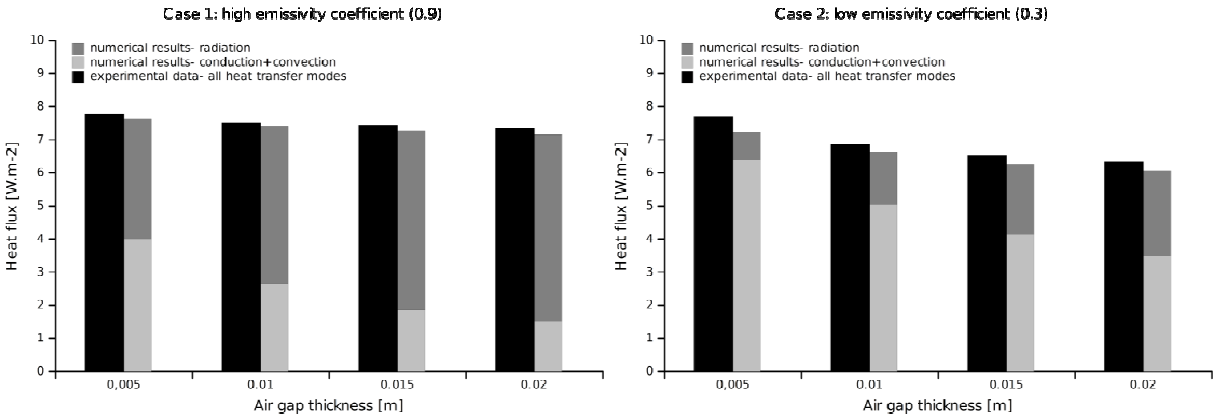

Paper V. Figure 5 Comparison of experimentally and numerically calculated total heat flux values for cases 1 and 2.

As predicted, the direction of the heat flow is decisive in laminar flow development. The characteristics of heat transfer through a horizontal enclosure depend whether the hotter plate is at the top (downward flow) or at the bottom (upward flow). If the downward flow is applied, no convection will develop in the enclosure since the lighter fluid is still on the top of the heavier fluid (see Figure 6, Cases 1 and 2). The heat flow in the enclosure is then caused purely by conduction and radiation heat transfer. If the upward flow is induced, the buoyancy driven flow will occur in the enclosure. The heat transfer is still by pure conduction, until the lighter hotter fluid rise to the colder top plate and cools down. At certain Rayleigh number (Ra>1708), the buoyant force overcomes the fluid resistance and

initiates natural convection currents (Çengel and Ghajar, 2011). The convection current in the form of hexagonal Bénard cells is evident in Figure 6, Case 4.

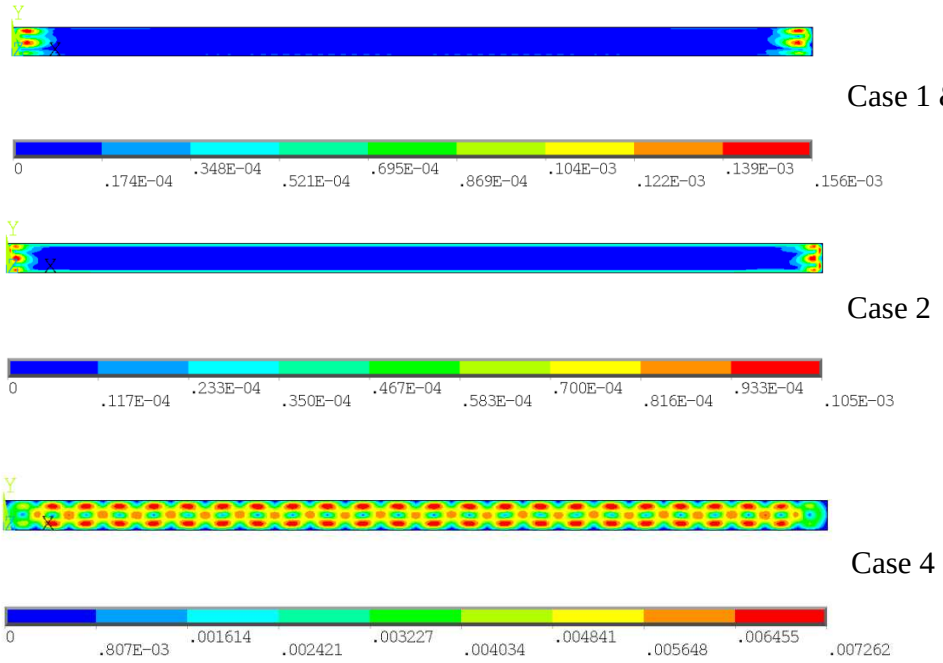

Paper V. Figure 6 The average air velocity [m.s^{-1}] within the enclosure at 20 mm thickness for all computed cases

The uneven temperature distribution within the air cavity arises from the low emissivity coefficient of inner surfaces which leads to Rayleigh-Bénard convection at thinner enclosures. The velocity field distribution (0.007 m.s^{-1}) originates in case 3 (ε=0.9) at 28 mm thick enclosure, while the same velocity field originates in case 4 (ε=0.3) at thickness 20 mm. Air velocities of cases 1 and 3 are equal at the 20 mm thickness, as the Rayleigh number does not exceed critical value to enable buoyant flow.

The laminar flow results solely from density gradients brought about by temperature variations. Those natural convection currents occur at the 18 mm thick air enclosure (case 4) bringing the increase in total heat flux value, see Figure 7. This statement was proved by the calculated air velocity distribution in the enclosure (Figure 6, Case 4). The differences between heat flux values in cases with low emissivity surfaces (ε=0.3) at upward (case 4) and downward (case 2) heat flow are shown in Figure 7. Total heat flux values are equal up

to the thickness 18 mm. The total heat flux decreases constantly with increasing enclosure thickness in case 2, as the convection heat transfer does not affect it.

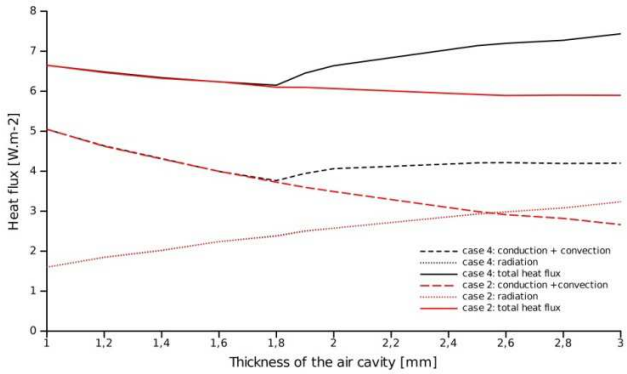

Paper V. Figure 7 Comparison of heat flux values of cases 2 and 4 in thickness range of the enclosure 1-3 mm

9.4. Conclusion

The experimental and numerical study of conjugate heat transfer in horizontal enclosure (560x560 mm and thickness 5-20 mm) at different heat flow directions was presented. Numerical models dealing with heat transfer in composed samples subjected to downward heat flow were verified by experimental data. The heat flow meter method was used to measure effective thermal conductivity of samples. Based on the close agreement between data, the numerical analyses of samples at upward heat flow direction were held and the total heat flux calculated. The obtained experimental and numerical results led to the following conclusions:

- The effective thermal conductivity increases with increasing thickness of the enclosure. Radiation heat transfer contributes to the decrease of total heat flow significantly. The thicker is the air gap, the more dominant is the decrease of heat flow caused by radiation
- The thermal transmittance value decreases with increasing air gap thickness because of the low thermal conductivity of air. This statement is valid for samples subjected to downward heat flow where no convection occurs.
- Direction of the heat flow is decisive in development of a buoyant driven flow. Rayleigh-Bénard convection occurs at enclosures thicker than 18 mm at upward

heat flow direction. Low emissivity of surfaces causes laminar convection at thinner cavities than at cases with higher emissivity coefficients which limits the cavity usage.

- Overall, the reflective materials with low emissivity coefficient decrease total heat transferred through the structure based on low radiation heat transfer. The total heat flux was decreased by 13.8% when using low emissivity foils (ε=0.3) inside 20 mm thick air enclosure at downward heat flow direction. The best application of air enclosure is in building components subjected to downward heat flow, as e.g. ground floor of a building. The advantage of air enclosures in structures where upward heat flow occurs is limited to small dimensions of the enclosure, as at thicker cavities convection heat transfer occurs. The possible solution is the division of thick enclosure into several thinner cavities.

The results demonstrated the possible application of air enclosures in certain building component. The numerical analysis can furthermore serve for prediction of heat flows in enclosures with higher dimensions or other boundary conditions.

Acknowledgement

The authors gratefully acknowledge the financial support of the International Grant Agency of the Mendel University (project no. 19/2014).

9.5. References

Anderson J.D. (1995) *Computational Fluid Dynamics: The basics with Applications*, McGraw-Hill, Inc., United States : 1-383.

ANSYS Theory reference, Release 5.5 ANSYS Inc., Canonsburg PA, USA, 1998.

Armando G.-M., Armando B.-B. J., Christian V.-C., Rangel-Hernández V.H., Belman-Flores J.M. (2010) *Analysis of the conjugate heat transfer in a multi-layer wall including an air layer,* Applied Thermal Engineering 30 : 599-604.

Aviram D.P., Fried A.N., Roberts J.J. (2001) *Thermal properties of a variable cavity wall*, Building and Environment 36 : 1057–1072.

Baetensa R., Jellea B. P., Thueb J. V., Tenpierik M. J., Grynninga S., Uvsløkka S., Gustavsene A. (2010) Vacuum insulation panels for building applications: A review and beyond, Energy and Buildings 42 : 147-172.

Çengel, A.J. Ghajar (2011) *Heat and Mass Transfer: Fundamentals and Applications*, Fourth Edition in SI Units, McGraw-Hill : 1-902.

Escudero C., Martin K., Erkoreka A., Flores I., Sala J.M. (2013) *Experimental thermal characterization of radiant barriers for building insulation*, Energy and Buildings 59 : 62-72.

Kessentinia H., Capdevilaa R., Castroa J., Olivaa A., Boudenb C. (2014) *Three dimensional heat transfer analysis of combined conduction and radiation in honeycomb transparent insulation*, Solar Energy 105 : 58-70.

Kosnya J., Asizb A., Smith I., Shresthad S., Fallahi A. (2014) A review of high R-value wood framed and composite wood wall technologies using advanced insulation techniques, Energy and Buildings 72 : 441-456.

Mahlia T.M.I., Iqbal A. (2010) *Cost benefits analysis and emission reductions of optimum thickness and air gaps for selected insulation materials for building walls in Maldives*, Energy 23 : 2242-2250.

Mavromatidis L. E., Bykalyuka A., Mankibia M. El, Michela P., Santamourisb M. (2012) *Numerical estimation of air gaps' influence on the insulating performance of multilayer thermal insulation*, Building and Environment 49 : 227-237.

Pásztory Z. (2013) *Improved heat insulation system (Mirrorpanel) for construction of wood buildings*, Holzforschung 67 (6) : 715-718.

Pelzers R.S., Schijndel A.W.M. (2013) *Numerical analysis of the thermal resistance of a multi-layer reflective insulation material enclosed by cavities under varied angles*, Comsol Conference Rotterdam October 23-25 : 1-8.

Saber H. H. (2012) *Investigation of thermal performance of reflective insulations for different applications*, Building and Environment 52 : 32-44.

Troppová E., Švehlík M., Tippner J., Wimmer R. (2014) *Influence of temperature and moisture content on the thermal conductivity of wood-based fibreboards*, Materials and Structures, DOI: 10.1617/s11527-014-0467-4.

Xie G.F., Li X.D., Wang R.S. (2010) *Study on the heat transfer of high-vacuum-multilayer-insulation tank after sudden, catastrophic loss of insulating vacuum,* Cryogenics 50 : 682-687.

Xie Z., Chen L., Sun F. (2014) *Constructal optimization for an insulating wall combining heat flow, strength and volume,* International Communications in Heat and Mass Transfer 54 : 141-147.

10. Paper VI.

Thermal bridges in a prefabricated wooden house: experimental and numerical characterization

Eva Troppová[1], Jan Klepárník[1], Jan Tippner[1]

a: Department of Wood Science, Mendel University in Brno, Czech Republic

Manuscript

Abstract

The major aim of this study was to create a numerical model of thermal bridges in a wooden structure and to discover differences between factual values of linear thermal transmittance utilized in the FE modelling and values given by the European normative method (EN ISO 14683). Thermal bridges of wooden structures were detected using thermocamera FLIR S65 for infrared detection. These measurements allow displaying the temperature distribution of the thermal scan and proving the positive correlation between heat flux and change in the evaluated temperatures of a thermal bridge. A three-dimensional FE model of the structure was prepared for thermal analysis using the engineering software ANSYS Workbench 13. The transmission heat loss coefficients of a prefabricated wooden house were established based on Czech normative method (ČSN 73 0540-4). Linear thermal transmittance values calculated from thermal analysis and the normative method given by EN ISO 10211 were compared. The results show that even if the transmission heat loss coefficients meet the requirements designated by standards, the real heat losses are increased by thermal bridges involved in the construction. Their influence is determined by the linear transmittance value which is usually not exactly established.

Keywords: Thermal bridges; Infrared thermography; Linear thermal transmittance; Numerical simulation

10.1.Introduction

Globally, minimization of energy consumption is emphasized to reduce environmental impacts. This trend is expressed in the building industry with common energy efficiency, but also during their construction and life cycle. Increasing demand for low-energy and passive houses accompanies assumption of stricter European norms. Energy saving requires both optimal choice of heating and energy-efficient construction of wooden structures. Every local raise of heat flux therefore significantly increases the energy consumption of building.

The relative influence of thermal bridges in the overall heat losses is integrated in the linear thermal transmittance (ψ- value in $W.m^{-1}.K^{-1}$), in the context of standard calculations (EN ISO 14683, 2009 and EN ISO 10211, 2007). Déqué et al. (2001) stated that the method underestimated the global heat losses through the walls in most cases. Svoboda and Kubr (2010) studied significant errors in calculation of the linear and point thermal transmittances for specific two-dimensional and three-dimensional thermal bridges. Kosny and Kossecká (2001) indicated that for some constructional and material solution of building envelope with three-dimensional thermal bridges can two-dimensional analysis cause remarkable faults. One suitable solution is to utilize numerical methods for evaluating heat transfer in construction. Zalewski et al. (2010) evaluated heat losses by thermal bridges using the three-dimensional unsteady analysis to perform more realistic results.

The infrared (IR) thermography is a valuable tool for inspecting and performing non-destructive detecting of heat losses from building´s envelopes (Balaras and Argiriou 2002). As all objects radiate energy, the IR inspections enable detection of IR electromagnetic radiation emitted by the object. The emitted energy is then converted by a sensor to the digital temperature. The possibility of indication variations in thermal resistance, air leaks or abnormally moist spots in buildings is discussed in the work of Grinzato et al. (1998) and Barreira and Freitas (2007). Asdrubali et al. (2012) performed quantitative analysis of some types of thermal bridges through thermographic surveys and subsequent numerical analyses.

In this paper, we discuss the possibility of detecting thermal bridges in a prefabricated wooden house by infrared thermography. The influence of thermal bridges is indicated by thermal transmittance values which were calculated according to the standard method and compared with the data from numerical calculations. The article presents also three-dimensional numerical models that could be used in further parametric studies.

10.2.Material and Methods

The investigated construction is a prefabricated wooden house considered as diffusion closed system (isolated by diffusion foil at the inner part of the wall). The outer wall and the ceiling panel were chosen for the calculation of thermal transmittances. For all the calculations, the material properties and constructional dimensions were necessary. One significant constructional detail with the appearance of a thermal bridge was analyzed. The thermal bridge was indicated by the results of infrared detection. The calculated constructional detail includes the connection of a ceiling beam and a wooden horizontal beam (Figure 1). The material properties are presented in Table 1. All results were compared to the norm values so the material properties are isotropic, without any dependence on temperature and moisture content.

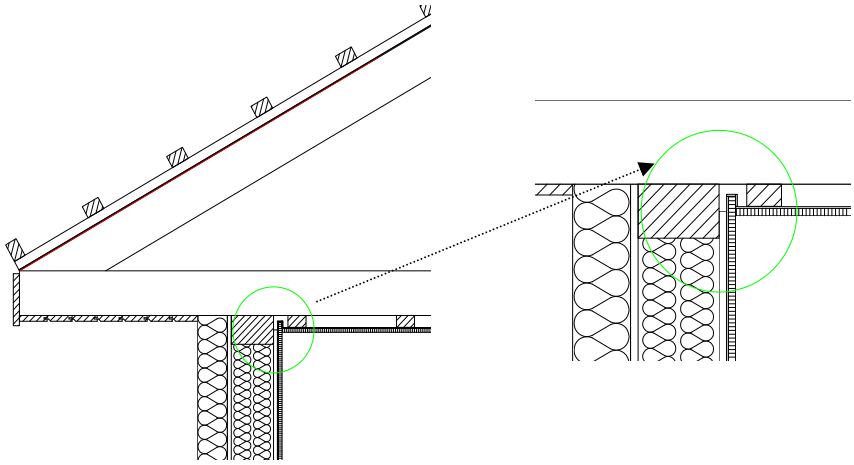

Paper VI. Figure 1 Calculated constructional part with connection of a ceiling beam and a wooden horizontal beam

The thermal transmittance (known as U-value) is the rate of heat transfer through a structure subjected to temperature gradient. For the evaluation of the thermal transmittance it is necessary to calculate the thermal resistance at the thermal bridge and at the “ideal”

segment of the construction (EN ISO 14683), see Figure 2. The equivalent thermal conductivity coefficient describes the heat transfer through a variety of materials ranked parallel to the heat flow (ČSN 730540-1). The constructional detail is divided into two structural parts (enclosure wall and ceiling) which are calculated separately.

Paper VI. Table 1 Isotropic material properties of the constructional parts

Material	**Thermal conductivity coefficient** λ [W.m^{-1}.K^{-1}]	**Source of the material property**
Gypsum board	0.23	Rigips, DIN EN 520, type A, A2-s1
Particle board V20 (interior)	0.18	EN 13 986, P4
Spruce timber *(Picea abies spp.)*	0.11	Bodig (1982)
Mineral wool	0.04	Rockwool, DIN EN 13501-1
Particle board V100 (exterior)	0.12	EN 13 986, P5
Polystyrene	0.04	Rigips, EPS 100 F
Air gap in the lower ceiling	0.02	ISO 6946 (2007)

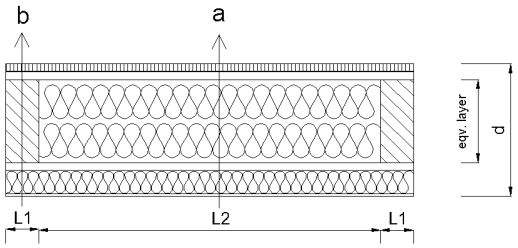

$$U = \frac{1}{\sum R} = \frac{1}{\frac{1}{\alpha_{\text{int}}} + \sum \frac{d}{\lambda_{(ekv)}} + \frac{1}{\alpha_{ext}}} \quad (1)$$

$$\lambda_{eqv.} = \frac{\lambda_1 L_1 + \lambda_2 L_2}{L_1 + L_2} \quad (2)$$

$$q = U.A.(T_i - T_e) = -\lambda_{eqv.} \frac{T_i - T_e}{d} \quad (3)$$

Paper VI. Figure 2 Description of the wall structure (a- "ideal" segment of the construction, b- a segment with the thermal bridge) and the calculation of equivalent thermal conductivity coefficient

The linear thermal transmittance value defines thermal properties of two-dimensional thermal bridges. It describes the amount of heat coming through unit length of thermal bridge by unit temperature difference. A positive value means an increase in the total heat loss coefficient. The heat flow of a thermal bridge will be already included in the heat loss of the construction, if the value is negative. The calculation methods based on European standards (ISO 10211, ISO 14683, ČSN 73 0540) establish the linear thermal transmittance values as the difference between the thermal coupling coefficient (L^{2D}) and heat thermal transmittance values of typical constructional segments, see Figure 3. Such value evaluates the thermal flux in the connection of two structures related to one length meter. The

calculation method in FEM based software is founded on evaluation of average heat flux in the connection of structures. It is possible to reach the linear thermal transmittance value directly based on this evaluation. The basic difference between both methods is the approach to the heat flux evaluation. The heat flux value is calculated according the eq. 3 given by standards in the analytical evaluation, while the heat flux is calculated based on FEM in the numerical approach. The calculation methods are described as follows:

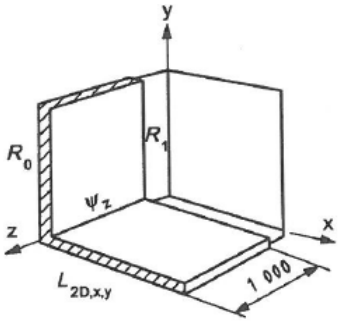

$$L_{x,y}^{2D} = \frac{q_{x,y}}{l_z.\Delta T}$$

$$L_{x,z}^{2D} = \frac{q_{x,z}}{l_y.\Delta T}$$

$$L_{y,z}^{2D} = \frac{q_{y,z}}{l_x.\Delta T}$$

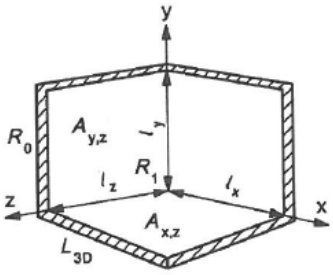

$$\psi_z = L_{x,y}^{2D} - U_{x,z}.l_x - U_{y,z}.l_y$$

$$\psi_x = L_{y,z}^{2D} - U_{x,y}.l_y - U_{x,z}.l_z$$

$$\psi_y = L_{x,z}^{2D} - U_{x,y}.l_y - U_{y,z}.l_z$$

$$\chi = L^{3D} - L_{x,y}^{2D}.l_z - L_{y,z}^{2D}.l_x - L_{x,z}^{2D}.l_y + U_{x,y}.A_{x,y} + U_{x,z}.A_{x,z} + U_{y,z}.A_{y,z}$$

Paper VI. Figure 3 Calculation method of linear (ψ) and point (χ) thermal transmittance (ISO 10211,2007)

The numerical model was created in the engineering software Ansys Workbench 13 and displays the 3D connection of enclosure walls and the ceiling panel. The load conditions were simplified for the numerical task (see Table 2). The convection (heat transfer from ambient air to the construction) was added as a heat transfer coefficient which differs on each side of the building envelope. Inner and outer temperatures were established in compliance with the normative method (ČSN 730540-3). The airspace above the ceiling is not heated which decreases the temperature by – 8.8 °C (ISO 13789). The numerical task consists of creating a numerical model (using application Design Modeler), assigning material properties (isotropic, without any dependence), analysis selection (steady-state thermal analysis), meshing (mapped face meshing with local refinement), solving and evaluating results.

Paper VI. Table 2 The load conditions used in a calculation and a numerical model (based on ČSN 730540-3)

Construction	**Inner temperature** T_i [°C]	**Outer temperature** T_e [°C]	**Internal resistance** α_{int} [W.m^{-2}.K^{-1}]	**External Resistance** α_{ext} [W.m^{-2}.K^{-1}]
Wall	+21	-15.0	7.7	23
Ceiling	+21	-8.8	10.0	25

The model was created in compliance with EN ISO 10211, which specifies the decomposition of the construction into several parts, see Figure 3. The material properties and the connection between the geometry parts were assigned. The temperature gradient is consistent in the numerical model. The steady-state thermal analysis was used to calculate the effects of steady thermal loads on the part of the construction. The mapped face meshing with local sizing method on the smaller parts of construction was used. The application determines a suitable number of divisions for the edges on the boundary faces (Ansys 2009). The results of the analysis are the temperature field in the construction part and the heat flux value. A script based on the calculation of an average heat flux in a defined nodal set is used for the evaluation of the directional heat flux.

In order to detect thermal bridges, a number of measurements were taken by thermocamera FLIR S65. A thermal bridge occurs where changing the heat flux results in a change of the inner surface temperature. There is a positive correlation between the heat flux and the change in evaluated temperatures. The change of temperature is caused by the lowered thermal resistance in specific parts of the constructional detail. The wall temperature should not be lower than 13.53 °C (based on ČSN 730540-3). Lower temperatures can cause condensation of water vapour on the wall surfaces and enable the mould to develop. The results of infrared measurements are analysed by Therma CAM^{TM} Researcher software. A histogram and a diagram describing the temperature distribution of a few lines situated on the thermal scan are required for the evaluation. The histogram is a graphical representation showing the distribution of temperatures of the thermal scan in a specific location which enables us to figure out the minimal and the most frequently occurring temperature observation on the thermal scan. The thermal scan of an object depends on the heat transfer between the surface and the surroundings. If there are no

external heat sources, the surface temperature of a building element is a function of temperature difference between the inside and the outside environments and the heat resistance of the various layers. The distance from the measured construction part, atmospheric temperature, relative humidity and emissivity of materials are the most influencing factors during the measurement which are described by many authors as e.g. Bareira (2012), Hart (1991), Balaras and Argiriou (2002). To avoid these effects, all the measurements were taken in the inner environment before the sunrise.

10.3.Results

The recordings (Figure 4 and Figure 5) show results of the infrared detection. The colour scope of the thermogram defines the temperature field on the structure. The linear thermal bridges on the wall are caused by the connection of two conductive materials, which increase the heat flow in the area (Figure 4a). The point thermal bridge (Figure 4b) is caused by an insufficient thermal insulation in the area of the ceiling panel.

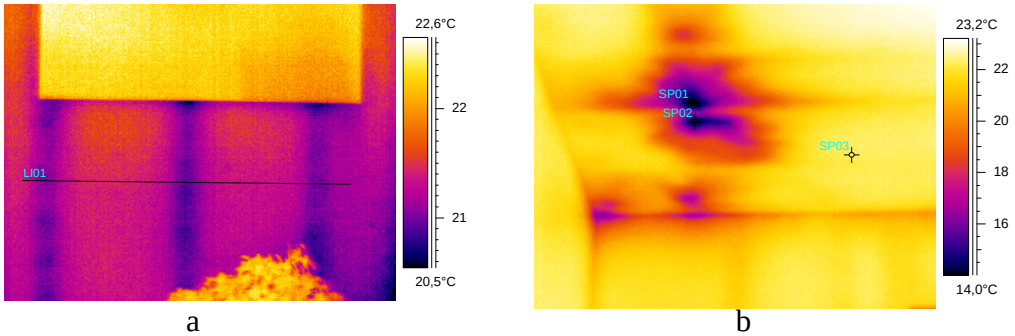

a b

Paper VI. Figure 4 a) linear thermal bridges on the enclosure wall, b) point thermal bridge on the ceiling

Two lines depicting the temperature behavior of the “ideal” part of the construction (LI02) and the part of the construction with the thermal bridge (LI01) were analyzed (Figure 5a). The average temperature on the wall (through line LI01) is 21.2 °C. As shown in Figure 6, the temperatures following line LI01 decrease to the minimum value of 16.9 °C, which demonstrates the occurrence of the thermal bridge. Two drops in the temperature are visible on line LI01. The first drop is caused by the lower thermal resistance at the place of connection to the ceiling beam. The second drop is caused by the insufficient thermal

insulation in the false ceiling. These analyzed point thermal bridges repeat regularly in the direction of two subsequent ceiling beams.

The corner connection between enclosure walls and the ceiling panel is shown in Figure 5b. Line LI01 describes a three-dimensional heat transfer and a point thermal bridge in the corner. The increased heat flow in the corner is a typical example of a geometrical thermal bridge. The geometrical thermal bridges are included in the heat loss coefficient value only when the outer dimensions are used in the calculation. Line LI02 describes a linear thermal bridge in the connection of the false ceiling and a gypsum board. The histogram (Figure 7) demonstrates the average temperature (17.9 °C), the most frequent temperature (18.5 °C) and the minimal measured temperature (13.8 °C) in the corner connection.

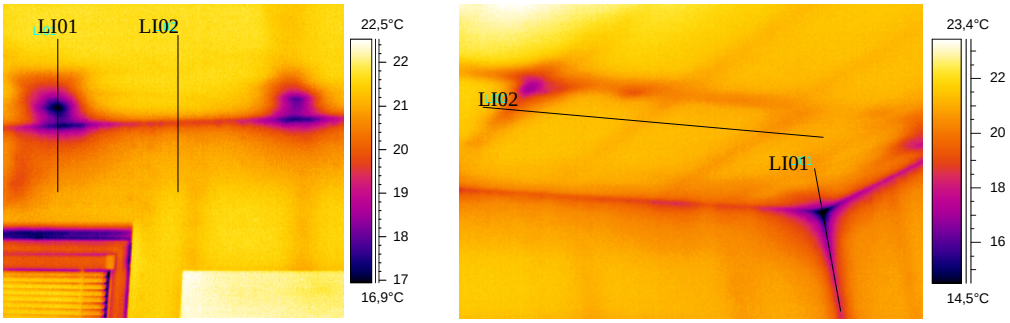

a b

Paper VI. Figure 5 A picture of the temperature field of a) a connection between a ceiling panel and the enclosure wall (LI01- point thermal bridge, LI02- linear thermal bridge) b) a corner connection (LI01- point thermal bridge, LI02- linear thermal bridges)

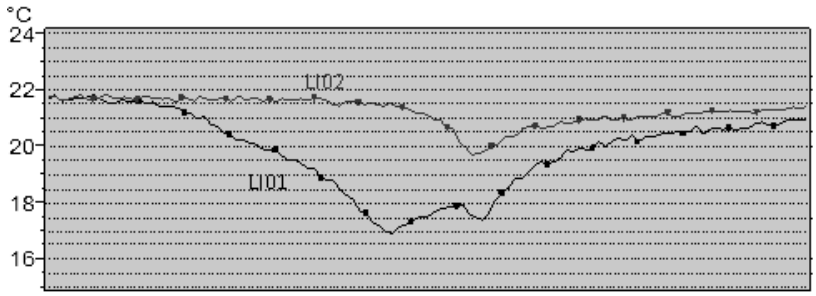

Paper VI. Figure 6 Temperature behaviour in a part of the thermal bridge (LI01) and in the “ideal” part of the construction (LI02) – (related to Figure 6a)

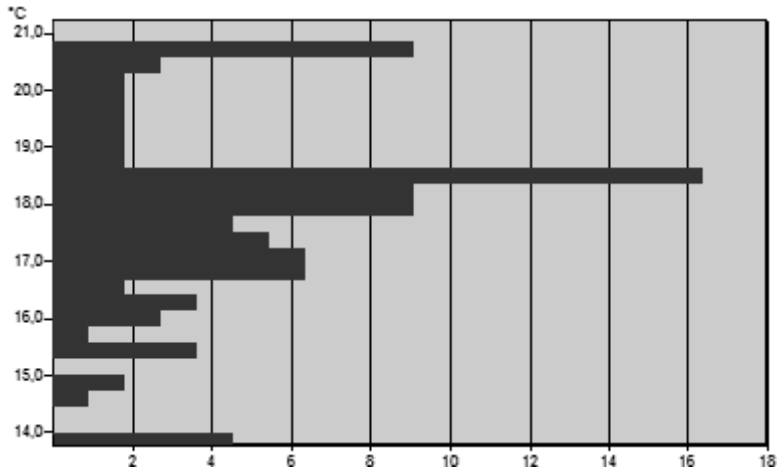

Paper VI. Figure 7 The histogram of the line LI01 - (related to Figure 6b)

Within the framework of the project, the heat thermal transmittances of the enclosure wall and the ceiling were calculated (Table 3). All the calculated constructional parts meet the requirements given by ČSN 73 0540-2. The heat thermal transmittances calculated following the numerical results are based on the heat flux evaluation established using Ansys 13. The analytical calculation method is based on ČSN 730540-1. The same load conditions and material properties were used to enable comparison of both methods. The insignificant difference between these values (max. 0.007 $W.m^{-2}.K^{-1}$) confirms the accuracy of the numerical solution.

Paper VI. Table 3 Results of calculations evaluated by the two different methods

Heat thermal transmittance [$W.m^{-2}.K^{-1}$]	**Enclosure wall**		**Ceiling**	
	numerical	analytical	numerical	analytical
	0.171	0.168	0.206	0.213
Heat flux [$W.m^{-2}$]				
$q_{ideal\ part}$	5.613	5.622	5.939	6.333
$q_{thermal\ bridge}$	9.819	8.621	12.008	12.026

The results of the numerical models prove the occurrence of linear thermal bridges in the thermograph. Figure 8a shows the numerical model of the enclosure wall with the heat flux field. The increased heat flux through the structure causes a decrease in temperature on the inner part of the construction. The approximate value of the heat flux at the enclosure wall is 6.166 $W.m^{-2}$ (when calculated by norms the value is 6.065 $W.m^{-2}$). The difference

between numerical and analytical solution counts to 0.101 W.m^{-2}. The maximum heat flux value of the ceiling panel occurs in the connection of the ceiling beam and wooden laths (Figure 8b). The average heat flux value makes 6.123 W.m^{-2} (when calculated by norms the value is 6.333 W.m^{-2}). Provided that the finite element method is more accurate (Šubrt and Volf, 2003), the maximum difference between numerical and analytical solution amounts to 3.43 %.

The results of the linear thermal transmittance (ψ) of all structural part connections are presented in Table 4. The comparison of linear thermal transmittances gained by two different methods confirms the underestimation of the analytical approach. The values gained from ISO 10211 calculations are considerably lower in comparison with the values from the numerical solution. The results confirm the negative influence of simplified thermal transmittance calculation based on the standard on the heat flux in the structural connections. The values of linear thermal transmittance are twice higher in the FEM calculation for the ceiling-enclosure wall connections than the ones calculated by standards. The calculations testify to the accuracy of the numerical methods given by standard. The accuracy of the standard values in the catalog is about ± 20%, while the accuracy of the numerical computation is about ± 5% (EN ISO 14683).

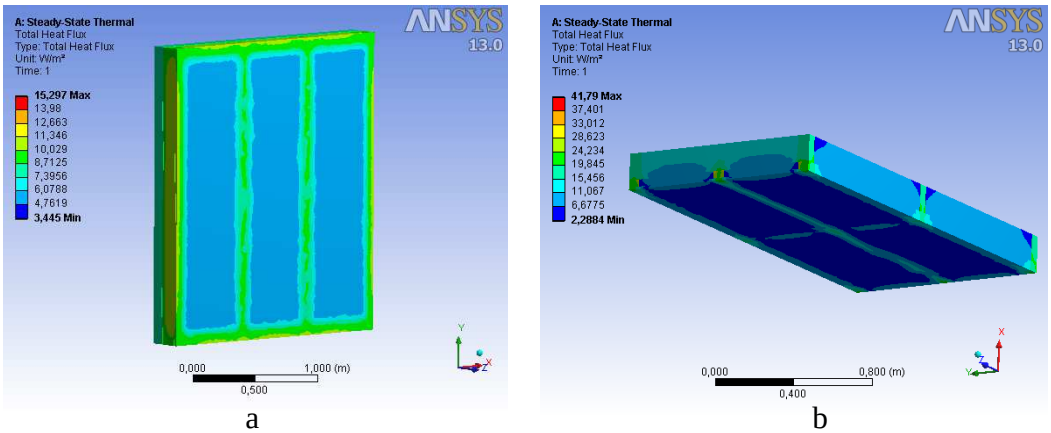

a b

Paper VI. Figure 8 Constructions with the regularly repeating elements, a) the enclosure wall, b) the ceiling panel

Paper VI. Table 4 Results of linear (ψ) and point (χ) thermal transmittances

Linear thermal transmittance ψ [W.m^{-1}.K^{-1}]			
	ISO 10211	ISO 14683	FEM
ψ_x (enclosure wall+ceiling)	0.0657	0.800	0.1274
ψ_y (enclosure walls)	0.0682	0.100	0.0970
ψ_z (enclosure wall+ceiling)	0.0644	0.800	0.1393
Point thermal transmittance χ [W.K^{-1}]			
χ (enclosure walls+ceiling)	0.0220	---	0.1103

* for all calculations inner dimensions were used

The connection of the ceiling beam to the enclosure horizontal beam is the most problematic part of the construction (see Figure 9). In the connection, the heat flux reaches 9.185 W.m^{-2}. The point thermal transmittance (χ) of the point thermal bridge rises to 0.1103 W.K^{-1} and occurs regularly at the ceiling beam locations on the enclosure wall. The presence of regular thermal bridges in the ceiling is confirmed also by the infrared detection.

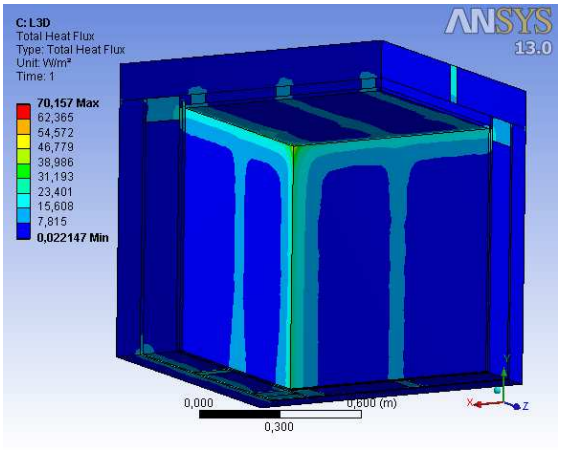

Paper VI. Figure 9 Numerical model of the whole construction for calculation of L^{3D}

Directory information about thermal bridge catalog values can be found in EN ISO 14683. If the constructional detail is not listed in the catalog, the linear thermal transmittance values can be taken from the most similar one. The catalog of thermal bridges is markedly overvalued which reflects on the real linear thermal transmittance values. Point thermal bridges are not specified in the thermal bridge catalog and the standard methodology (ISO 10211) does not include point thermal bridges under the value of 0.1 W.K^{-1} at all. As shown, in some cases it is not possible to neglect these values. This

corresponds with most of the literature, as evidenced in Svoboda and Kubr (2010). The thermal bridges influence the heat consumption of the building and the amount of energy required for heating. The influence of thermal bridges on the transmission heat loss coefficient and energy intensity of the wooden house is non-negligible (Šubrt and Volf, 2003). Numerical calculations are recommended for the most accurate expression of the linear and point thermal transmittance values. Comprehension of the influence of the dimension and the thermal conductivity coefficients on the linear transmittance values is recommended for the catalog of thermal bridges.

10.4. Conclusion

The infrared detection was used to monitor thermal bridges in a prefabricated wooden house. The infrared thermography illustrates the occurrence of thermal bridges, but it does not impinge on the finite element analysis validation. The measured temperatures where compared with the calculated ones (in compliance with ČSN 730540-3) to exclude the possibility of water vapor condensation. The lowest measured temperature reaches 13.8 °C, which is over the required condensation point value. Although the thermal measurements are influenced by many factors, the maximum deviation average is 1.5 %, which makes max. ±2 °C in the internal environment. Numerical simulations of the constructional parts were created using the FE computational system ANSYS. The load conditions of numerical simulations created for comparison with the standard methods were simplified.

The transmission heat loss coefficients (U value) and the heat fluxes in ideal parts of the construction and in the locations of thermal bridges were established. All the calculated constructional parts meet the requirements for the transmission heat loss coefficients given by ČSN 73 0540-2 (max. value of 0.3 $W.m^{-2}.K^{-1}$) and the comparison of the values calculated by both methods prove the accuracy of numerical models (max. deviation 3.43 %). The results prove the hypothesis that the standard calculation method includes inaccuracies arisen from the simplified calculation of heat thermal transmittances with equivalent thermal conductivity coefficient which decreases the impact of thermal bridges on the total heat flux.

The results of this study indicated the significant influence of thermal bridges in wooden constructions. The calculated ψ values of the structural connections differ from the standard value in EN ISO 14683 notably and prove the overestimation of the values mentioned in the catalog. The two methods, based on the standards (EN ISO 10211) and the software based on FEM differ from each other. The differences between them are caused by the exclusion of the thermal relations between structural elements in the analytical methodology. The comparison of linear thermal transmittances gained by those methods confirms the underestimation of analytical approach. The accuracy of the standard values is about ± 20% which is caused by undifferentiated material properties of lightweight constructions. It can be stated that the neglected point thermal bridges influence the thermal losses of the building as well. The connection of the ceiling beam to the enclosure horizontal beam is the most problematic part of the construction. The calculated point thermal transmittance (χ) value (0.1103 $W.K^{-1}$) of the connection proves the influence and can also predict the quality of the building system facture.

Generally, thermal bridges occur in any types of constructions. Wood based constructions are usually well insulated and their low total heat assumption declares their status of passive and low-energy houses. Nevertheless, thermal bridges can appear in such constructions too, which signifies improperly designed constructional details or poor quality construction work. By using FEM software it is possible to reach more accurate values for linear and point thermal bridges. An interesting task for the future may be the use of optimization functions to reach the optimal solution of problematic constructional details. Such parametric models can be transformed in order to meet the requirements given by European norms or the building industry.

Nomenclature

A Area [m^2]

d Thickness of a material [m]

H_d Heat loss coefficient [$W.K^{-1}$]

$l_{(x,y,z)}$ Length of the structural part [m]

L_1 Length of the construction part with a thermal bridge [m]

L_2 Length of the “ideal” segment of the construction [m]

L^{2D} Thermal coupling coefficient- 2D [$W.m^{-1}.K^{-1}$]

L^{3D} Thermal coupling coefficient- 3D [$W.K^{-1}$]

q Heat flow [W]

$\dot{q}$ Heat flux [$W.m^{-2}$]

R Thermal resistance [(m2.K)/W]

ΔT Temperature difference [K]

T_e Outer temperature [K]

T_i Inner temperature [K]

U Transmission heat loss coefficients [$W.m^{-2}.K^{-1}$]

α_{ext} External surface resistance [$W.m^{-2}.K^{-1}$]

α_{int} Internal surface resistance [$W.m^{-2}.K^{-1}$]

λ Thermal conductivity coefficient [$W.m^{-1}.K^{-1}$]

λ_{ekv} Equivalent thermal conductivity coefficient [$W.m^{-1}.K^{-1}$]

χ Point thermal transmittance [$W.K^{-1}$]

ψ Linear thermal transmittance [$W.m^{-1}.K^{-1}$]

Acknowledgement

The authors want to thank to the Internal Grant Agency of Mendel University in Brno for the partial financial support of this research (project no. 8/2011).

10.5.References

Ansys Release 12.1 (2009) *Documentation for ANSYS WORKBENCH*, Canonsburg: SAS IP, Inc.

Asdrubali F, Baldinelli G, Bianchi F (2012) *A quantitative methodology to evaluate thermal bridges in buildings*, Applied Energy 97: 365-373.

Balaras CA, Argiriou AA (2002) *Infrared thermography for building diagnostics*, Energy and Buildings 34: 171-183.

Bareira E, Freitas V.P, Delgado J.M.P.Q, Ramos N.M.M (2012) *Thermography Apllications in the Study of Buildings Hydrothermal Behaviour*, Ifrared Thermography. Chapter 8, Portugal: InTech

Barreira E, VP de Freitas (2007) *Evaluation of building materials using infrared thermography*, Construction and Building Materials 21: 218-224.

ČSN 730540-1 (2005) *Thermal protection of buildings - Part 1: Terminology*. Prague: Czech office of standard, metrology and testing

ČSN 730540-2 (2011) *Thermal protection of buildings – Part 2: Requirements*. Prague: Czech office of standard, metrology and testing

ČSN 730540-3 (2005) *Thermal protection of buildings - Part 3: Design value quantities*. Prague: Czech office of standard, metrology and testing

ČSN 730540-4 (2005) *Thermal protection of buildings - Part 4: Calculation methods.* Prague: Czech office of standard, metrology and testing

Déqué F, Ollivier F, Roux JJ (2001) *Effect of 2D modelling of thermal bridges on the energy performance of buildings: numerical application on the Matisse apartment*, Energy and Buildings 33(6): 583-587.

EN ISO 10211 (2007) *Thermal bridges in building construction- Heat flows and surface temperatures- Detailed calculations*. Brussels: CEN

EN ISO 13789 (2007) *Thermal performance of buildings – Transmission and ventilation heat transfer coefficients – Calculation method*. Brussels: CEN

EN ISO 14683 (2009) *Thermal bridges in building construction – Linear thermal transmittance – Simplified methods and default values*. Brussels: CEN

Grinzato E, Vavilov V, Kauppinen T (1998) *Quantitative infrared thermography in buildings*, Energy and Buildings 29: 1-9.

Hart J.M (1991) *A Practical Guide to Infra-red Thermography for Building Surveys United Kingdom: IHS BRE Press*

Kosny J, Kossecka E (2001) *Multi-dimensional heat transfer through complex building envelope assemblies in hourly energy simulation programs*, Energy and Buildings 34: 445-454.

Svoboda Z, Kubr M (2010) *Numerical simulation of heat transfer through hollow bricks in the vertical direction*, Journal of Building Physics 34(4): 325-350.

Šubrt R, Volf M (2003) *Construction details- Thermal bridges*, Prague: Grada Publishing

Zalewski L, Lassue S, Rousse D, Boukhalfa K (2010) *Experimental and numerical characterization of thermal bridges in prefabricated building walls*, Energy Conversion and Management 51 (12): 2869-2877.

11. Conclusion

A primary motivation for this dissertation thesis was to research thermal properties of wood (beech wood and Lignamon) and wood-based materials (low density fibreboards and MDF) using advanced experimental and numerical techniques. Three different experimental methods were used to measure thermal properties of selected materials. Natural beech wood (*Fagus sylvatica* L.) and the ammonia-treated compressed beech wood (Lignamon) were measured by using the quasi-stationary method. The analysis proved that there are statistically significant differences between the results of all the measured properties of modified and native beech wood. The results indicated that the well-known ascending character of thermal conductivity and a descending one for diffusivity is dependent on the density in a moist environment. The thermal conductivity of the samples increased with increasing density (increasing compression rate of Lignamon). Our measurement proved also the independence of specific heat capacity on density. The device based on the quasi-stationary method was also used to measure the thermal conductivity and the thermal diffusivity in both directions (perpendicular and parallel to the plane). It was found out that the in-plane thermal conductivity and thermal diffusivity along fiber is 2 to 2.4 times greater than in the perpendicular direction. The higher in-plane thermal conductivity corresponds with the main in-plane orientation of wood fibers. Thermal properties (thermal conductivity, thermal diffusivity, and specific heat capacity) of medium density fiberboards with different thicknesses (12 and 18 mm) was also measured using the pulse-transient method. A week positive correlation between density and thermal conductivity was found. The X-ray densitometry measurements were carried out to further investigate the vertical density profiles. The variation of density in the thickness direction profoundly affects the physical properties of MDF. The heat flow meter method was used to assess thermal conductivity of insulation fiberboards at different temperatures (ranging from -10 °C to +60 °C at 10 °C increments) and moisture contents (gravimetrically determined after conditioning at 15%, 50%, 85% RH). A relationship between thermal conductivity, temperature and MC of low density fiberboards was established. It was also proved that the conductivity increases as temperature and moisture content raises. The

differences between conductivity values at oven-dry conditions and at 85% RH increased remarkably as temperature went up.

The results from the numerical studies showed differences in thermal properties of all materials depending on chosen measurement method and different parameters' setup during measuring processes. Density proved to be one of the most influencing factors for all three measurement techniques. The high-density faces of MDF influence the pulse-transient measurements by adding higher resistance to the heat transfer at the surface of samples. The extensive experimental evaluation of the relationship between density and thermal properties as well as the incorporation of realistic density profiles into the numerical model could improve the results of the sensitivity analysis. The relevancy of non-stationary measurements is also influenced by the choice of the proper ratio between thickness and width of the sample. The accuracy of the quasi-stationary method and pulse-transient method depends on the precision of measurement and fulfillment of conditions during measurement, especially the test duration. The reliability of experiments may be increased by avoiding heat losses (ie. by insulating all lateral parts of samples) so that the size of samples would not affect the determination of thermal parameters. Temperature and moisture content are also important parameters affecting thermal evaluation of wood and wood-based materials. Therefore, stable environment conditions are needed for all experiments as well as the stable moisture content of samples.

Quantitative data are required to better characterize the thermal performance of wood and wood-based materials. Accurate data on the thermal behavior of insulation materials are also needed to improve numerical modelling approaches that enable high efficient optimization of building envelopes. The contribution of radiation and convection heat transfer modes to the total heat flow through a construction composed of fiberboards and horizontal enclosure was investigated experimentally. Numerical models dealing with heat transfer in such composed samples subjected to downward heat flow were verified by experiments based on the heat flow meter method. The emissivity coefficient was proved to be the most influential factor contributing to the decrease of total heat flow. The significance of radiation transfer increases with increase in the air gap thickness. Direction of the heat flow is decisive in development of a buoyant driven flow. It was proved that the

best application of the air enclosure is in building components subjected to downward heat flow. The advantage of air enclosures in structures where upward heat flow occurs is limited to small dimensions of the enclosure, as at thicker cavities Rayleigh-Bénard convection occurs.

Finally, the temperature distribution in a wooden construction was studied with help of infrared thermography. The results of this study indicated the significant influence of thermal bridges in wooden constructions on heat losses which are generally not sufficiently evaluated.

12. References

Almanza O, Rodríguez-Pérez MA, De Saja JA (2004) *Applicability of the transient plane source method to measure the thermal conductivity of low-density polyethylene foams*, Journal of Polymer Science: Part B: Polymer Physics: 42: 1226-1234.

Al-Sanea SA, Zedan MF (2011) *Improving thermal performance of building walls by optimizing insulation layer distribution and thickness for same thermal mass*, Applied Energy 88(9): 3113-3124.

Al-Sanea SA, Zedan MF, Al-Ajlan SA, Abdul Hadi AS (2003*) Heat transfer characteristics and optimum insulation thickness for cavity walls*, Journal od Thermal Envelope and Building Science 26: 285-307.

Arasteh D, Beck F, Griffith B, Acevedo-Ruiz M (1992) *Using infrared thermography for the study of heat transfer through building envelope components*, ASHRAE Transactions 98(1): 1-12.

Armando GM, Armando BBJ, Christian VC, Rangel-Hernández VH, Belman-Flores JM (2010) *Analysis of the conjugate heat transfer in a multi-layer wall including an air layer*, Applied Thermal Engineering 30: 599-604.

Asdrubali F, Baldinelli G, Bianchi F, Libbra A, Muscio A (2010*) Comparative analysis of different methods to evaluate the thermal conductivity of homogenous materials*, ASME-ATI-UIT Conference of Thermal and Environmental Issues in Energy systems, 1-5.

Asdrubali F, Baldinelli G, Bianchi F (2011) *A quantitative methodology to evaluate thermal bridges in buildings*, Third International Conference on Applied Energy, Italy, 1241-1252.

ASTM C518 (2010) *Standard test method for steady-state thermal transmission properties by means of the heat flow meter apparatus*, American Society for Testing and Materials (ASTM).

Barreira E, Freitas VP (2004) *Infrared thermography applications in the study of building hygrothermal behavior*, CIB W40 Meeting, Caledonian University, Glasgow, 1-22.

Bareira E, Freitas VP, Delgado JMPQ, Ramos NMM (2012) *Thermography Apllications in the Study of Buildings Hydrothermal Behaviour*, Ifrared Thermography, Chapter 8, Portugal: InTech.

Balaras CA, Argiriou AA (2002) *Infrared thermography for building diagnostics*, Energy and Buildings 34(2): 171-183.

Bjarløv SP, Vladykova P (2011) *The potential and need for energy saving in standard family detached and semi-detached wooden houses in arctic Greenland*, Building and Environment 46: 1525-1536.

Boháč V, Dieška P, Vretenár V (2012) *The measurement of thermophysical properties of sandstone by pulse transient method using model for cuboid form samples and influence of heat loss effect*, in Thermophysics 2012, Proc. of the Meeting of the Thermophysical Society - Working Group of the Slovak Physical Society, 23-32.

Bomberg M, Shirtliffe CJ (1978) *Influence of moisture and moisture gradients on heat transfer through porous building materials*, in: Thermal Transmission Measurements of Insulation, ASTM International 211-234.

Brombacher V, Michel F, Niemz P, Volkmer T (2012) *Investigation of thermal conductivity and moisture behaviour of fiberboards and material combinations*, Bauphysik 34:157-169.

Carvalho LM, Costa CAV (1998) *Modeling and simulation of the hot-pressing process in the production of medium density fiberboard (MDF),* Chemical Enginering Communications 170: 1-21.

Clarke LN, Kingston RST (1950) *Equipment for the simultaneous determination of thermal conductivity and diffusivity of insulating materials using a variable state methods*, Australian Journal of Basic and Applied Sciences 1(2): 172-187.

Dai C, Yu C (2004) *Heat and mass transfer in wood composite panels during hot-pressing: Part I., A physical-mathematical model*, Wood and Fibre Science 36(4): 585-597.

Deltiski N (2013) *Computation of the wood thermal conductivity during defrosting of the wood*, Wood Research 58(4): 637-650.

Deru M, Judkoff R, Neymark J (2003) *Whole-building energy simulation with a three dimensional ground-coupled heat transfer model,* Conference paper, American Society of Heating, Refrigerating and Air-Conditioning Engineers, Chicago, Illinois.

Desta TZ, Langmans J, Roels S (2010) *Experimental data set for validation of heat, air and moisture transport models of building envelopes*, Building and Environment 46: 1038-1046.

DIN EN 12667 (2001) *Thermal performance of building materials and products- Determination of thermal resistance by means of guarded hot plate and heat flow meter methods- Products of high and medium thermal resistance*, German Institute for Standardization.

Domínguez-Muňos F, Anderson B, Cejudo-López JM, Carrillo-Andrés A (2009) *Uncertainty in the thermal conductivity of insulation materials*, Building Simulation, Eleventh International IBPSA Conference, Glasgow, Scotland, 1008-1013.

Dubois S, Lebeau F (2013) *Design, construction and validation of a Guarded Hot Plate Apparatus for thermal conductivity measurement of high thickness crop-based specimens*, Materials and Structures 1-15.

Dündar T, Kurt S, As N, Uysal B (2012) *Nondestructive evaluation of wood strength using thermal conductivity*, BioResources 7(3): 3306-3316.

Dupleix A, Kusiak A, Hughes M, Rossi F (2013) *Measuring the thermal properties of green wood by the transient plane source (TPS) technique*, Holzforschung 67(4): 437-443.

EN ISO 6946 (2005) *Building components and building elements- thermal resistance and thermal transmittance- calculation method*, Brussels, European standard.

EN ISO 14683 (2007) *Thermal bridges in building construction- Linear thermal transmittance- Simplified methods and default values*, Brussels, European standard.

EN ISO 10211 (2007) *Thermal bridges in building construction- Heat flows and surface temperatures- Detailed calculations*, Brussels, European standard.

Fenton TE, Budman HM, Pritzker MD (2003) *Modeling and Simulation of oriented strandboard pressing*, Industrial and Engineering Chemistry Research 42: 5229.

Fotsing JAM, Takam M (2004) *A prediction of the thermal conductivity of sapelli*, Academic Open Internet Journal 11: 1-10.

Gerlich V (2011) *Modelling of heat transfer in buildings*, Proceedings 25th European Conference on Modelling and Simulation: 1-5.

Gibson P, Lee C (2006) *Application of nanofiber technology to nonwoven thermal insulation*, Report OMB No. 0704-0188, U.S. Army Soldier System Center, Natick, Massachusetts.

Grønli MG (1996) *Theoretical and experimental study of the thermal degradation of biomass*, Ph.D. thesis, Norwegian University of Science and Technology, Faculty of Mechanical Engineering, Trondheim, Norway.

Gu HM (2001) *Structure based, two-dimensional anisotropic, transient heat conduction model for wood*, Ph.D. dissertation, Virginia Polytechnic Institute and State University, Blacksburg, Virginia.

Gu HM, Hunt JF (2007) *Two-dimensional finite element heat transfer model of softwood. Part III. Effect of moisture content on thermal conductivity*, Wood and Fiber Science 39: 159-166.

Gu HM, Zink-Sharp A (2005) *Geometrical model for softwood transverse thermal conductivity*, Part1, Wood and Fiber Science 37(4): 699-711.

Gustavsson SE (1991) *Transient plane source techniques for thermal conductivity and thermal diffusivity measurements of solid materials*, Review of Scientific Instruments 62: 797.

Hankalin V, Ahonen T, Raiko R (2009) *On thermal properties of a pyrolysing wood particle*, Finnish-Swedish Flame Days 2009, Naantali, Finland

Harada T, Hata T, Ishihara S (1998) *Thermal constants of wood during the heating process measured with the laser flash method*, Journal of Wood Science 44: 425-431.

Hart JM (1991) *A Practical Guide to Infra-red Thermography for Building Surveys*, United Kingdom: IHS BRE Press.

Heibati SM, Atabi F, Khalajiassadi M, Emamzadeh A (2013*) Integrated dynamic modeling for energy optimmization in the building: Part I.: The development of the model*, Journal of Building Physics 37(1): 28-54.

Hrčka R, Kurjatko S (2006) *Thermal properties of Elm wood (Ulmus Scabra, mill.)*, Wood Structure and Properties, Arbora Publishers, 245-249.

Hrčka R, Babiak M (2012) *Some non-traditional factors influencing thermal properties of wood*, Wood Research 57(3): 367-374.

Humphrey PE, Bolton AJ (1989) *The hot pressing of dry-formed wood-based composites: Part II: A simulation model for heat and moisture transfer and typical results*, Holzforschung 43(3): 199-206.

Chew MYL (1998) *Assessing building facades using infra-red thermography*, Structural Survey 16(2): 81-86.

Chown GA, Burn KN (1983) *Thermographic identification of buildings enclosure defects and deficiencies*, Canadian Building Digest 229, Canada.

ISO 8301 (2014) *Thermal insulation- Determination of steady-state thermal resistance and related properties- Heat flow meter apparatus*, International Organization for Standardization

Janssen H, Blocken B, Carmeliet J, *Conservative modeling of the moisture and heat transfer in building components under atmospheric excitation*, International Heat and Mass Transfer 50(5-6): 1128-1140.

Joy FA (1957) *Thermal conductivity of insulation containing moisture*, Symposium on thermal conductivity measurements and applications of thermal insulation ASTM STP 217, 65-80.

Kandemir-Yucel A, Tavukcuoglu A, Caner-Saltik EN (2007) *In situ assessment of structural timber elements of a historic building by infrared thermography and ultrasonic velocity*, Infrared Physics and Technology 49: 243-248.

Kato S, Kuroki K, Hagihara S (2007) *Method of in-situ measurement of thermal insulation performance of building elements using infrared camera*, 6th International Conference on Indoor Air Quality, Ventilation & Energy Conservation in Buildings.

Kavazović Z, Deteix J, Fortin A, Cloutier A (2012) *Numerical modeling of the medium-density fiberboard hot pressing process, part 2: Mechanical and Heat and Mass transfer models*, Wood and Fibre Science 44(3): 243-262.

Kawasaki T, Kawai S (2006) *Thermal insulation properties of wood-based sandwich panel for use as structural insulated walls and floors*, Journal of Wood Science 52: 75-83

Kawasaki T, Zhang M, Kawai S (1998) *Manufacture and properties of ultra-low-density fiberboard*, Journal of Wood Science 44: 354-360.

Kirscher O, Esdorn H (1954) *Simple short-term method for the simultaneous determination of thermal conductivity, heat capacity and thermal effusivity of solids*, VDI- Forsch.-H. 450.

Kol HS (2009) *The transverse thermal conductivity coefficients of some hardwood species grown in Turkey*, Forest Product Journal 59(10): 58-63.

Kolář V, Němec I (1997) *FEM- principy a praxe metody konečných prvků*, Praha: Computer press, p. 401, ISBN80-7226-021-9.

Kollmann FFP (1951) *Technology of wood and wood-based materials*, Springer-Verlag (in German).

Kosny J (1995) C*omparison of thermal performance of wood stud and metal frame wall systems*, Journal of Building Physics 19(1): 59-71.

Kosny J, Asiz A, Smith I, Shrestha S, Fallahi A (2014) *A review of high R-value wood framed and composite wood wall technologies using advanced insulation techniques*, Energy and Buildings 72: 441-456.

Krempaský J (1969) Measurement of thermophysical parameters, Veda SAV, 288.

Krisher O, Esdorn H (1954) *Simple short-term method for the simultaneous determination of thermal conductivity, heat capacity and thermal effusivity of solids*, VDI-Forsch.-H. 450, (in German).

Kubičár L´, Boháč V, Vretnár V, Barta Š, Neuer G, Brandt R (2005*) Thermophysical properties of heterogeneous structures measured by pulse transient method*, International Journal of Thermophysics 26(6): 1949-1962.

Kubičár L´, Boháč V (2002) *Intercomparison measurements by pulse transient and stepwise transient methods on Perspex and stainless steel A310*, High Temperature-High Pressures 34(2): 135-146.

Kühlmann G (1962) *Investigation of the thermal properties of wood and particleboard in dependency from moisture content and temperature in hygroscopic range*, Holz als Roh- und Werkstoff 20(7): 259-270.

Labans E, Bikovs A, Kalninš K (2012) FEM *Simulation of mechanical and thermal properties of wood based sandwich panels with cellular wood core*, in: 10th International Conference on Sandwich Structures, France, Nantes, 169-170.

Labat M, Woloszyn M, Garnier G, Piot A, Roux J-J (2013) *Simulation of coupled heat, air and moisture transfers in an experimental house exposed to natural climate*, 13th Conference of International Building Performance Simulation Association, France.

Leon G, Cruz-de-Leon J, Villasenor L (2000) *Thermal characterization of pine wood by photoacoustic and photothermal techniques*, Holz als Roh- und Werkstoff 58: 241-246.

Lewis WC (1967) *Thermal conductivity of wood-based fiber and particle panel materials*, Research paper FPL77, USDA Forest Service, Forest Products Laboratory, Madison, Wisconsin.

López G, Basterra LA, Acuňa L (2013) *Estimation of wood density using infrared thermography*, Construction and Building Materials 42: 29-32.

Lorente S, Bejan A (2002) *Combined „flow and strength" geometric optimization: internal structure in a vertical insulating wall with air cavities and prescribed strength*, Internatinal Journal of Heat and Mass Transfer 45(16): 3313-3320.

Ludwig N, Redaelli V, Rosina E, Augelli F (2004) *Moisture detection in wood and plaster by IR thermography*, Infrared Physics & Technology 46(1-2): 161-166.

MacLean JD (1941) *Thermal conductivity of wood*, Heating Piping and Air Conditioning 13: 380-391.

Mackerle J (2005) *Finite element analyses in wood research: a bibliography*, Wood Science and Technology 39: 579-600.

Madenci E, Guven I (2006) *The Finite Element Method and Applications in Engineering Using ANSYS*, Springer, United States of America.

Mahlia TMI, Iqbal A (2010) *Cost benefits analysis and emission reductions of optimum* Energy 35: 2242-2250.

Manohar K, Kochhar G, Ramlakhan D, Haldar SC (2005) *Thermal conductivity measurement of wood by means of a water-activated, guarded-hot-plate apparatus*, West Indian Journal of Engineering 28(1): 61.

Markus TA, Morris EN (1980*) Buildings, climate and energy*, Pitman Publishing Limited, London.

Martínez I (1988) *Liquid bridge modeling of floating zone processing*, Physicochemical Hydrodynamics, Interfacial Phenomena, Velarde, Plenum Press, New York, 25-51.

Matias L, Santos C, Reis M, Gil L (1997) *Declared value for the thermal conductivity coefficient of insulation corkboard*, Wood Science and Technology 31:355-365.

Mavromatidis LE, Bykalyuk A, Mankibi ME, Michel P, Santmouris M (2012) *Numerical estimation of air gaps' influence on the insulating performance of multilayer thermal insulation*, Building and Environment 49: 227-237.

Meinlschmidt P (2005) *Thermographic detection of defects in wood and wood-based materials*, 14th International Symposium of nondestructive testing of wood, Hannover, Germany, 1-6.

Mlakar J, Štrancar J (2013) *Temperature and humidity profiles in passive-house building blocks*, Building and Environment 60: 185-193.

Moaveni S (2008) *Finite element analysis, Theory and Application with ANSYS*, Third Edition, Pearson International Edition, United States of America, 6-8.

Mohesnin NM (1980) *Thermal properties of food and agricultural materials*, Gordon and Breach Science Publishers, New York.

Nässén J, Hedenus F, Karlsson S, Holmberg J (2012) *Concrete vs. wood in buildings- An energy system approach*, Building and Environment 51: 361-369.

Niemz P, Sonderegger W, Hering S (2010) *Thermal conductivity of Norway spruce and European beech in the anatomical directions*, Annals of Warsaw University of Life Sciences, Forestry and Wood Technology 72: 66-72.

Parker WJ, Jenkins RJ, Butler CP, Abbott GL (1961) *Method of determining thermal diffusivity, heat capacity and thermal conductivity*, Journal of Applied Physics 32(9): 1679.

Plescanu C, Cochior MT, Klein C, Ibarra-Castenado A, Bendada A, Maldagie X (2008) *Localization of wood floors structure by infrared thermography*, Proceedings of the 30th SPIE (Thermosense XXX), USA, Orlando.

Požgaj A, Chovanec D, Kurjatko S, Babiak M (1997) *Wood structure and properties*, Bratislava, Priroda, 486.

Rice RW, Shepard R (2004) *The thermal conductivity of plantation grown white pine (Pinus stropus) and red pine (Pinus resinosa) at two moisture content levels*, Forest Product Journal 54(1): 92-94.

Rosina E, Robison EC (2002) *Applying infrared thermography to historic wood-framed buildings in North America*, APT Bulletin 33(4): 37-44.

Rowley FB (1933) *The heat conductivity of wood at climatic temperature differences*, Heating Piping and Air Conditioning 5: 313-323.

Saber HH, Maref W, Swinton MC, St-Onge C (2011) *Thermal analysis of above-grade wall assembly with low emissivity materials and furred airspace*, Building and Environment 46: 1403-1414.

Salmon D (2001) *Thermal conductivity of insulations using guarded hot plates, including recent developments and sources of reference materials*, Measurement Science and Technology 12 (12) R89.

Sebera V (2013) *Computational modeling of chosen wood-based composites*, PhD thesis, Mendel University in Brno, p. 117.

Seo J, Jeon J, Lee JH, Kim S (2011) *Thermal performance analysis according to wood flooring structure for energy conservation in radiant floor heating systems*, Energy and Buildings 43: 2039-2042.

Siau JF (1984) *Transport processes in wood*, Springer-Verlag, New York, 245.

Simpson W, TenWolde A (1999*) Physical Properties and Moisture Relations of Wood*, In: Forest Products Laboratory, Wood Handbook – Wood as an engineering material, Gen, Tech. Rep. FPL-GTR-113. Madison, WI:U.S. Department of Agriculture, Forest Service, Forest Products Laboratory, 463.

Sonderegger W, Hering S, Niemz P (2011) *Thermal behaviour of Norway spruce and European beech in and between the principal anatomical directions*, Holzforschung 65: 369-375.

Sonderegger W, Niemz P (2009) *Thermal conductivity and water vapour transmission properties of wood-based materials*, European Journal of Wood and Wood Products 67:313-321.

Sonderegger W, Niemz P (2012) *Thermal and moisture flux in soft fibreboards*, European Journal of Wood and Wood Products 70: 25-35.

Spencer M, Nychka J, Penn L, Boyer L, Everlade L, Liebertz J (2008) *Applying infrared thermography for the purpose of identifying concealed wood framing member type and*

subsurface anomalies with intended application towards historic structures, National Center for Preservation Technology and Training, USA.

Steinhagen HP (1977) *Thermal properties of wood, green or dry, from -40°to +100°C*; A literature review, USDA Forest Service General Technical Report FPL-9, Forest Products Laboratory, Madison, WI.

Steskens PWMH, Janssen H, Rode C (2009) *Influence of the convective surface transfer coefficients on the Heat, Air, and Moisture (HAM) building performance*, Indoor and Built Environment 18: 245- 256.

Suleiman BM, Larfeldt J, Leckner B, Gustavsson M (1999) *Thermal conductivity and diffusivity of wood*, Wood Science and Technology 33: 465-473.

Suleiman BM (2011) *Measurements of thermal conduction in partially saturated specimens using the transient hot-disk technique*, Journal of Testing and Evaluation 39(4): 529-534.

Šubrt R (2005) *Thermal bridges in building constructions*, Grada Publishing, (in Czech).

TenWolde A, McNatt JD, Krahn L (1988) *Thermal properties of wood and wood panel products for use in buildings*, U.S. Department of Energy, Oak Ridge National Laboratory, Oak Ridge, Tennessee, 40.

Tippner J (2010) *Numerical simulation of grand piano soundboard*, PhD thesis, Mendel University in Brno, p. 327.

Totten PE, Pazera M (2009) *Thermal Inefficiencies in Building Enclosures—Causes of Moisture Related Performance Problems*, Forensic Engineering, 43-54.

Troppová E, Tippner J, Hrčka R, Halachan P (2013) *Quasi-stationary measurements of Lignamon thermal properties*, BioResources 8(4): 6288-6296.

Tsilingiris PT (2006) *The influence of heat capacity and its spatial distribution on the transient wall thermal behaviour under the effect of harmonically time-varying driving forces*, Building and Environment 41: 590-601.

Van Dusen MS (1920) *The thermal conductivity of heat insulators*, American Society of Heating and Ventilating Engineers 26: 385-414.

Venkateswaran A (1974) *A note on the relationship between electrical properties and thermal conductivity of woods*, Wood Science and Technology 8: 50-55.

Wangaard FF (1940) *Transverse heat conductivity of wood*, Heating Piping and Air Conditioning 12: 459-464.

Ward RJ, Skaar C (1960) *A continuous measurement of the specific heat and conductivity of particle board as functions of temperature*, Society of Wood Science and Technology, 22.

Wood S, Weber B (2003) *IR Thermography use in the building science industry*, InfraMation Proceedings 4: 1-4.

Wood S, VanBree K (2006) *Using thermography to find a class of latent construction defects*, Thermal Solutions, 1-6.

Wyckhuyse A, Maldague X (2011) *A study of wood inspection by infrared thermography, Part II: Thermography for wood defects detection*, Research in Nondestructive Evaluation 13(1): 13-22.

Xie Y, Tong Q, Chen Y, Liu J, Lin M (2011) *Manufacture and properties of ultra-low density fibreboard from wood fibre*, BioResources 6(4): 4055-4066.

Xie Z, Chen L, Sun F (2014) *Constructal optimization for an insulating wall combining heat flow, strength and volume*, International Communications in Heat and Mass Transfer 54: 141-147.

Xing Ch, Folsom Ch, Jensen C, Ban H, Marshall DW (2014) *A correction scheme for thermal conductivity measurement using the comparative cut-bar technique based on 3D numerical simulation*, Measurement Science and Technology 25(5).

Yapici F, Ozcifci A, Esen R, Kurt S (2011) *The effect of grain angle and species on thermal conductivity of some selected wood species*, BioResources 6(3): 2757-2762.

Yu ZT, Xu X, Fan LW, Hu YC, Cen KF (2011) *Experimental measurements of thermal conductivity of wood species in China: effects of density, temperature and moisture content*, Forest Product Journal 61(2): 130-135.

Zarr RR, Burch DM, Fanney AH (1995) *Heat and moisture transfer in wood-based wall construction: measured versus predicted*, NIST Building Science Series 173, Building and Fire Research Laboratory 28-34.

Zejda J (2009) *Numerical simulation of drying wood*, PhD thesis, Mendel University of Agriculture and Forestry in Brno, p. 121.

Zhai ZJ, Chen QY (2006) *Sensitivity analysis and application guides for integrated building energy and CFD simulation*, Energy and Buildings 38(9): 1060–1068.

Zhong Z, Braun J (2008) *Combined heat and moisture transfer modeling for residential building*, U.S. National Institute of Standards and Technology, HL 2008-3: 1-190.

Zhou J, Zhou H., Hu Ch, Hu S (2013) *Measurements of thermal and dielectric properties of medium density fiberboard with different moisture contents*, BioResources 8(3): 4185-4192.

Zimmerman W B J (2006*) Multiphysics Modeling with Finite Element Methods*, World Scientific Publishing, p. 432, ISBN: 978-981-256-843-4.

13. Annexes

1. Annex: APDL script for heat transfer in MDF by quasi-stationary measuring method
2. Annex: Probabilistic analysis of the quasi-stationary measuring method
3. Annex: ADPL script for heat transfer in MDF by pulse-transient measuring method
4. Annex: Conjugate heat transfer- the air enclosure

13.1.Annex 1.

```
!-------------------------------------------------------------------------------------------------------------------------------------------------------------
!                                                    MDF MODEL- quasi-stationary method
!-------------------------------------------------------------------------------------------------------------------------------------------------------------
!
/prep7
sir=0.04985                                          ! X axis
del=0.04966                                          ! Z axis
tl=0.01820                                           ! Y axis
n_div=4                                              ! mesh division
krit_der=-0.0000001                                  ! criterium for 1. der. = 0
krit1=1                                              ! criterium for the beginning of the linear part (100%)
krit2=0.9998                                         ! criterium of the end of the linear part (99,98%)
!
kx_1=0.235                                           ! thermal conductivity according exp.data
ky_1=0.251
h1=772.66                                            ! density of the measured sample
c_1=2741                                             ! specific heat
conv_1=14                                            ! heat transfer coefficient
!
temp_1=294.15                                        ! initial temperature on the lateral surfaces (21°)
hf_1=925                                             ! heat flow applied on the upper and down surface
n_sub=2e4                                            ! number of step
t_ime=2e4                                            ! time of the transient analysis (= time of the measurement)
!
! INPUT PARAMETERS
par1=(conv_1*tl)/ky_1                                ! Biot number
par2=ky_1/(c_1*h1*tl)                                ! Fourier number (thickness)
par3=kx_1/(c_1*h1*sir)                               ! Fourier number (surface)
par4=c_1*h1
par5=par2/par3
!
! OUTPUT PARAMETERS
!nod_num ,  208.0000000000                           ! node number in the middle of the sample
!nsub_deriv_0,                                       ! number of steps where  the fisrt derivation=0 at krit_der
!t_deriv_0,                                          ! time when the deriv_t=0
!max_deriv_t,                                        ! maximal first derivation of temperature deriv_t=max
!nsub_deriv_max,                                     ! number of substeps
!t_deriv_max,                                        ! time at deriv_t=max
!min_deriv_t,                                        ! minimal first derivation of temperature deriv_t=min
!nsub_deriv_min,                                     ! number of substeps
!t_deriv_min,                                        ! time at deriv_t=min
!nsub_deriv_lin1,                                    ! number of substeps at the beginning of the linear part
!t_deriv_lin1,                                       ! time at the beginning of the linear part
!nsub_deriv_lin2,                                    ! number of substeps at the end of the linear part
!t_deriv_lin2,                                       ! time at the end of the linear part
!max_deriv2_t,                                       ! maximal second derivation of temperature
!nsub_deriv2_max,                                    ! number of substeps
!t_deriv2_max,                                       ! time at deriv2_t=max
!min_deriv2_t,                                       ! minimal second derivation of temperature
!nsub_deriv2_min,                                    ! number of substeps
!t_deriv2_min,                                       ! time at deriv2_t=min
!avg_der_at_lin,                                     !  average value of the first derivations at the linear part
!stdev_der_at_lin,                                   !  standard deviation of avg_der_at_lin
!var_der_at_lin,                                     ! coefficient of variation
! GEOMETRY (x=sir, y=tl, z=del)
block,0,sir,0,tl,0,del                               !lower mdf
wpoffs,0,tl,0
block,0,sir,0,tl,0,del                               !upper mdf
vsel,all
vglue,all
!
mptemp,
 mp,kxx,1,kx_1                                       ! thermal conductivity in width
 mp,kyy,1,ky_1
 mp,kzz,1,kx_1                                       ! thermal conductivity in width= in length
 mp,dens,1,h1
```

```
 mp,c,1,c_1
!
et,1,solid279
vsel,all
vatt,1,,1,
allsel,all
!
esize,,n_div                                ! size of elements
mshape,0,3d
mshkey,1                                    ! mapped mesh
vsel,all
vmesh,all
!
csys,0
nsel,s,loc,x,0,sir
nsel,r,loc,y,0,0
nsel,r,loc,z,0,del
cm,plocha1,node
sf,plocha1,hflux,hf_1                       ! heat flux on the lower surface
allsel,all
nsel,s,loc,x,0,sir
nsel,r,loc,y,2*tl,2*tl
nsel,r,loc,z,0,del
cm,plocha2,node
sf,plocha2,hflux,hf_1                       ! heat flux on the upper surface
allsel,all
/replot
!
asel,s,,,1
asel,a,,,13
asel,a,,,5
asel,a,,,16
asel,a,,,2
asel,a,,,14
asel,a,,,6
asel,a,,,15
cm,konv1,area
con_v=conv_1
sfa,konv1,1,conv,con_v,temp_1               ! convection on the lateral surfaces
finish
!
/solu
antype,4                                    ! transient analysis
allsel,all
ic,all,temp,temp_1                          ! initial temperature
solcontrol,0
kbc,1                                       ! step boundary conditions
time,t_ime                                  ! time at end of transient
autots,off                                  ! automatic time stepping
nsubst,n_sub,n_sub,n_sub
outres,erase $ outres,all,all               ! saving of outputs
solve
finish
!
/post1
file,file,rth
csys,0
nod_num=node(sir/2,tl,del/2)                ! node in the center of the middle sample
!
*dim,temp_stred,array,n_sub                 ! temperatures array
*dim,ti_me,array,n_sub                      ! time array
!
*do,i,1,n_sub                               ! finding temperature in time for nod_num
 set,,,1,,,,%i%,
 temp_stred(i)=temp(nod_num)
 *get,ti_me(i),active,0,set,time
*enddo
!
```

```
*voper,deriv_t,temp_stred,der1,ti_me                ! first temperature derivation in time for nod_num
*voper,deriv2_t,temp_stred,der2,ti_me               ! second temperature derivation in time for nod_num
*vscfun,max_deriv_t,max,deriv_t                     ! maximal first derivation in time for nod_num
 *vscfun,min_deriv_t,min,deriv_t                    ! minimal first derivation in time for nod_num
*vscfun,max_deriv2_t,max,deriv2_t                   ! maximal second derivation in time for nod_num
*vscfun,min_deriv2_t,min,deriv2_t                   ! minimal second derivation in time for nod_num
finish
!
/post26
numvar,200                                          ! number of variables
nsol,2,nod_num,temp,, temp_2,                       ! assign temperature temp_2 in nod_num
vput,deriv_t(1,1,1),200
realvar,3,200,,,der1
vput,deriv2_t(1,1,1),200
realvar,4,200,,,der2
xvar,1
plvar,2,                                            ! plot temp_2 to a graph
!/show,png,,0
!pngr,comp,1,-1
!pngr,orient,horiz
!pngr,color,2
!pngr,tmod,1
!/gfile,1000,
!/cmap,_tempcmap_,cmp,,save
!/rgb,index,100,100,100,0
!/rgb,index,0,0,0,15
!/replot
!/wait,3
!/cmap,_tempcmap_,cmp
!/delete,_tempcmap_,cmp
!/show,close
!/device,vector,0
!/rename,file000,png,,temp_vs_time,png,
xvar,1                                              ! plot first derivation to a graph
plvar,3,
!/show,png,,0
!pngr,comp,1,-1
!pngr,orient,horiz
!pngr,color,2
!pngr,tmod,1
!/gfile,1000,
!/cmap,_tempcmap_,cmp,,save
!/rgb,index,100,100,100,0
!/rgb,index,0,0,0,15
!/replot
!wait,3
!/cmap,_tempcmap_,cmp
!/delete,_tempcmap_,cmp
!/show,close
!/device,vector,0
!/rename,file000,png,,der1temp_vs_time,png,
xvar,1                                              ! plot second derivation to a graph
plvar,4,
!/show,png,,0
!pngr,comp,1,-1
!pngr,orient,horiz
!pngr,color,2
!pngr,tmod,1
!/gfile,1000,
!/cmap,_tempcmap_,cmp,,save
!/rgb,index,100,100,100,0
!/rgb,index,0,0,0,15
!/replot
!/wait,3
!/cmap,_tempcmap_,cmp
!/delete,_tempcmap_,cmp
!/show,close
!/device,vector,0
```

```
!/rename,file000,png,,der2temp_vs_time,png,
!
*do,i,1,n_sub
  *if,deriv_t(i),eq,max_deriv_t,then                    ! finding the maximum of the first derivation
 t_deriv_max=ti_me(i)
nsub_deriv_max=(i)
  *endif
    *if,deriv_t(i),eq,min_deriv_t,then                  ! finding the minimum of the first derivation
 t_deriv_min=ti_me(i)
 nsub_deriv_min=(i)
  *endif
     *if,deriv2_t(i),eq,max_deriv2_t,then               ! finding the maximum of the second derivation
t_deriv2_max=ti_me(i)
nsub_deriv2_max=(i)
  *endif
      *if,deriv2_t(i),eq,min_deriv2_t,then              ! finding the minimum of the second derivation
t_deriv2_min=ti_me(i)
nsub_deriv2_min=(i)
  *endif
*enddo
!
*do,i,1,n_sub-1                                       ! finding the part of the curve approximating to zero value
   *if,deriv_t(i+1)-deriv_t(i),gt,krit_der,and,i,gt,10000,then
     t_deriv_0=ti_me(i)
     nsub_deriv_0=(i)
     *exit
   *endif
*enddo
!
*do,i,1,n_sub-2
   *if,(deriv_t(i+2)-deriv_t(i+1))/(deriv_t(i+1)-deriv_t(i)),lt,krit1,and,i,gt,nsub_deriv_max,then
    t_deriv_lin1=ti_me(i)                               ! finding the beginning of the linear part of the curve
    nsub_deriv_lin1=(i)
    *exit
   *endif
*enddo
!
*do,i,1,n_sub-2
   *if,(deriv_t(i+2)-deriv_t(i+1))/(deriv_t(i+1)-deriv_t(i)),lt,krit2,and,i,gt,nsub_deriv_lin1,then
    t_deriv_lin2=ti_me(i)                               ! finding the end of the linear part of the curve
    nsub_deriv_lin2=(i)
    *exit
   *endif
*enddo
!
*dim,der_range,array,nsub_deriv_lin2-nsub_deriv_lin1
*if,nsub_deriv_lin2,gt,nsub_deriv_lin1,then
 *do,i,nsub_deriv_lin1,nsub_deriv_lin2-1
  der_range(i-(nsub_deriv_lin1)+1)=deriv_t(i)
 *enddo
*else
 *msg,warn
  Range for AVG > NSUB
  /wait,2
*endif
!
*vscfun,avg_der_at_lin,mean,der_range                 ! set the average value of the first derivation in the linear part
*vscfun,stdev_der_at_lin,stdv,der_range               ! set the standard deviation
var_der_at_lin=stdev_der_at_lin/avg_der_at_lin        ! set the coefficient of variation
t_deriv_delta=t_deriv_lin2-t_deriv_lin1               ! the time difference between times of the linear part
```

13.2.Annex 2.

```
!-------------------------------------------------------------------------------------------------------------------------------------------------------------
!                Sensitivity probabilistic analyses (PDS)- quasi-stationary method
!-------------------------------------------------------------------------------------------------------------------------------------------------------------
!
/inp,mdf_m,mac                                          ! input of the macro file
/pds                                                    ! switching to probabilistic analyses
!
pdanl,mdf_m,mac
!
pdvar,kx_1,gaus,0.235,0.1*0.235          ! thermal conductivity with Gaussian distribution (average and the standard deviation)
pdvar,ky_1,gaus,0.251,0.1*0.251          ! thermal conductivity with Gaussian distribution (average and the standard deviation)
pdvar,h1,gaus,772.66,0.1*772.66          ! density with Gaussian distribution (average and the standard deviation)
pdvar,c_1,gaus,2741,0.1*2741             ! specific heat with Gaussian distribution (average and the standard deviation)
pdvar,conv_1,gaus,14,0.1*14              ! heat transfer coeff. with Gaussian distribution (average and the standard deviation)
pdvar,hf_1,gaus,925,0.1*925              ! heat flux with Gaussian distribution (average and the standard deviation)
!
!pdcor,kx_1,ky_1,0.5                     ! correlation coefficient between parameters
!
pdvar,avg_der_at_lin,resp                ! parameters response
pdvar,var_der_at_lin,resp
pdvar,min_deriv_t,resp
pdvar,max_deriv_t,resp
pdvar,min_deriv2_t,resp
pdvar,max_deriv2_t,resp
pdvar,t_deriv_min,resp
pdvar,t_deriv_max,resp
pdvar,t_deriv2_min,resp
pdvar,t_deriv2_max,resp
pdvar,t_deriv_0,resp
pdvar,t_deriv_lin2,resp
pdvar,t_deriv_delta,resp
pdvar,par1,resp
pdvar,par2,resp
pdvar,par3,resp
pdvar,par4,resp
pdvar,par5,resp
!
pdmeth,mcs,dir                                          ! direct Monte Carlo simulation
pddmcs,4000,none,all,,,,123457                          ! 4000 samples, initial seed of 123457
!
pdexe,mdf_m                                             !start of the analyses
pdsesns,mdf_m,avg_der_at_lin,both,rank,0.025            !sensitivity graph (this step is done for all of the parameters consequently)
!
/show,png,,0                                            ! saving the graph
pngr,comp,1,-1
pngr,orient,horiz
pngr,color,2
pngr,tmod,1
/gfile,1000,
/cmap,_tempcmap_,cmp,,save
/rgb,index,100,100,100,0
/rgb,index,0,0,0,15
/replot
/wait,3
/cmap,_tempcmap_,cmp
/delete,_tempcmap_,cmp
/show,close
/device,vector,0
/rename,file000,png,,avg_der_at_lin,png,
/wait,5
!!
pdcmat,mdf_m,io,'       ','       ',rank,0.025,1    ! prints the correlation coefficients matrix
save
/eof
```

13.3.Annex 3.

```
!-----------------------------------------------------------------------------------------------------------------------------------------------------------
!           ADPL script for heat transfer in MDF by pulse-transient measuring method
!-----------------------------------------------------------------------------------------------------------------------------------------------------------
/prep7
sir=0.05056                                     !X axis
del=0.05079                                     !Z axis
tl=0.01205                                      !Y axis
tl2=0.0182
n_div=12
ky_1=0.187                                      !physical properties of MDFs gained by experiments
kx_1=ky_1
ky_2=0.187
h1=781.87
c_1=1751.645
conv_1=10                                       !heat transfer coefficient
temp_1=298.05
temp_2=298.05                                   !bulk temperature
t_ime=1800                                      !time of the measurement
n_sub=7200                                      !calculate in ¼ of a second
t_1=25                                          !beginning of the pulse in second
t_2=48                                          !end of the heat pulse
t_delta=t_2-t_1                                 !duration of the heat pulse
block,0,sir,0,tl2,0,del                         !creation of blocks- outer sample 1
wpoffs,0,tl2,0
block,0,sir,0,tl,0,del                          !creation of blocks- middle sample
wpoffs,0,tl,0
block,0,sir,0,tl2,0,del                         !creation of blocks- outer sample 2
vsel,all
vglue,all
mptemp,
mp,kxx,1,ky_1                                   !assigning material propeties to middle sample
mp,kyy,1,ky_1
mp,kzz,1,ky_1
mp,dens,1,h1
mp,c,1,c_1
mp,kxx,2,ky_2                                   !assigning material propeties to outer samples
mp,kyy,2,ky_2
mp,kzz,2,ky_2
mp,dens,2,h1
mp,c,2,c_1
et,1,solid279
vsel,all
vsel,u,loc,y,tl2,tl2+tl
vatt,2,,1,
vsel,inve
vatt,1,,1,
allsel,all
esize,,n_div
mshape,0,3d                                     !meshing the geometry
vmesh,all
!
/solu
antype,4                                        !transient analysis
trnopt,full
kbc,1
solcontrol,on,on
ic,all,temp,temp_1
time,t_ime
nsubst,n_sub,n_sub,n_sub
outres,erase $ outres,all,all
asel,s,loc,y,0,0
asel,a,loc,y,2*tl2+tl,2*tl2+tl
nsla,s,1
d,all,temp,temp_1                               !boundary condition: temperature to the outer surfaces
allsel,all
asel,u,loc,y,0
```

```
asel,u,loc,y,tl2
asel,u,loc,y,tl2+tl
asel,u,loc,y,2*tl2+tl
sfa,all,,conv,conv_1,temp_2          !boundary condition: heat transfer coefficient  at bulk temperature
allsel,all
asel,s,loc,y,tl2
nsla,s,1
*get,po_cet,node,0,count             !give nuber of all nodes in the selected area
*DIM,pulse,table,t_ime,1             !create table with assigned heat values
*do,i,1,t_ime
pulse(0,1)=0
pulse(i,0)=i
pulse(i,1)=0
*if,i,gt,t_1,and,i,lt,t_2,then
pulse(i,0)=i
pulse(i,1)=8.77/po_cet               !calculation of heat at certain nodes
*endif
*enddo
f,all,heat,%pulse%                   !assign heat value for each node in the selected area
allsel,all
solve
finish
!
/post1
file,,rth
csys,0
nod_num=node(sir/2,tl+tl2,del/2)
*dim,temp_stred,array,n_sub          !list the temperature field in the selected node
*dim,ti_me,array,n_sub               !list the time field in the selected node
*do,i,1,n_sub                        !find the temperature and time in selected node for all subsets
 set,,,1,,,,%i%,
 temp_stred(i)=temp(nod_num)
 *get,ti_me(i),active,0,set,time
*enddo
finish
!
/post26                              !time history postprocessor
numvar,200
nsol,2,nod_num,temp,, temp_2,
xvar,1
plvar,2,
/show,png,,0                         !show the temperature vs. time as a picture
pngr,comp,1,-1
pngr,orient,horiz
pngr,color,2
pngr,tmod,1
/gfile,800,                          !save picture
/cmpa,_tempcmap_,cmp,,save
/rgb,index,100,100,100,0
/rgb,index,0,0,0,15
/replot
/cmap,_tempcmap_,cmp
/delete,_tempcmap_,cmp
/show,close
/device,vector,0
*create,ansuitmp
*cfopen, 'out_temp','txt',' '
*vwrite,ti_me(1),temp_stred(1), , , , , , ,      !write a text file with temperature values
%g %g
*cfclos
*end
/input,ansuitmp
/eof
```

13.4.Annex 4.

```
!geom.mac
!-----------------------------------------------------------------------------------------------------------------------------------------------------------
/prep7
tl_sp=0.56                                  !parameters describing the geometry
vys_sp=0.02
tl_fibre=0.032
rectng,0,tl_sp,0,vys_sp                     !create rectangles (2D)
rectng,-0.02,tl_sp+0.02,-0.032,vys_sp+0.032
aovlap,all
aplot
!
et,1,fluid141                               !fluid element
et,2,fluid141                               !solid part of the element
asel,s,,,1
aatt,1,,1
asel,inve,
aatt,2,,2,
allsel,all
!
lsel,s,loc,x,0
lsel,a,loc,x,tl_sp
lesize,all,vys_sp/20
allsel
!
lsel,s,loc,x,-0.02                          !assigning different mesh demands (finer mesh in fluid part)
lsel,a,loc,x,tl_sp+0.02
lesize,all,vys_sp/10
allsel
!
lsel,s,loc,y,-tl_fibre                      !assigning different mesh demands (rough mesh in solid part)
lsel,a,loc,y,tl_fibre+vys_sp
lsel,a,loc,y,0
lsel,a,loc,y,vys_sp
lesize,all,vys_sp/10
allsel
!
amesh,all                                   !mesh all areas
allsel,all
!
!-----------------------------------------------------------------------------------------------------------------------------------------------------------
!               Conjugate heat transfer- the air enclosure
!-----------------------------------------------------------------------------------------------------------------------------------------------------------
geom.mac                                    !open geom.mac with created geometry
!
/prep7
!
ic,all,temp,293,                            !boundaty condition: initial temperature of all areas
tref,293
toff,0
kx_2=0.053                                  !thermal properties of the solid part
h2=195
c2=2100
!
mptemp,                                     !assign the thermal properties to the solid
mp,kxx,2,kx_2
mp,kyy,2,kx_2
mp,dens,2,h2
mp,c,2,c2
!
temp_down=287.288
temp_up=297.312                             !temperature at the upper surface
!
csys,0
lsel,s,loc,y,-tl_fibre
nsll,s,1
d,all,temp,temp_down                        !assigning the temperature temp_down
```

```
allsel,all
!
lsel,s,loc,y,vys_sp+tl_fibre                !assigning the temperature temp_up
nsll,s,1
d,all,temp,temp_up
allsel,all
!
asel,s,,,3
asll,s
nsll,s,1
d,all,,,,,,vx,vy                            !boundary condition: zero velocity in the cavity
allsel,all
!
asel,s,,,1
lsla,s
nsll,s,1
sfl,all,rdsf,0.3,,-1                        !boundary condition: surface to surface radiation within the cavity
!
nsel,all
esel,all
tref,293                                    !reference temperature
stef,5.67e-8
radopt,0.5,0.0001
toff,0
!
fldata1,solu,temp,1                         !material properties of air
fldata2,iter,exec,1000
fldata2,iter,over,50
fldata5,outp,sumf,50
fldata13,vary,dens,1
fldata7,prot,dens,air-si
fldata7,prot,visc,air-si
fldata7,prot,cond,air-si
fldata8,nomi,cond,-1
fldata7,prot,spht,air-si
!
acel,0,9.81,0                               !gravity acceleration
fldata18,meth,pres,1                        !solvers in Flotran
fldata19,tdma,pres,100
fldata18,meth,temp,6
!
/solu
solve
finish
/post1
set,last
plnsol,temp                                 !show temperature field
!
lsel,s,loc,y,vys_sp
nsll,s,1
*get,n_count,node,0,count
*get,n_min,node,0,num,min
*get,temp_up%1%,node,%n_min%,temp,sum
!
*do,i,2,n_count
 *get,n_next,node,%n_min%,nxth
 *get,temp_up_sum%i%,node,%n_next%,temp,sum
 n_min=n_next
*enddo
!
temp_up_sum%0%=0
*do,i,1,n_count
 temp_up_sumsum=temp_up_sum%i-1%+temp_up_sum%i%
 temp_up_sum%i%=temp_up_sumsum                  !get average temperature for selected nodes
*enddo
!
temp_up_avg=temp_up_sumsum/n_count
lsel,s,loc,y,vys_sp
```

```
nsll,s,1
*get,n_count,node,0,count
*get,n_min,node,0,num,min
*get,temp_down%1%,node,%n_min%,temp,sum
!
*do,i,2,n_count
 *get,n_next,node,%n_min%,nxth
 *get,temp_down_sum%i%,node,%n_next%,temp,sum
 n_min=n_next
*enddo
!
temp_down_sum%0%=0
*do,i,1,n_count
 temp_down_sumsum=temp_down_sum%i-1%+temp_down_sum%i%
 temp_down_sum%i%=temp_down_sumsum
*enddo
!
temp_down_avg=temp_down_sumsum/n_count                    !get average temperature for selected nodes
!
lsel,s,loc,y,0
nsll,s,1
*get,n_count,node,0,count
*get,n_min,node,0,num,min
*get,flx_down%1%,node,%n_min%,hflu,sum
!
*do,i,2,n_count
 *get,n_next,node,%n_min%,nxth
*get,flx_down_sum%i%,node,%n_next%,hflu,sum
 n_min=n_next
*enddo
!
flx_down_sum%0%=0
*do,i,1,n_count
 flx_down_sumsum=flx_down_sum%i-1%+flx_down_sum%i%
 flx_down_sum%i%=flx_down_sumsum
*enddo
!
flx_down_avg=flx_down_sumsum/n_count                      !get average heat flux for selected nodes at down line
!
lsel,s,loc,y,vys_sp
nsll,s,1
*get,n_count,node,0,count
*get,n_min,node,0,num,min
*get,flx_up%1%,node,%n_min%,hflu,sum
!
*do,i,2,n_count
 *get,n_next,node,%n_min%,nxth
*get,flx_up_sum%i%,node,%n_next%,hflu,sum
 n_min=n_next
*enddo
!
flx_up_sum%0%=0
*do,i,1,n_count
 flx_up_sumsum=flx_up_sum%i-1%+flx_up_sum%i%
 flx_up_sum%i%=flx_up_sumsum
*enddo
!
flx_up_avg=flx_up_sumsum/n_count                          !get average heat flux for selected nodes at upper line
!
flx_down_avg2=abs(flx_down_avg)
flx_avg=(flx_down_avg2+flx_up_avg)/2
!
lsel,s,loc,y,0
nsll,s,1
*get,n_count,node,0,count
*get,n_min,node,0,num,min
*get,radi%1%,node,%n_min%,rdfl,sum
*do,i,2,n_count
```

```
 *get,n_next,node,%n_min%,nxth                    !get value of next higher node number
 *get,radi_sum%i%,node,%n_next%,rdfl,sum          !get heat flux sum for node with next number in the selected set
 n_min=n_next
*enddo
!
radi_sum%0%=0                                    !loop for sumation of heat flux sums
*do,i,1,n_count
radi_sumsum=radi_sum%i-1%+radi_sum%i%
radi_sum%i%=radi_sumsum
*enddo
!
radi_avg=radi_sumsum/n_count                     !get average value of radiation heat flux
```